

**SOUTHAMPTON OCEANOGRAPHY CENTRE**

**CRUISE REPORT No. 45**

**RRS *CHARLES DARWIN* CRUISE 139  
01 MAR - 15 APR 2002**

Trans-Indian Hydrographic Section across 32°S

*Principal Scientist*  
**H L Bryden**

**2003**

School of Ocean and Earth Sciences  
Southampton Oceanography Centre  
University of Southampton  
Waterfront Campus  
European Way  
Southampton  
Hants SO14 3ZH  
UK

Tel: +44 (0)23 8059 6437  
Fax: +44 (0)23 8059 6204  
Email: [H.Bryden@soc.soton.ac.uk](mailto:H.Bryden@soc.soton.ac.uk)



# DOCUMENT DATA SHEET

<b>AUTHOR</b> BRYDEN, H L et al	<b>PUBLICATION DATE</b> 2003
<b>TITLE</b> RRS <i>Charles Darwin</i> Cruise 139, 01 Mar-15 Apr 2002. Trans-Indian Hydrographic Section across 32°S.	
<b>REFERENCE</b> Southampton Oceanography Centre Cruise Report, No. 45, 122pp.	
<b>ABSTRACT</b> <p>A modern hydrographic section was made across the Indian Ocean at a latitude of about 32°S during a 46-day voyage from Durban to Fremantle aboard RRS <i>Charles Darwin</i> in March-April 2002. The principal goal of this work was to measure the flows of mass, heat, freshwater, inorganic and organic nutrients, and carbon dioxide across the southern boundary of the Indian Ocean in order to determine the meridional overturning circulation for the Indian Ocean, to define the heat, freshwater, nutrient and carbon transports across 32°S, and to produce overall physical and biogeochemical budgets for the Indian Ocean. A second goal was to examine the climate variability in ocean circulation from comparisons of these new measurements with previous surveys in 1936, 1965, 1987 and 1995. A total of 146 hydrographic stations were made along this transoceanic section. At each station an instrument package consisting principally of a CTD, 3 Lowered ADCP's and 24 10-litre sampling bottles was lowered from the surface down to the ocean bottom to measure temperature, salinity, oxygen and eastward and northward current profiles throughout the water column. On the way back to the surface, 24 water samples were collected at various depths and these samples were analysed on board ship for salinity and oxygen (to calibrate the continuous electronic profiles), for inorganic nutrients, constituents of the carbon system, and chlorofluorocarbons. Samples were also collected and stored for later, shore-based analyses of helium, tritium, and organic nutrients. Throughout the cruise velocity data in the upper few hundred meters of the water column were provided by an ADCP mounted in the ship's hull, meteorological variables were monitored and samples of air and rainfall were periodically collected. In addition, 25 Argo floats were launched along the section to provide continuing profiles over the next 5 years. This report describes the methods used to acquire and process the measurements on board ship during the cruise.</p>	
<b>KEYWORDS</b> ADCP, AGULHAS CURRENT, ARGO FLOATS, BIOGEOCHEMICAL BUDGETS, CARBON CHEMISTRY, CFC, CHARLES DARWIN, CLIMATIC CHANGES, CRUISE 139 2002, CTD OBSERVATIONS, HELIUM-TRITIUM SAMPLES, HYDROGRAPHIC SECTION, INDIAN OCEAN, LADCP, LOWERED ACOUSTIC DOPPLER CURRENT PROFILER, MERIDIONAL OVERTURNING CIRCULATION, NUTRIENTS, OCEAN CIRCULATION, TRACER MEASUREMENTS, VESSEL MOUNTED ADCP	
<b>ISSUING ORGANISATION</b> Southampton Oceanography Centre Empress Dock European Way Southampton SO14 3ZH UK	
Copies of this report are available from: National Oceanographic Library, SOC PRICE: £26.00 Tel: +44(0)23 80596116 Fax: +44(0)23 80596115 Email: nol@soc.soton.ac.uk	



**CONTENTS**

<b>SCIENTIFIC PERSONNEL</b>	<b>7</b>
<b>SHIPS PERSONNEL</b>	<b>8</b>
<b>ITINERARY</b>	<b>9</b>
<b>BACKGROUND AND OBJECTIVES</b>	<b>9</b>
<b>Chart of Hydrographic Station – Cruise Track for CD 139</b>	<b>13</b>
<b>Hydrographic Station positions and depths</b>	<b>14</b>
<b>NARRATIVE</b>	<b>18</b>
<b>CTD DATA PROCESSING AND CALIBRATION</b>	<b>22</b>
<b>WATER SAMPLE SALINITY ANALYSIS</b>	<b>46</b>
<b>DISSOLVED OXYGEN</b>	<b>48</b>
<b>NUTRIENTS</b>	<b>50</b>
<b>CO<sub>2</sub> COMPONENTS</b>	<b>57</b>
<b>CHLOROFLUOROCARBON (CFC) MEASUREMENTS</b>	<b>61</b>
<b>SAMPLING FOR HELIUM AND TRITIUM</b>	<b>65</b>
<b>LOWERED ACOUSTIC DOPPLER CURRENT PROFILER</b>	<b>68</b>
<b>SHIPBOARD INSTRUMENTATION AND COMPUTING</b>	<b>100</b>
<b>NAVIGATION</b>	<b>105</b>

<b>VESSEL-MOUNTED ACOUSTIC DOPPLER CURRENT PROFILER (VMADCP)</b>	<b>109</b>
<b>UNDERWAY METEOROLOGICAL MEASUREMENTS</b>	<b>113</b>
<b>ATMOSPHERIC SAMPLING</b>	<b>115</b>
<b>ARGO FLOATS</b>	<b>119</b>

**SCIENTIFIC PERSONNEL**

<b>Name</b>	<b>Role</b>	<b>Affiliation</b>
Harry L. Bryden	Principal Scientist	SOES-SOC
Brian A. King	Watch Leader-LADCP	JRD-SOC
Stuart A. Cunningham	Watch Leader-CTD	JRD-SOC
Louise M. Duncan	Watch Leader-VMADCP	JRD-SOC
Lisa M. Beal	LADCP	SIO, San Diego
Jeffrey R. Benson	CTD	UKORS-SOC
John B. Wymar	Instrumentation	UKORS-SOC
Richard Sanders	Nutrients-Leader	GDD-SOC
Valerie Latham	Nutrients	CSIRO, Hobart
Angela Landolfi	Nutrients	SOES-SOC
Aida Rios	CO2-Leader	IIM, Vigo
Marta Álvarez	CO2	IIM, Vigo
David P. Wisegarver	CFC-Leader	PMEL, Seattle
Kevin McHugh	CFC	PMEL, Seattle
W. Kevin Smith	Winch	UKORS-SOC
Steve Whittle	Winch	UKORS-SOC
Matthew D. Palmer	CTD	SOES-SOC
Melanie Witt	Atmosphere Trace Metals	UEA, Norwich
Martin Bridger	Computing	UKORS-SOC

SOC=Southampton Oceanography Centre

PMEL=Pacific Marine Environmental Laboratory

JRD=James Rennell Division

CSIRO=Commonwealth Scientific and Industrial Research Organisation

SOES=School of Ocean and Earth Science

GDD=George Deacon Division

UKORS=UK Ocean Research Services

IIM=Instituto de Investigaci3n Marinas

SIO=Scripps Institution of Oceanography

UEA=University of East Anglia

**SHIP'S PERSONNEL**

<b>Name</b>	<b>Rank</b>
LONG, G. M.	Master
NEWTON, P. W.	Chief Officer
OLDFIELD, P. T.	2 <sup>nd</sup> Officer
HOOD, M. P.	2 <sup>nd</sup> Officer
MOSS, S. A.	Chief Engineer
HOLT, J. M.	2 <sup>nd</sup> Engineer
CLARK, J. R. C.	3 <sup>rd</sup> Engineer
SLATER, G.	3 <sup>rd</sup> Engineer
BAKER, J. G. L.	ETO
POOK, G. A.	CPO(D)
LUCKHURST, T. G.	PO(D)
ALLISON, P.	S1A
COOK, S. C.	S1A
CRABB, G.	S1A
MACLEAN, A.	S1A
HILLIER, L. J.	POMTR
BELL, R.	SCM
FAHEY, F.	Chef
KUJAWIAK, A.	M/S
MINGAY, G. M.	Steward



## ITINERARY

*RRS Charles Darwin* departed Durban, South Africa on Friday 1 March at 1500 local time to take a transindian hydrographic section along a nominal latitude of 32°S. We made 2 transects of the Agulhas Current and then began the coast-to-coast section just offshore of Port Edward 60 miles south of Durban. On Monday, 15 April at 0800 local time *RRS Charles Darwin* arrived in Fremantle Australia after 146 hydrographic stations over 46 days at sea (Figure 1).

## BACKGROUND AND OBJECTIVES

The size and structure of the overturning circulation in the Indian Ocean is one of the foremost issues in observing the large-scale ocean circulation today. Taking advantage of the scheduling of a UK research vessel to work in the Indian Ocean in 2001/2002, we proposed a transindian hydrographic section across the southern boundary of the Indian Ocean at 32°S to measure this overturning circulation. Transoceanic hydrographic sections across the southern boundaries of the Atlantic Ocean at about 40°S and Pacific Ocean at about 32°S during the World Ocean Circulation Experiment (WOCE) have provided estimates of the basin-scale meridional circulation and meridional heat, freshwater and biogeochemical fluxes that then define the ocean-scale heat, freshwater and biogeochemical budgets in effect defining the overall contribution of each ocean to the global heat, water and nutrient balances (Saunders and King, 1995a; Tsimplis, Bacon and Bryden, 1998; Wijffels, Toole and Davis, 2000). Unfortunately a hydrographic section across the southern boundary of the Indian Ocean was not carried out during WOCE.

There was a 1987 transindian section across 32°S of the Indian Ocean aboard *RRS Charles Darwin* (Toole and Warren, 1993), but that section consisted primarily of traditional hydrographic stations with CTD profiles and water sample analyses without the technological improvements that became standard during WOCE fieldwork. The technological improvements made during WOCE focussed on making velocity measurements with underway acoustic Doppler current profiler (ADCP) measurements combined with three-dimensional GPS navigation providing continuous velocity information in the upper 400 m (King, Alderson and Cromwell, 1996), on making full-depth Lowered ADCP (L-ADCP) measurements of velocity throughout the water column on each hydrographic station (King, Firing and Joyce, 2001), and on deploying neutrally buoyant floats to define the deep velocity field (Davis, 1998). Each of these velocity techniques has proven useful for determining the reference level velocity for geostrophic velocity profiles (Saunders and King, 1995b; Beal and Bryden, 1997; Wijffels, Toole and Davis, 2000). Without having these velocity techniques available,

analyses of the 1987 transindian hydrographic section have had to rely on traditional water mass analysis techniques to define the zero velocity surface for the geostrophic velocity profile for each station pair across the basin.

Another problem with the 1987 section across 32°S is that it took stations over the Broken Plateau for about 1300 km from 88°E to 101°E so that it preferentially sampled relatively shallow waters over the Plateau rather than the deeper waters to the north or south of the Plateau. Such sampling forces a shallow reference level for geostrophic velocity estimates in analyses using the 1987 32°S section and this shallow reference level may compromise estimates of the meridional overturning circulation (Bryden and Beal, 2001).

Thus, the principal objective of the resulting *RRS Charles Darwin* cruise was to take a modern hydrographic section across 32°S in the Indian Ocean in order to measure the flows of mass, heat, freshwater, inorganic and organic nutrients, and carbon dioxide across the southern boundary of the Indian Ocean, to quantify the meridional overturning circulation for the Indian Ocean, and to produce overall physical and biogeochemical budgets for the Indian Ocean. The 2002 section followed the track of the 1987 section out to 80°E but then, to avoid the problems of shallow reference levels, took a course to the south of Broken Plateau in order to take stations in deep water from 80°E to Australia. A second objective was to examine the climate variability in ocean circulation from comparisons of these new measurements with previous surveys along 32°S in 1936, 1965 and 1987. Because changes in subantarctic mode water along this section have been suggested to be fingerprints of anthropogenic climate change based on Hadley Centre climate model runs (Banks and Wood, 2002; Banks and Bindoff, 2003), analysis of the actual changes is of much current interest. Since the 2002 track follows the track of the 1987 section from the coast of South Africa out to 80°E, climate changes can most easily be assessed in the western part of the section from 30°E to 80°E.

During the 46-day voyage (1 March to 15 April 2002) from Durban to Fremantle aboard *RRS Charles Darwin* across the southern boundary of the Indian Ocean, a total of 146 CTD/LADCP stations were taken along the 9000 km track (Figure 1, Table 1). On each station, continuous top-to-bottom profiles of temperature, salinity, oxygen and east and north velocities were made and up to 24 water samples were analysed for salinity, oxygen, nitrate, phosphate, silicate, CFC's and carbon system components alkalinity and pH. The CFC measurements were made by collaborating American scientists from PMEL in Seattle and the carbon system measurements were made by collaborating Spanish scientists from IIM in Vigo. In addition, 25 Argo floats were launched along the section to provide continuing profiles over the next 5 years, 385 paired water samples were collected for subsequent analysis of helium and tritium concentrations in the Noble Gas Laboratory in Southampton, and atmospheric trace metal measurements were made by a UEA scientist.

## REFERENCES

- Banks, H. T. & Bindoff, N.L.** 2003 Comparison of observed temperature and salinity changes in the Indo-Pacific with results from the coupled climate model HadCM3: Processes and mechanisms. *Journal of Climate*, **16**, 156-166.
- Banks, H. & Wood, R.** 2002 Where to look for anthropogenic climate change in the ocean. *Journal of Climate*, **15**, 879-891.
- Beal, L.M. & Bryden, H.L.** 1997 Observations of an Agulhas Undercurrent. *Deep-Sea Research, I*, **44**, 1715-1724.
- Bryden, H.L. & Beal, L.M.** 2001 Role of the Agulhas Current in Indian Ocean circulation and associated heat and freshwater fluxes. *Deep-Sea Research, I*, **48**, 1821-1845.
- Davis, R.** 1998 Preliminary results from directly measuring mid-depth circulation in the tropical and South Pacific. *Journal of Geophysical Research*, **103**, 24619-24640.
- King, B.A., Alderson, S.G. & Cromwell, D.** 1996 Enhancement of shipboard ADCP data using DGPS position and GPS heading measurements. *Deep-Sea Research, I*, **43**, 937-947.
- King, B.A., Firing, E. & Joyce, T.M.** 2001 Shipboard observations during WOCE. In *Ocean Circulation and Climate*, edited by G. Siedler, J. Church and J. Gould, Academic Press, 99-122.
- Saunders, P.M. & King, B.A.** 1995a Oceanic fluxes on the WOCE A11 section. *Journal of Physical Oceanography*, **25**, 1942-1958.
- Saunders, P.M. & King, B.A.** 1995b Bottom currents derived from a shipborne ADCP on WOCE cruise A11 in the South Atlantic. *Journal of Physical Oceanography*, **25**, 329-347.
- Toole, J.M. & Warren, B.A.** 1993 A hydrographic section across the subtropical South Indian Ocean. *Deep-Sea Research, I*, **40**, 1973-2019.

**Tsimplis, M.N., Bacon, S. & Bryden, H.L.** 1998 The circulation of the sub-tropical South Pacific derived from hydrographic data. *Journal of Geophysical Research*, **103** (10), 21443-21468.

**Wijffels, S.E., Toole, J.M. & Davis, R.** 2000 Revisiting the South Pacific subtropical circulation: A synthesis of World Ocean Circulation Experiment observations along 32°S. *Journal of Geophysical Research*, **106**, 19481-19514.

# Hydrographic Section across 32°S in the Indian Ocean

RRS Charles Darwin March-April 2002

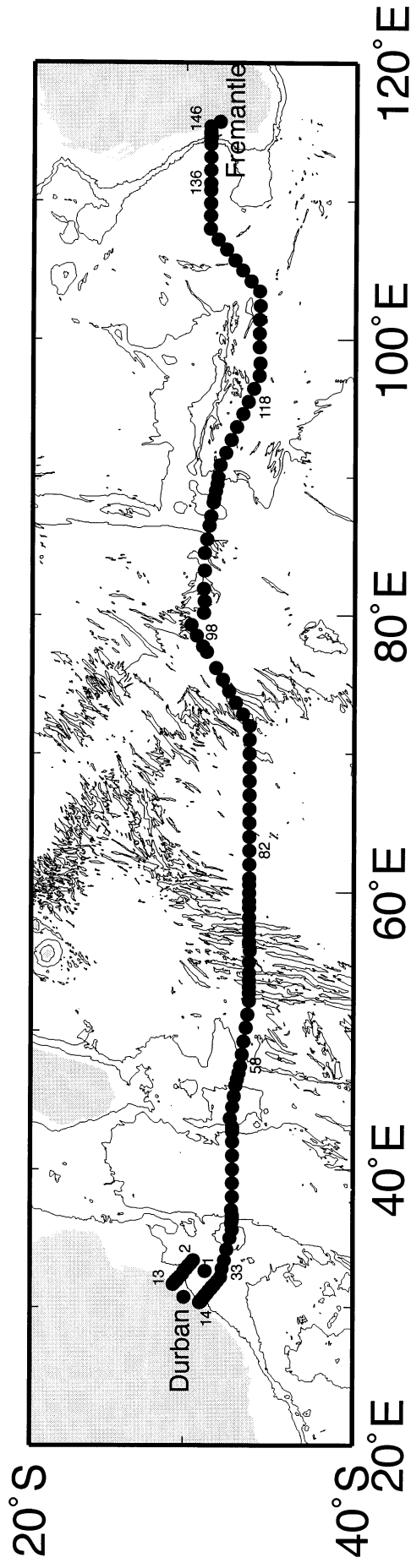


Figure 1. Hydrographic Stations showing Cruise Track

Table 1. Hydrographic station positions and depths.

station#	lat (°S) deg min	lon (°E) deg min	distance km	depth m	Notes
Durban	-30 05.00	30 42.00	0	0	Depart 1Mar 1400
1	-31 22.00	32 38.00	236	3410	Test station
2	-30 37.00	33 24.00	347	3153	
3	-30 28.00	33 11.00	373	2912	
4	-30 19.50	32 59.00	398	2387	
5	-30 11.00	32 47.00	423	1808	Winch stuck
6	-30 3.50	32 36.00	445	1753	
7	-29 56.00	32 25.00	468	1540	
8	-29 48.00	32 14.00	491	1479	
9	-29 41.00	32 4.00	512	1131	
10	-29 37.00	31 58.00	524	868	
11	-29 33.00	31 52.50	535	485	
12	-29 29.00	31 47.00	547	99	
13	-29 23.00	31 38.75	564	67	
14	-31 0.89	30 19.97	785	213	
15	-31 2.00	30 20.86	788	346	
16	-31 2.90	30 22.10	790	549	
17	-31 4.40	30 24.20	795	977	
18	-31 5.80	30 25.40	798	1280	
19	-31 7.30	30 28.30	803	1628	CTD Suspended
20	-31 9.10	30 32.10	810	1877	
21	-31 12.10	30 35.80	818	2387	He/Trit Samples
22	-31 15.60	30 39.30	827	2904	
23	-31 19.05	30 44.70	837	3295	
24	-31 22.50	30 50.10	848	3304	
25	-31 25.95	30 55.50	859	3257	
26	-31 29.40	31 0.90	869	3206	
27	-31 34.70	31 9.70	886	3338	
28	-31 43.12	31 18.86	907	3198	
29	-31 48.32	31 25.98	922	3380	He/Trit Samples
30	-31 56.60	31 36.30	945	3647	
31	-32 6.84	31 52.26	976	3582	Float deployment
32	-32 18.57	32 8.75	1010	3408	
33	-32 25.69	32 46.73	1071	3537	End of Week 1
34	-32 32.80	33 24.70	1131	3551	
35	-32 41.50	34 10.30	1204	2301	
36	-32 54.00	35 0.10	1285	1640	He/Trit Samples
37	-33 0.10	35 35.00	1341	1477	
38	-32 59.40	36 4.70	1387	1862	
39	-33 0.90	36 20.60	1412	2329	Float deployment
40	-33 0.77	36 27.13	1422	3298	
41	-33 0.70	36 30.90	1428	4265	He/Trit Samples
42	-33 0.30	36 40.50	1443	4598	
43	-32 59.70	37 4.80	1480	5105	
44	-33 0.40	38 0.00	1566	4950	
45	-33 0.00	39 0.00	1659	5173	He/Trit Samples

46	-33	0.00	40	0.00	1752	5142	Float deployment
47	-33	0.30	41	0.30	1846	5120	
48	-33	0.00	42	0.00	1939	4430	
49	-32	59.93	42	42.45	2005	4372	
50	-32	59.92	42	50.18	2017	3371	Float deployment
51	-32	59.90	43	2.50	2036	2270	He/Trit Samples
52	-32	52.00	43	40.10	2094	891	
53	-32	59.60	44	29.40	2171	958	
54	-33	6.00	45	18.00	2247	1290	
55	-33	12.40	46	4.80	2321	2172	
56	-33	18.70	46	30.20	2362	2678	
57	-33	22.80	46	55.00	2401	3039	
58	-33	29.90	47	26.80	2452	3608	He/Trit Samples End of week 2
59	-33	33.70	48	14.70	2526	3987	Float deployment CTD stop at 300m
60	-33	40.20	49	13.80	2618	4196	Reterminate wire
61	-33	46.80	50	12.60	2709	4277	CTD stop at 550m
62	-33	53.40	51	11.40	2801	4348	SIO LADCP install Wire in block
63	-33	59.50	52	10.60	2892	4414	Float deployment
64	-33	59.90	52	44.70	2945	4638	He/Trit Samples
65	-34	0.40	53	10.20	2984	4633	
66	-34	0.40	53	36.90	3025	4302	
67	-34	0.70	54	7.10	3071	3955	
68	-34	0.13	54	54.99	3145	3610	
69	-34	0.00	55	46.44	3224	3985	
70	-33	59.66	56	15.09	3268	2725	Float deployment
71	-33	59.33	56	26.80	3286	3847	
72	-33	58.30	57	2.10	3340	4440	He/Trit Samples
73	-33	59.70	57	29.10	3382	5083	
74	-33	59.90	58	10.00	3444	4865	
75	-33	59.70	58	53.60	3511	4169	
76	-33	59.66	59	19.31	3551	5304	He/Trit Samples
77	-33	59.60	59	57.00	3609	4841	
78	-33	59.83	60	32.90	3664	5337	Float deployment
79	-34	0.00	61	0.00	3705	4871	He/Trit Samples
80	-33	59.40	61	59.70	3797	4846	
81	-34	0.00	63	0.00	3890	4721	
82	-33	59.50	63	59.90	3982	4599	He/Trit Samples End of week 3
83	-34	0.00	65	0.00	4074	4567	Float deployment
84	-33	59.80	66	0.20	4166	4581	
85	-34	0.00	67	0.00	4258	4900	He/Trit Samples
86	-34	0.10	67	59.90	4350	4489	
87	-34	0.00	69	0.00	4442	4429	Float deployment
88	-34	0.00	70	0.30	4535	4160	He/Trit Samples Wire in block
89	-34	0.00	71	0.00	4627	4605	
90	-34	0.10	71	59.80	4718	4771	Reterminate wire

91	-33	35.00	72	50.00	4809	4233	Float deployment Snap on wire-kink
92	-33	10.00	73	40.00	4899	4166	
93	-32	45.00	74	30.00	4989	3668	He/Trit Samples
94	-32	20.00	75	20.00	5080	3350	
95	-31	55.00	76	10.00	5171	3199	
96	-31	20.30	77	19.30	5298	3009	Wind/Swell 31 h Position Revised
97	-31	7.70	77	44.40	5344	3183	Float deployment
98	-30	45.00	78	29.80	5427	3513	He/Trit Samples End of week 4
99	-30	22.40	79	15.30	5511	3706	Evade cyclone
100	-31	11.60	80	8.80	5636	3693	Float deployment
101	-31	12.00	81	1.41	5719	4171	
102	-31	12.00	81	54.02	5803	3688	
103	-31	12.00	83	12.00	5926	3907	Float deployment
104	-31	12.00	84	30.00	6050	3858	He/Trit Samples
105	-31	20.88	85	30.00	6146	3627	
106	-31	30.03	86	30.00	6242	3516	
107	-31	36.13	87	10.00	6307	2109	
108	-31	45.29	88	10.00	6403	2095	He/Trit Samples
109	-31	48.34	88	30.00	6435	2917	Float deployment
110	-31	52.91	89	0.00	6483	3305	
111	-31	57.49	89	30.00	6530	3709	
112	-32	2.07	90	0.00	6578	3887	
113	-32	10.00	90	52.00	6661	3772	Float deployment
114	-32	30.00	91	48.00	6756	4311	
115	-32	50.00	92	44.00	6851	4402	He/Trit Samples
116	-33	10.00	93	40.00	6946	4301	
117	-33	30.00	94	36.00	7040	4381	Float Cluster
118	-33	50.00	95	32.00	7134	4558	He/Trit Samples End of Week 5
119	-34	10.00	96	28.00	7227	4521	Wind delay 5h
120	-34	30.00	97	24.00	7321	4512	
121	-34	30.00	98	25.00	7414	4222	Float deployment
122	-34	30.00	99	26.00	7507	4591	
123	-34	30.00	100	27.00	7600	4337	He/Trit Samples
124	-34	30.00	101	28.00	7693	4255	
125	-34	30.00	102	29.00	7786	5343	Float deployment
126	-34	30.00	103	30.00	7879	5732	
127	-34	0.00	104	15.00	7968	5383	
128	-33	30.00	105	0.00	8057	5332	He/Trit Samples
129	-33	0.00	105	45.00	8146	5332	
130	-32	30.00	106	30.00	8235	4355	Float deployment Reterminate wire
131	-32	0.00	107	15.00	8325	5125	
132	-31	30.00	108	0.00	8415	5293	
133	-31	30.00	108	55.00	8502	5327	He/Trit Samples
134	-31	30.00	109	50.00	8589	5207	Float deployment
135	-31	30.00	110	45.00	8676	5100	



136	-31	30.00	111	19.00	8729	4924	End of Week 6
137	-31	30.00	112	14.00	8816	5444	Clearance delay7h
138	-31	30.00	113	9.00	8903	5199	Float deployment He/Trit Samples
139	-31	30.00	114	4.00	8990	4447	
140	-31	30.00	114	30.00	9031	3332	
141	-31	30.00	114	35.82	9040	2292	
142	-31	30.00	114	40.00	9047	1351	
143	-31	30.00	114	50.00	9063	622	
144	-31	30.00	114	56.00	9072	373	
145	-31	30.00	115	2.00	9081	172	
146	-31	30.00	115	25.00	9118	4	On deck 14Apr1600
Fre	-32	04.80	115	42.00	0		

mantle

## NARRATIVE

Most of the scientists arrived in Durban on Monday, 25 February, and spent Tuesday, Wednesday and Thursday setting up the ship for the long hydrographic cruise. Networking the laboratory computers was an initial holdup, but was accomplished by noontime on Wednesday. The remainder of setup went steadily. We had a Safety Briefing for all scientists on Thursday afternoon and we were basically ready to sail Friday morning. One of the scientists, however, was ill and required a doctor's appointment Friday morning so we set a sailing time for 1400. We actually left the pier at 1500 on 1 March 2002 and were out in open water by 1545. As usual, most of the scientists retired to their cabins to adjust and prepare for the station work ahead.

For this cruise, two changes were made to normal scientific manning for long hydrographic cruises. First, negotiations with UKORS and RVS resulted in taking 2 UKORS mechanical technicians rather than the standard 3 to operate the winches for continuous 24-hour hydrographic station work, and entraining one RVS deckman (P. Allison) to operate the winch for 8 hours each day. Second, an additional scientist was berthed in the hospital for the duration of the cruise. These two changes allowed us to accommodate 2 additional scientists beyond *Charles Darwin's* normal capacity to carry out the CFC (chlorofluorocarbon) measurement programme. We very much appreciate RVS and UKORS cooperation in making these changes possible.

We sailed directly across the Agulhas Current to a test station in deep water (3410 m) at 0430 on 2 March. Wire tension seemed abnormally high and investigation found that improper calibration coefficients were being used, likely due to a system reset when the winches were started up. Installing the correct coefficients reduced the wire tension to normal levels, confirming that we would be able to do stations to 5500 m depth as required across the section.

Following the test station, we proceeded northeastward to begin a hydrographic section across the Agulhas Current (stations 2 to 13) at 1500 on 2 March. On station 5, the winch would not work and required repair for about 4 hours. We finished the northern Agulhas section in shallow water (67 m) at 1100 on 4 March, and spent the remainder of the day steaming along the coast with the Agulhas Current in beautiful weather before beginning the southern Agulhas section (and the main hydrographic section) at 2100 on 4 March. On station 19, the winch stopped as the CTD was coming on deck and the package remained suspended above the deck for 3 hours while a fitting was rethreaded. On station 21, we took our first set of helium-tritium samples and after station 31 on 7 March we deployed our first Argo float. By the end of one week at sea we had accomplished 33 hydrographic stations.

Winds were persistently out of the east at about 20 to 25 knots, hampering our steaming eastward and sometimes forcing us to sample the rosette while hove to. The problem seemed to be related to Hurricane Hary travelling slowly southeastward from the coast of Madagascar. While our progress was slow, Brian King compared the EM log speed used by the Bridge with the GPS speed over ground for between-station steaming and found that the EM log displayed 1 knot faster than the actual ship speed. Because we feared that the Bridge Officers were aiming for a 10-knot EM log speed and blaming the 8.5 knot true speed on wind and swell, we decided to change the calibration coefficients for the EM log to reflect true speed. Nice weather set in following the change in coefficients, as Hurricane Hary decayed and moved away, but agreeably the EM log speed now matched the GPS speed over ground. By the end of Week 2 we had accomplished 58 stations.

On station 59, the CTD signal ceased on the way down at 300m depth, always a scary moment. We brought the package back on board and found that the electrical connection at the wire termination had failed, so the wire was reterminated. Again at station 61, the CTD signal stopped at 550m on the way up. This time the problem was a fuse in the deck unit, most likely a power surge on the ship had blown the fuse. For station 62 we changed from the SOC Broadband LADCP to the SIO Broadband LADCP and, being happy with the SIO instrument performance, we continued with the SIO instrument for the remainder of the cruise. For these stations over the Southwest Indian Ridge, Elaine McDonagh had planned out station positions to be in the valleys between the series of mini-ridges based on the Smith and Sandwell bathymetry. As we steamed between stations over the mini-ridges that extended up to 2000 m depth, we were impressed that each of the planned station positions was indeed in the deepest part of the valleys at about 5000 m. We had generally good weather from 14 to 22 March.

For 23 March we planned a barbecue on deck in the evening to mark the temporal mid-point of the cruise. As the barbecue started the rain began. Stuart Cunningham was heard to comment that it was perfectly acceptable Scottish barbecue weather, but spirits were dampened. The weather continued to deteriorate so we began to sample while hove to. There was a terrific roll in the early morning hours of 25 March followed by a terrific rain storm at 0600. Weather continued to be marginal but we pressed ahead with stations until 27 March at 0700 when the Captain decided it was too rough to start station 96. After 30 hours of steaming slowly into the weather, we set out for the next station position which started at 1500 on 28 March. We then went back westward 25 miles to do another station to help fill in the gap. As a consequence there is a sizeable separation between stations 95 and 96 and a small separation between 96 and 97. Stations 98 and 99 were accomplished in difficult wind and swell conditions. Before station 100, the Captain decided we must run southeastward to get away from tropical cyclone Ikeda. We had been following Ikeda on weather maps and it had been menacing us for nearly a week. It was a large system drawing in air from the

east so the winds had been strongly against us. It appeared to wait for us at 20°S, 80°E and as we approached 80°E it moved south toward us. We diverted south then southeast as it circled around behind us and began to chase us.

As a result of avoiding Ikeda, we modified the section to head southeastward a bit earlier than planned. Wind and swell remained difficult for stations 100, 101, 102 and 103 and steaming between stations was slow as Ikeda passed by us and dissipated. At the start of station 103, a kink in the wire was noticed and retermination was needed. Seriously worried now whether there would be enough time to finish the section into Australia, we opted to eliminate a station while we were reterminating. As a result there are larger than normal separations between stations 102 and 103 and between 103 and 104. Finally at station 105 on 1 April, Easter Monday, the weather calmed and we began to work steadily for the first time in 10 days. At this point we estimated that we had just enough time to finish the section if there were no more problems with equipment or weather. On 5 April, we deployed a "cluster" of 4 floats near 95°E to study their dispersion over horizontal separations of 8 to 59 km. There was a freak squall during recovery of the CTD on the morning of 5 April that cut out the power to the bow thruster. Otherwise, for most of the remainder of the cruise, the wind came around behind us so that our steaming time between stations shortened considerably and we actually stored up some hours of time, enough to reterminate the wire after station 130 and to cover the 7-hour delay due to Australian clearance problems.

Slow progress due to adverse weather coloured the first 4 weeks of the cruise. We had not expected such adverse winds crossing the subtropical south Indian Ocean in late austral summer and I had never seen it rain so much at sea. Melanie Witt had come on the cruise hoping to fill a few small jars with rainwater and she posted a request in the Main Lab to awaken her if it rained. After being constantly awakened and filling all available containers by mid cruise, she removed the request. We were perhaps unlucky to encounter 2 tropical cyclones in Hary and Ikeda, neither of which hit us with much force but each of which created adverse winds for a week to ten days which slowed our progress.

About 1 April when we were about as far from land as possible, one of the CO<sub>2</sub> chemists became ill with first an earache (and a constant headache), then a sore throat, then a swollen left cheek. Initially she used eardrops and aspirin. After several days of worsening pain, the Captain put her on antibiotics and telephoned for medical advice. By 7 April, her condition seemed to stabilise and she started to work for a few hours each day. She was able to help with the CO<sub>2</sub> analysis (but not to sample on deck) but still complained of constant headache. When we docked in Fremantle, she went to the doctor for a diagnosis, which was that she had somehow contracted shingles out at sea. There was really no cure other than antibiotics and time, so the doctor prescribed antibiotics and patience pills for her subsequent holiday in Australia. Thus, the second major issue was a serious

illness for one of the scientists over the last two weeks of the cruise. The scientific party stepped forward to do the necessary CO<sub>2</sub> work, so there was no effect on the measurement programme. But the concern for her health and the worry about what we could do about it when we were so far from any port were all-consuming for about 10 days.

The final problem surprisingly was Australian diplomatic clearance to take stations within 200 miles of the coast of Australia. In planning the cruise we had expected such clearance to be a formality given the historically friendly relations between the United Kingdom and Australia. But in early March after departing Durban, the Captain mentioned that we did not yet have Australian clearance and in fact the clearance request had been 'lost' so that only in March had it been sent to Australia for consideration. Easter holidays from 24 March to 7 April of course slowed progress on the clearance, so that about 5 April I began emailing Australian colleagues for help with the clearance request while SOC called the Foreign Office in London each day. At noontime on Friday, 12 April, we finished our last planned station outside the 200-mile Australian territorial waters and began our wait for clearance. Because it was already Friday afternoon and we did not expect much diplomatic activity over the weekend before docking on Monday, I made a contingency plan to connect our section to a line of WOCE stations into the Australian coast as a way of creating a coast-to-coast transindian section for post-cruise analysis. We started this station plan late Friday afternoon (1600 local time) when it was already 1900 hours in Canberra where permission was being sought. Spirits around the ship were extremely glum: after 6 weeks at sea and 136 stations, it appeared that we would have no clearance to finish the last 10 stations before docking in Fremantle on Monday morning. Then at 1630 the Captain took a telephone call to say that clearance had been granted. We abandoned the contingency plan, recovered the CTD package and steamed off to do the final 10 stations. In 10 minutes the entire ship's party went from desolation to jubilation.

We finished the final hydrographic station at 1600 on 14 April, with just about 12 hours to spare. We proceeded offshore and then alongshore to do a ground-track calibration for the shipboard ADCP and then proceeded to Fremantle to tie up at the pier by 0800 on Monday, 15 April. The equipment was rapidly dismantled and packed away in shipping containers or in the hold for a subsequent cruise. By 1600, nearly all the scientific party had left the ship and only a short re-visit by King and Bryden was required on 16 April to finalise the packing and shipping.

With completion of 146 stations over 46 days, worries about weather, illness and diplomatic clearance faded quickly. All of the equipment had worked extremely well; we had complete data sets for all components of the planned hydrographic section; and the scientific and ship's party had worked harmoniously for nearly 7 weeks toward achieving the scientific and technical objectives of the cruise.

H. L. Bryden

## CTD DATA PROCESSING AND CALIBRATION

### CTD Package

The CTD package consists of a frame on which the CTD, fluorometer, altimeter, LADCP's, battery packs and rosette system with 24 10-litre water samplers. The package also has 500 kg of weight strapped to the frame to improve its descent.

### Instruments

A total of 146 CTD casts were undertaken on the cruise. The initial package configuration was as follows:

Sea-Bird 9/11 *plus* CTD system  
 24 by 10L NOAA/PMEL CFC-Free water samplers  
 Sea-Bird 43B Oxygen sensor  
 Benthos PSA-916T Altimeter  
 10KHz beacon  
 SOC RDI Broadband 150 KHz LADCP & battery pack  
 Upward-Looking RDI Workhorse 300 KHz LADCP  
 Downward-Looking RDI Workhorse 300 KHz LADCP  
 Battery pack for both Workhorse LADCP's

The Sea-Bird CTD configuration was as follows:

SBE 9 *plus* Underwater unit s/n 09P-19817-0528  
 Frequency 0—SBE 3P Temperature sensor s/n 03P-4107 (primary)  
 Frequency 1—SBE 4C Conductivity sensor s/n 03P-2573 (primary)  
 Frequency 2—Digiquartz temperature compensated pressure sensor s/n 73299  
 Frequency 3—SBE 3P Temperature sensor s/n 03P-4103 (secondary)  
 Frequency 4—SBE 4C Conductivity sensor s/n 03P-2580 (secondary)  
 SBE 5T submersible pump s/n 05T-3002  
 SBE 5T submersible pump s/n 05T-3195  
 SBE 32 Carousel 24 position pylon s/n 32-24680-0344  
 SBE 11 *plus* deck unit s/n 11P-19817-0495

The auxiliary A/D output channels were configured for casts 001 through 146 as follows:

V0---SBE 43B Oxygen s/n 43B-0076

V3--- Benthos PSA-916T Altimeter s/n 874

After cast 013, Chelsea MKIII Aquatracka Fluorometer s/n 088243 was installed in V4. The cable was found to be defective and the fluorometer was removed for casts 022 through 034 whilst a replacement cable was spliced. The fluorometer was re-installed for casts 035 onwards.

### **Deployment Procedure**

The package is lifted by the winch from the starboard deck with guidance ropes to keep the package from swinging. As the winch moves the package outboard and lowers it into the water, the ropes are retrieved. Because the SeaBird pumps start between 30 seconds and 1 minute after the conductivity rises from zero, the package is initially lowered to 5 m depth and held for 1 minute to allow the pumps to start. The package is then raised to the surface and then the station begins as the package descends. On several stations when there was significant ship roll as CTD was deployed and it was not considered safe to hold the package at 5 m depth, the package was sent immediately down. This resulted in lost or contaminated data in the top 20m while the pumps switched on during these stations. Therefore, the preferred deployment procedure should always include a 1 minute wait at a few meters depth and then a return to near surface before beginning the downcast.

### **Data Logging Setup**

The signal from the SBE 9+ underwater unit is fed up the wire to the SBE 11+ deck unit and then to a PC with SBE software where the data is displayed and recorded to hard disk. For security of the basic data series, the acquisition PC is isolated from the shipboard computer network. After completing the station, the station data is put on a Zip Disk and carried to the processing system computer which is part of the shipboard computer network

### **CTD Data Processing**

CTD data processing is now split between two software packages: Sea-Bird's proprietary software SEASOFT and the traditional PSTAR. Sea-Bird CTD's are new to UKORS and we describe in detail the Sea-Bird processing path and its interface to PSTAR.

## Sea-Bird

Raw CTD data are returned up the seacable, translated by the deck unit and displayed as calibrated data in real time on dual logging PC's.

1. On completion of the CTD station copy the four CTD files to a zip disk. The files have the extensions: *ctdionnn*.BL, .CON, .HDR, .dat. File formats are described in Sea-Bird (2001b). Briefly, BL is created when a bottle fire confirmation is received, and contains bottle sequence number, position, date, time and beginning and end scan numbers; CON, contains the instrument configuration and calibration coefficients; HDR, header recorded when acquiring real time data; dat is the raw binary CTD data.
2. sneakernet CTD files on zip disk to processing PC. Put files in a sub folder of your cruise folder e.g. C:\CD139\data
3. Install the latest version of the Seabird-win32 processing software in the directory C:\CD139. If you don't have a copy of this software it may be found on the PC or can be downloaded prior to the cruise from the Sea-Bird www site. Sea-Bird processing routines for windows can be recognised from their name format, which appends "W" to each exe module. E.g. DatCnvW.exe
4. The next step is to process the first CTD station by hand, storing parameters in a .psu file. We can then create a batch processing routine for all subsequent stations based on these psu files. Run the following processing modules. This sequence below is recommended by Sea-Bird as the standard processing of SBE 9/11 CTD data with a SBE-43 oxygen sensor.

### i. Data Conversion (DatCnv)

Converts raw data to calibrated data. Using the processing form, click the File tab. Make sure to select the station stored in C:\CD139\data and tick the box to match file name to configuration file. Write output file to the same directory. Now click the Data Setup tab. Tick process to end of file, scans to skip 0, output format: binary. Convert data from: upcast and downcast. Create: both bottle and data file. Source of scan range data Bottle log (.BL) file. Scan range offset 0, scan range duration 0.001. These last parameters ensure that the .ros file contains a single scan of all the CTD variables including the time of that scan at each bottle fire. Subsequently in PSTAR, we will merge a 10s average CTD profile onto this data to create the firing file for CTD versus bottle calibration. Now select output variables (Table C1).



Table C1: CTD variables calibrated and output from SEASOFT module DatCnv

Parameter	Unit
Pressure, digiquartz	dbar
Temperature	ITS-90, degC
Conductivity	mS/cm
Temperature2	ITS-90, degC
Conductivity2	mS/cm
Pressure temperature	degC
Altimeter	m
Oxygen, SBE 43	μmol/kg
Temperature difference (2-1)	ITS-90, degC
Time, Elapsed	seconds
Fluorimeter	μg/l

## ii. AlignCTD

Can be used to advance or retard any of the data streams to minimise spiking or hysteresis. To minimise oxygen hysteresis below 1000 dbar we advance oxygen relative to pressure by five seconds. For the 9/11 CTD, conductivity must be advanced relative to pressure; the default is to advance conductivity by 1.75 scans. This is done in hardware by the deck unit for both primary and secondary conductivity.

## iii. WildEdit

The SBE manual suggests this should not be required for 9/11 CTD systems but give it as part of the standard processing and so we have included this module without checks of its results. Standard deviations for pass one and two are 2 and 10 respectively, applied to 500 scans/block and excluding scans marked bad for all variables.

## iv. CellTM

Uses a recursive filter to remove conductivity cell thermal mass effects (Lueck (1990), Lueck and Pickelo (1990)) from the measured conductivity. In areas of steep temperature gradient the thermal mass correction is on the order 0.005 PSU, and is negligible elsewhere. The algorithm used is:

$$dt=t(1)-t(-7) \quad (1)$$

$$c(t)tm = -1 \times b \times ctm(t-1) + a \times dcdt \times dt \quad (2)$$

$$C_{corr} = C + ctm \quad (3)$$

where

$$a=2\alpha/(\text{sample interval}\times\beta+2)$$

$$b=1-(2a/\alpha)$$

$$dcdt=0.1\times(1+0.006\times(T-20))$$

Typical values are  $\alpha=0.03$  and  $1/\beta=7.0$  for a SBE 9/11 plus TC ducted conductivity cell (3000rpm pump).

#### v. Filter

Low pass filter pressure,  $\tau=0.15s$

#### vi. RosSum

Writes out a summary of the bottle file .BL using the .ros file as input.

#### vii. Trans

Finally, create an ASCII version of the .CNV file.

### Batch Processing

Having run through the SBE processing and set the required parameters in each .psu file (one psu file per programme), a DOS batch script can be used to automatically complete this processing on subsequent stations (assuming the instrument setup remains unchanged). The file below (called sbeproc.bat) should be placed in the CD139 folder.

File:sbeproc.bat

```
DatCnv /cc:\CD139\data\ctdio%1.con /ic:\cd139\data\ctdio%1.dat /oc:\cd139\data /fctdio%1.cnv /pc:\CD139\DatCnv.psu
AlignCTD /ic:\cd139\data\ctdio%1.cnv /oc:\cd139\data /fctdio%1.cnv /pc:\CD139\AlignCTD.psu
WildEdit /ic:\cd139\data\ctdio%1.cnv /oc:\cd139\data /fctdio%1.cnv /pc:\CD139\WildEdit.psu
CellTM /ic:\cd139\data\ctdio%1.cnv /oc:\cd139\data /fctdio%1.cnv /pc:\CD139\CellTM.psu
Filter /ic:\cd139\data\ctdio%1.cnv /oc:\cd139\data /fctdio%1.cnv /pc:\CD139\Filter.psu
RosSum /cc:\cd139\data\ctdio%1.con /ic:\cd139\data\ctdio%1.ros /oc:\cd139\data /fctdio%1.btl /pc:\CD139\RosSum.psu
Trans /ic:\cd139\data\ctdio%1.cnv /oc:\cd139\data /fctdio%1.cnv /pc:\CD139\Trans.psu
```

This DOS batch file must be executed from a DOS window, and is the first argument to a SBE programme called *sbebatch*. In a DOS window, C:\CD139>sbebatch sbeproc.bat *nnn*. Station number is the argument %1 to sbeproc.bat.

## CTD Sensor Calibrations

In DatCnv the following calibration equations convert raw sensor frequencies to calibrated data.

Temperature

$$T_{cal}(ITS - 90)^{\circ}C = 1/\left\{g + h\left[l_n\left(\frac{f}{f_0}\right)\right] + i\left[l_n^2\left(\frac{f}{f_0}\right)\right] + j\left[l_n^3\left(\frac{f}{f_0}\right)\right]\right\} - 273.15 \quad (4)$$

where  $l_n$  is the natural log function,  $f$  is the output frequency in Hz,  $f_0 = 1000$  is an arbitrary scaling used for computational efficiency. Throughout this report all temperatures and calibration equations are given on the ITS-90 temperature scale. For equation of state calculations temperatures in ITS-90 are converted to ITS-68 using Saunders (1990),

$$T_{68} = 1.00024 \times T_{90} \quad (5)$$

The temperature calibrations were performed on the 4<sup>th</sup> of December and 2<sup>nd</sup> of November 2001 for the primary and secondary sensors respectively. Fitted temperature residuals were less than  $\pm 0.00007^{\circ}C$  for both sensors. The drift in temperature since the last calibrations (March 2001) was  $+0.00095^{\circ}C/year$  for the primary and  $-0.00004^{\circ}C/year$  for the secondary. See Table C2 for the calibration coefficients  $g$ ,  $h$ ,  $i$  &  $j$ .

Table C2: Temperature sensor calibration coefficients

Coefficient	Primary	Secondary
$g$	$4.40385186 \times 10^{-3}$	$4.42352698 \times 10^{-3}$
$h$	$6.49254747 \times 10^{-4}$	$6.47980623 \times 10^{-4}$
$i$	$2.35916338 \times 10^{-5}$	$2.36589809 \times 10^{-5}$
$j$	$2.12472851 \times 10^{-6}$	$2.16776478 \times 10^{-6}$

Conductivity

The conductivity sensors are calibrated over a range of 0 to 60 mS/cm using natural seawater; a water sample at each point is compared to IAPSO standard seawater using a Guildline AutoSal. The calibration equation is,

$$C(S/m) = \frac{g + hf^2 + if^3 + jf^4}{10[1 + \delta t + \epsilon p]} \quad (6)$$

where  $f$  is the instrument frequency (KHz),  $t$  is temperature ( $^{\circ}\text{C}$ ),  $p$  is pressure (db),  $\delta = -9.57 \times 10^{-8}$  is the bulk compressibility and  $\varepsilon = 3.25 \times 10^{-6}$  is the thermal coefficient of expansion of the borosilicate cell.

The primary and secondary conductivity cells were calibrated on the 30<sup>th</sup> and 2<sup>nd</sup> of November 2001 respectively. Conductivity residuals were all less than  $\pm 0.00003$  S/m in a seven point calibration. Drift since last calibration (6<sup>th</sup> and 20<sup>th</sup> March 2001) is 0.00000 psu/month for the primary and  $-0.00120$  psu/month for the secondary. Calibration coefficients are given in Table C3.

Table C3: Conductivity calibration coefficients

<b>Coefficient</b>	<b>Primary</b> (s/n 4107)	<b>Secondary</b> (s/n 4103)
g	$-1.05163057 \times 10^1$	$-1.04988214 \times 10^1$
h	$1.63468814 \times 10^0$	$1.54363454 \times 10^0$
i	$-1.02002185 \times 10^{-4}$	$2.34998282 \times 10^{-4}$
j	$1.59143440 \times 10^{-4}$	$7.50542098 \times 10^{-4}$

#### Pressure

Pressure is measured by a DIGIQUARTZ 410K-105 pressure transducer with quartz crystal pressure sensing and thermal compensation. Pressure is calibrated from,

$$P = C \left( 1 - \frac{T_0^2}{T^2} \right) \left( 1 - D \left( 1 - \frac{T_0^2}{T^2} \right) \right) \quad (7)$$

where  $T$  is pressure period ( $\mu\text{s}$ ).  $C, D, T_0$  are given by,

$$C = C_1 + C_2 U + C_3 U^2 \quad (8)$$

$$D = D_1 + D_2 U \quad (9)$$

$$T_0 = T_1 + T_2 U + T_3 U^2 + T_4 U^3 + T_5 U^4 \quad (10)$$

where  $U$  is temperature ( $^{\circ}\text{C}$ ) and the calibration coefficients are given in Table C4.

Table C4: Pressure sensor calibration coefficients.

<b>Coefficient</b>	
C1	$-5.087539 \times 10^{-4}$
C2	$-2.199664 \times 10^2$
C3	$1.589010 \times 10^{-2}$
D1	$3.721700 \times 10^{-2}$
D2	0
T1	$3.011152 \times 10^1$
T2	$-2.857091 \times 10^{-4}$
T3	$4.528990 \times 10^{-6}$
T4	$-5.48500 \times 10^{-11}$
T5	0

### CTD Conductivity Calibration using Bottle Conductivities

The Sea-Bird conductivity sensor usually drifts by changing the slope of the conductivity calibration (referred to by Sea-Bird as the span), and changes are typically toward lower conductivity readings with time. Offset error in conductivity is normally due to electronics drift, and is usually less than  $\pm 0.001$  mS/cm/year. Offsets greater than  $\pm 0.002$  mS/cm are symptomatic of sensor malfunction. Sea-Bird recommends that drift corrections to conductivity be made by assuming no offset error, unless there is strong evidence to the contrary Sea-Bird (2001a).

Therefore, compute,

$$K = \langle C_{\text{bot}} / C_{\text{ctd}} \rangle \quad (11)$$

where  $C_{\text{bot}}$  is bottle conductivity = Fn(upcast press, upcast temp, botsal) and  $C_{\text{ctd}}$  is upcast CTD conductivity at the time of the bottle sample and  $\langle \rangle$  denotes the station average. The corrected CTD conductivity is given by,

$$C_{\text{ctdcorr}} = KC_{\text{ctd}} \quad (12)$$

Bottle samples are excluded where they are obviously bad and rejected data mainly occur in upper ocean.

## CTD Oxygen Calibration

The Sea-Bird dissolved oxygen sensor (SBE43) is a Clark membrane polarographic oxygen detector. This sensor is similar in principle to the sensors we have used with the Neil Brown CTD, but has been redesigned with improved materials and electronics: the principal improvements are the elimination of hysteresis in the top 1000 m, continuous polarization which eliminates the wait time for stabilization after power up and coupling to a pumped system so that the effects of flow rate variation are removed. The sensor and its operating principles are described in Sea-Bird Application note no. 64 and the product specification sheet for the sensor (both available on the Sea-Bird www site).

### i. Sensor calibration

Voltage output in the range 0 to +5 volts is converted to oxygen concentration using a modified version of the algorithm by Owens and Millard (1985),

$$O_2 = \left( S_{oc} \times \left( (v + offset) + \left( \tau \times \frac{doc}{dT} \right) \right) + B_{oc} \times e^{-0.03T} \right) \times e^{(T_{corr} \times T + P_{corr} \times p)} \times O_{sat}(T, S) \quad (13)$$

Where,  $O_2$  is dissolved oxygen concentration (in the Sea-Bird routine datcnvW oxygen units may be specified – choose  $\mu\text{mol/kg}$ ),  $T$  is water temperature ( $^{\circ}\text{C}$ ),  $p$  is pressure (dbar),  $S$  is salinity (psu),  $v$  is temperature compensated oxygen current ( $\mu\text{amps}$ ),  $doc/dT$  is slope of oxygen current ( $\mu\text{amps/sec}$ ),  $S_{oc}$  is the oxygen current slope,  $B_{oc}$  is oxygen current bias,  $T_{corr}$  is residual temperature correction factor for membrane permeability,  $offset$  is the voltage produced for zero current,  $P_{corr}$  is the pressure correction factor for membrane permeability,  $\tau$  is the oxygen sensor response time and

$$O_{sat}(T, S) = \exp \left( \begin{array}{l} -173.4292 + 249.6339 \times \left( \frac{100}{T} \right) + 143.3483 \times \ln \left( \frac{100}{T} \right) + \\ S \times \left( -0.033096 + 0.014259 \times \left( \frac{100}{T} \right) - 0.00170 \times \left( \frac{T}{100} \right)^2 \right) \end{array} \right) \quad (14)$$

is oxygen saturation Weiss (1970). The calibration coefficients are given in Table C5.

Table C5: Oxygen calibration coefficients for SBE43 dissolved oxygen sensor s/n 0076

Calibration Date	17 September 2001
Soc	0.36960
Boc	0.0212
Offset	-0.6308
Tcor	0.0020
Pcor	0.000134
$\tau$	0.0

## ii. Reconciliation of CTD to bottle oxygens

Bottle oxygens in  $\mu\text{mol/l}$  are first converted to units of  $\mu\text{mol/kg}$  and then the differences to CTD oxygens are calculated. The CTD oxygens are taken from the downcast because of hysteresis below 1000 dbar. Downcast datacycles were found by matching potential temperature on the upcast at each bottle stop to a potential temperature on the downcast. Bottle-CTD oxygen residuals from the first 91 stations gave a mean curve versus depth (Table C6). This correction was merged on pressure with the CTD data and oxycorr added to CTD oxygen. For stations after 91 the oxygen correction residual with pressure changed rapidly over groups of ten or so stations. The reasons for this are not clear but may be due to contamination or ageing of the oxygen sensor.

For the first 91 stations the oxycorr values are constant between 125 and 1000 dbar, increase linearly to 4500 dbar, and are constant below 4500 dbar (though not well determined because of rather few samples). This is similar to the specification of the sensor for no hysteresis at pressures less than 1000 dbar. A subtle effect shallower than 125 dbar is evident in the oxycorr values. Clearly, the oxycorr values increase towards the surface, from 4.9 to 7.1  $\mu\text{mol/kg}$  (near surface oxygen is about 250  $\mu\text{mol/kg}$ ). The near surface increase in oxycorr is not explained by any systematic differences between the down and up CTD oxygen profiles.

Could the increase in oxycorr in the top 100dbar be explained by a problem with the bottle oxygens? We examined the percent saturation of the bottle oxygen values (Table C7). The bottle data

Table C6: oxycorr versus pressure, where oxycorr=<bto-uo> is the average of the oxygen residuals in the pressure interval for stations in the interval m-n.

1-91		95-117		118-127		128-135		136-146	
press	oxycorr	press	oxycorr	press	oxycorr	press	oxycorr	press	oxycorr
dbar	μmol/kg	dbar	μmol/kg	dbar	μmol/kg	dbar	μmol/kg	dbar	μmol/kg
-10	7.1	0	21.3	-10	27.8	-10	27.8	-10.0	28.3
0	7.1	25	21.3	25	27.8	25	27.8	25	28.3
25	7.1	75	20.8	75	29.5	75	29.5	75	27.3
75	6.2	125	20.3	125	27.1	125	27.1	125	26.2
125	4.9	175	20.1	175	26.9	175	26.9	175	26.0
175	4.7	250	17.7	250	26.7	250	26.7	250	23.9
240	4.4	350	17.9	350	25.1	350	25.1	350	24.1
340	4.1	450	17.6	450	23.8	450	23.8	450	23.9
440	4.2	550	17.5	550	23.1	550	23.1	550	21.4
540	4.3	650	17.4	650	23.1	650	23.1	650	18.3
640	4.3	750	17.5	750	23.1	750	23.1	750	18.0
740	4.3	850	16.3	850	21.0	850	21.0	850	15.1
840	4.3	950	15.6	950	18.7	950	18.7	950	15.3
940	4.3	1125	15.1	1125	17.2	1125	17.2	1125	12.7
1040	4.8	1375	13.2	1375	16.0	1375	16.0	1375	11.5
1250	5.9	1625	12.5	1625	13.5	1625	13.5	1625	13.8
1750	6.7	1875	13.3	1875	14.4	1875	14.4	1875	14.3
2250	7.9	2125	14.1	2125	15.1	2125	15.1	2125	14.1
2750	8.4	2375	14.7	2375	17.1	2375	17.1	2375	13.1
3250	8.8	2625	14.3	2625	16.9	2625	16.9	2625	15.1
3750	9.7	2875	14.9	2875	18.1	2875	18.1	2875	14.8
4250	10.6	3125	15.7	3125	17.8	3125	17.8	3125	15.2
4750	10.7	3375	15.7	3375	17.5	3375	17.5	3375	16.0
5250	10.5	3625	15.8	3625	17.0	3625	17.0	3625	16.0
5750	10.4	3875	15.6	3875	16.5	3875	16.5	3875	14.6
6000	10.4	4125	15.4	4125	16.8	4125	16.8	4125	15.1
		4375	15.0	4375	16.2	4375	16.2	4375	14.5
		4625	14.0	4625	17.6	4625	15.5	4625	16.5
		6000	14.0	4875	17.5	4875	14.7	4875	16.4
				6000	17.5	6000	14.0	6000	15.2



suggest that the water column is supersaturated at 52 dbar, decreasing toward 100% saturation at the surface and also decreasing in saturation below 52 dbar. The supersaturation at 52 dbar corresponds to a peak in fluorescence and is probably caused by phytoplankton producing oxygen at this depth. An identical analysis for CTD oxygen has about 3.2% less saturation at each depth than the values in Table C7. From this analysis of bottle oxygen saturations, we conclude that the bottle oxygens are probably accurate because it is expected that oxygen saturation is close to 100% near surface, and therefore the increase in oxycorr in the top 125 dbar is probably due to a reduction in the sensitivity of the CTD oxygen sensor near surface. These results have been passed to Sea-Bird and we await a response.

Table C7: Percent saturation of bottle oxygens (mean), where press is the average pressure of the nbot samples, sd is standard deviation of the mean and se is the standard error of the mean.

<b>press</b>	<b>nbot</b>	<b>mean %</b>	<b>sd</b>	<b>se</b>
11	95	1.004	0.014	0.001
42	21	1.008	0.016	0.003
52	30	1.013	0.016	0.003
77	22	0.982	0.035	0.007
100	32	0.927	0.052	0.009

After adding oxycorr to CTD oxygens, the residuals plotted against station number have a slowly changing low amplitude variation, which was removed as an offset on a station-by-station basis. This slow drift is broadly consistent with the sensor specification of 2% drift per 1000 hours of operation.

Figure C1 shows the distribution of oxygen residuals (bottle-CTD) versus bottle oxygen, station number and pressure. For points within  $\pm 2$  standard deviations of the mean the mean  $\pm$  standard deviation oxygen residuals is  $0.16 \pm 2.1 \mu\text{mol/kg}$ .

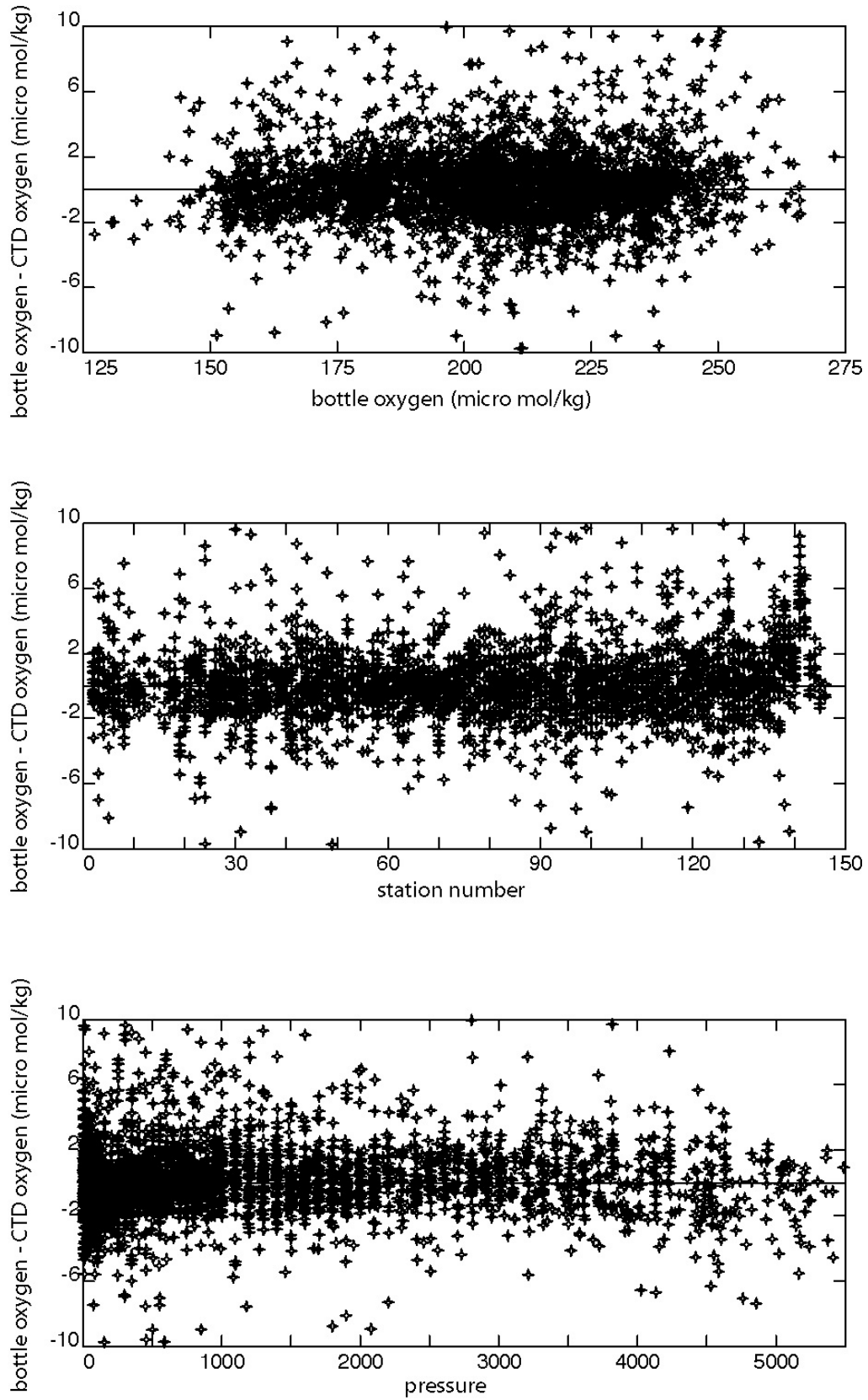


Figure C1: bottle-CTD oxygen versus i. bottle oxygen, ii. station number (limits are for  $-10 < (btO_2 - O_2) < 10$ ) and iii. Pressure.

## **Salinometry**

Salts were drawn for analysis from every bottle. These were analysed by salinometer, and usually a standard sea water was measured at the beginning of each analysis and then every twenty four samples thereafter. A timeseries of the standard seawater (SSW) conductivity ratio divided by the stated conductivity of the SSW plotted against station number shows changes in the values of the measured SSW. Note that the standardisation of the salinometer was adjusted at station 022 so the timeseries must be considered in two parts. If the SSW conductivity is constant within the batch, then variability of the conductivity ratio of the SSW is due to variations of the salinometer or to variations in operator method. Between stations 022 and 048 the measured SSW conductivity ratio is extremely stable, varying by less than 0.00001, equivalent to 0.0003 mS/cm at conductivity values around 32 mS/cm. If the salinometer is stable and the SSW varies sample to sample, then the variability of bottle conductivities will be apparent in the comparison of bottle-CTD conductivities if the CTD conductivity sensor is stable. We have compared the measured SSW values to the bottle-CTD conductivities and can see no evidence that the measured SSW conductivity variations are present. Either they are not present in the bottle-CTD conductivities or are swamped by the typical variability of bottle-CTD conductivities of about 0.002 mS/cm. The best we can conclude is that the measurement of conductivity by the salinometer and standardisation against SSW introduces a conductivity error of about 0.0003 mS/cm, which is much smaller than the error due to variability in the bottle-CTD conductivities.

## **Post Cruise CTD Sensor Calibrations**

The post cruise calibrations took place immediately after the cruise (Table C8) and we decided to implement corrections to the cruise data based on these calibrations. Pressure and temperature corrections are small and linear, and are a result of sensor changes either during the cruise or perhaps in transit. Here, we assume that changes occurred during the cruise and use the post-cruise calibrations to obtain the linear corrections to the cruise data. Conductivity residuals (bottle-CTD), were found to be quadratic with depth and linear with temperature. These were subsequently found to be due to an error in the calibration coefficients provided by SeaBird. After the post-cruise calibrations, dependent variables were recalculated.

Table C8: Timeline in days between pre and post cruise calibrations

<b>Event</b>	<b>Time</b> (days)
Pre-cruise calibrations	0
Cruise start	90
Cruise end	135
Post-cruise calibrations	157

### Pressure

Post-cruise the pressure sensor (s/n 73299) was tested against a stable reference pressure sensor on 8<sup>th</sup> May 2002: input pressures are generated using a Ruska model 5201 dead-weight tester, s/n 23330/380, and eleven calibration points were obtained between 0 and 7000 and back to 0 dbar. The pressure difference between pre and post cruise calibrations, is given by

$$P_{corr} = -0.78 + 0.99989 \times P_{CTD} \quad (15)$$

where  $P_{CTD}$  is the pressure measurements during the cruise using the pre-cruise calibrations and  $P_{corr}$  is corrected pressure. The standard deviation of pressure residuals corrected using (15) to the post-cruise calibration data is 0.1 dbar.

### Temperature

The post-cruise temperature calibration coefficients are given in Table C9. The average temperature change $\pm$ sd from pre to post cruise calibrations is  $0.91\pm 0.26$  m°C and  $0.13\pm 0.09$  m°C for the primary and secondary sensors respectively, such that both sensors now read cold and these corrections could be added to temperatures measured during the cruise. These changes were calculated by applying the pre-cruise calibration coefficients to the post-cruise CTD calibration data and taking the difference to the post cruise calibration bath temperatures.

The primary sensor has a much larger offset and sd than the secondary sensor. This prompted us to look at these residuals as a function of temperature. For the primary sensor, the CTD reads cold by  $0.66$  m°C at  $-1.5$  °C and cold by  $-1.25$  m°C at  $32.5$ °C, varying linearly between. Therefore, we corrected the cruise data using the following,

$$T_{corr} = 0.000569 + 1.00002214 \times T_{CTD} \quad (16)$$

where  $T_{CTD}$  is the primary temperature measured during the cruise and  $T_{corr}$  is corrected temperature. Secondary temperature has not been adjusted.

Table C9: Temperature sensor calibration coefficients for post-cruise calibrations on 07May2002

Coefficient	Primary (s/n 4107)	Secondary (s/n 4103)
g	$4.40361941 \times 10^{-3}$	$4.42341950 \times 10^{-3}$
h	$6.48783845 \times 10^{-4}$	$6.47681379 \times 10^{-4}$
i	$2.32699968 \times 10^{-5}$	$2.34539360 \times 10^{-5}$
j	$2.05383746 \times 10^{-6}$	$2.12200464 \times 10^{-6}$

### Conductivity

Calibrated bottle-CTD conductivity residuals show an exponential shape with depth. Below 1500 m the conductivity difference is constant. Between 1500m and 500m the conductivity difference increases by 0.001 mS/cm; shallower than 500 m the conductivity difference increases by 0.005 mS/cm. The bottle-CTD conductivity difference plotted against in situ temperature is linear; decreasing from 0.005 mS/cm at 25 °C to 0 mS/cm at 0 °C. Initially this was thought to be due to the vertical separation of the CTD and Niskin bottles in the CTD frame in the presence of large vertical conductivity gradients. However, this was incorrect and SeaBird after long and detailed inspection of our data and their calibration data discovered an egregious error in their calibration coefficients.

The CTD conductivity sensor is calibrated as follows. The sensor is immersed in a bath of seawater with an approximate salinity of 35 psu. The bath is heated from 0 to 35 °C and readings of conductivity from the CTD are noted at eight precisely measured temperatures. The bath salinity is measured by Autosal using samples drawn from the bath at each calibration point and the bath conductivity is back calculated using bath temperature and pressure. i.e.  $C_{bath} = fn(P, T_{T68}, S)_{bath}$  where  $S_{bath}$  is the bath salinity calculated from the conductivity ratio of water samples taken from the bath. The error made by Sea-Bird in calculating  $C_{bath}$  was using bath temperatures measured on the ITS-90 temperature scale and not converting them to ITS-68 temperatures and this error affects the calibration coefficients given in Table C3. The error in CTD conductivity  $C_{error}$  (Table C10) closely matches the error observed during the cruise ( $C_{btc} - C_{CTD}$ ), the mean±sd of  $C_{\Delta} = (C_{btc} - C_{CTD}) - C_{error}$  is  $-0.0004 \pm 0.0002$  mS/cm.

Confident that the error introduced in  $C_{CTD}$  during the cruise is correctly explained we corrected the CTD conductivities by,

$$C_{corr} = C_{CTD} - 0.000474 + 0.00025667 * T_{insitu}_{T90} \quad (17)$$

predicted from 2915 bottle samples taken during the cruise. The mean±sd of  $C_{btc} - C_{corr}$  is  $0.0000 \pm 0.0009$  mS/cm.

Table C10: Conductivity error  $C_{error} = C(P, T_{68}, S)_{bath} - C(P, T_{90}, S)_{bath}$  arising from T90 temperatures in the calculation of conductivity instead of T68 temperatures ( $C_{corr} = C_{CTD} + C_{error}$ ).  $C_{btc}$  is bottle conductivity and  $C_{CTD}$  is conductivity measured by the CTD during the cruise, predicted from 2915 bottle samples taken during the cruise  
 $(C_{btc} - C_{CTD}) = 0.00025667 * T_{insitu_{T90}} - 0.000474$ ,  $R^2 = 0.793$ .  $C_{\Delta} = (C_{btc} - C_{CTD}) - C_{error}$  is the residual CTD conductivity error after correction.

Bath temp	Bath temp	$C_{bath} = fn(P, T_{68}, S)_{bath}$	$C_{error}$	$C_{btc} - C_{CTD}$	$C_{\Delta}$
T90 (°C)	T68 (°C)	mS/cm	mS/cm	mS/cm	mS/cm
0.01	0.01	29.03603	0	-0.0005	-0.0005
2	2.00048	30.77615	0.00042	0.0000	-0.0004
5	5.00120	33.45538	0.00109	0.0008	-0.0003
10	10.0024	38.08971	0.00228	0.0021	-0.0002
20	20.0048	47.91804	0.00487	0.0047	-0.0002
24	24.00576	52.02918	0.00598	0.0057	-0.0003
30	30.00720	58.35696	0.00769	0.0072	-0.0005
35	35.00840	63.75694	0.00915	0.0085	-0.0006

### CTD Salinity Residuals

The distribution of bottle-CTD salinity versus bottle salinity, station number and pressure is given in Figure C2a, C2b and Table C11. The low scatter and small number of wild points is an

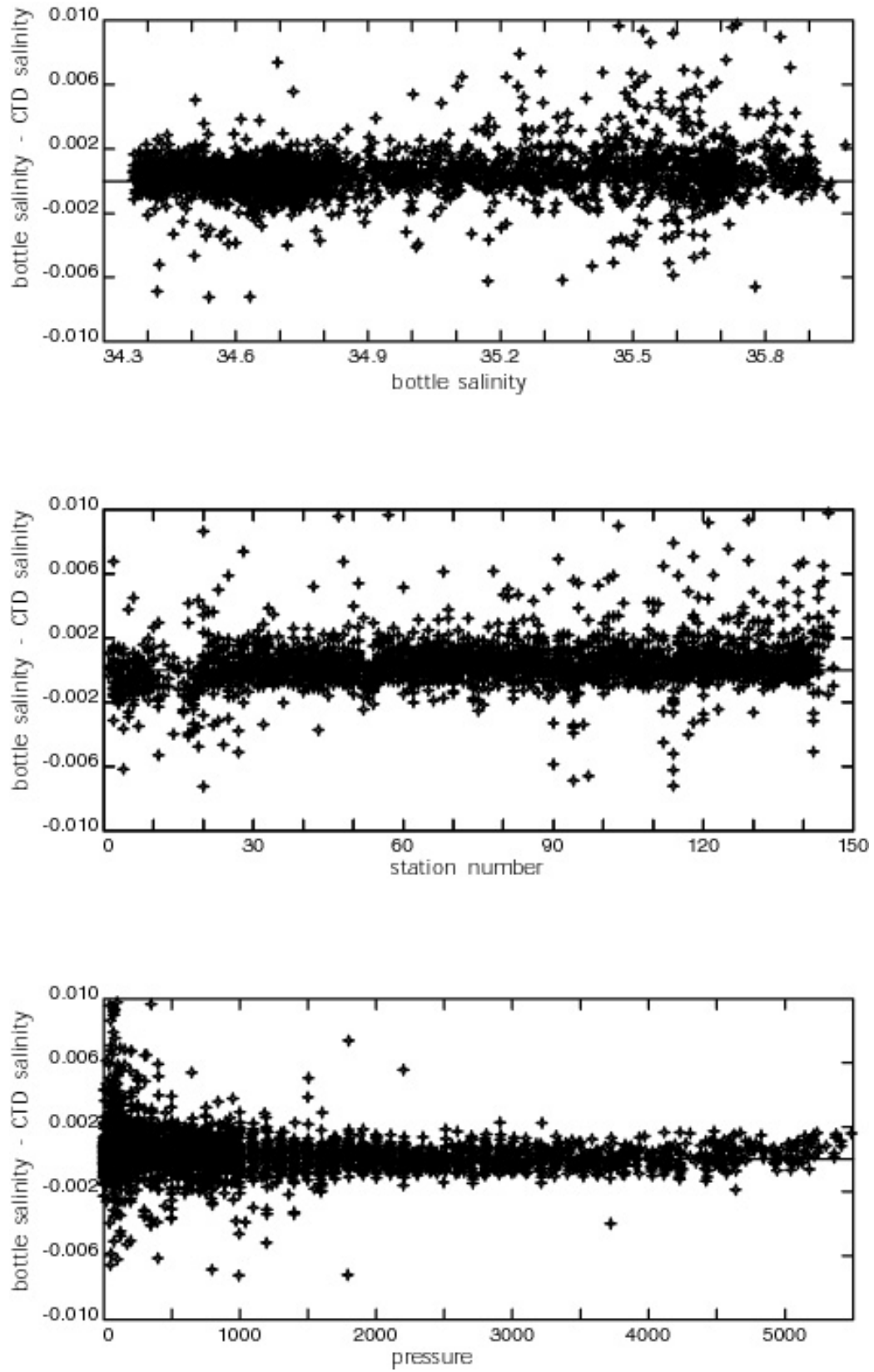


Figure C2a. bottle-CTD salinity versus i. bottle salinity, ii. station number (limits are for  $-0.014 < (\text{bts} - \text{s}) < 0.014$ ) and iii. Pressure.

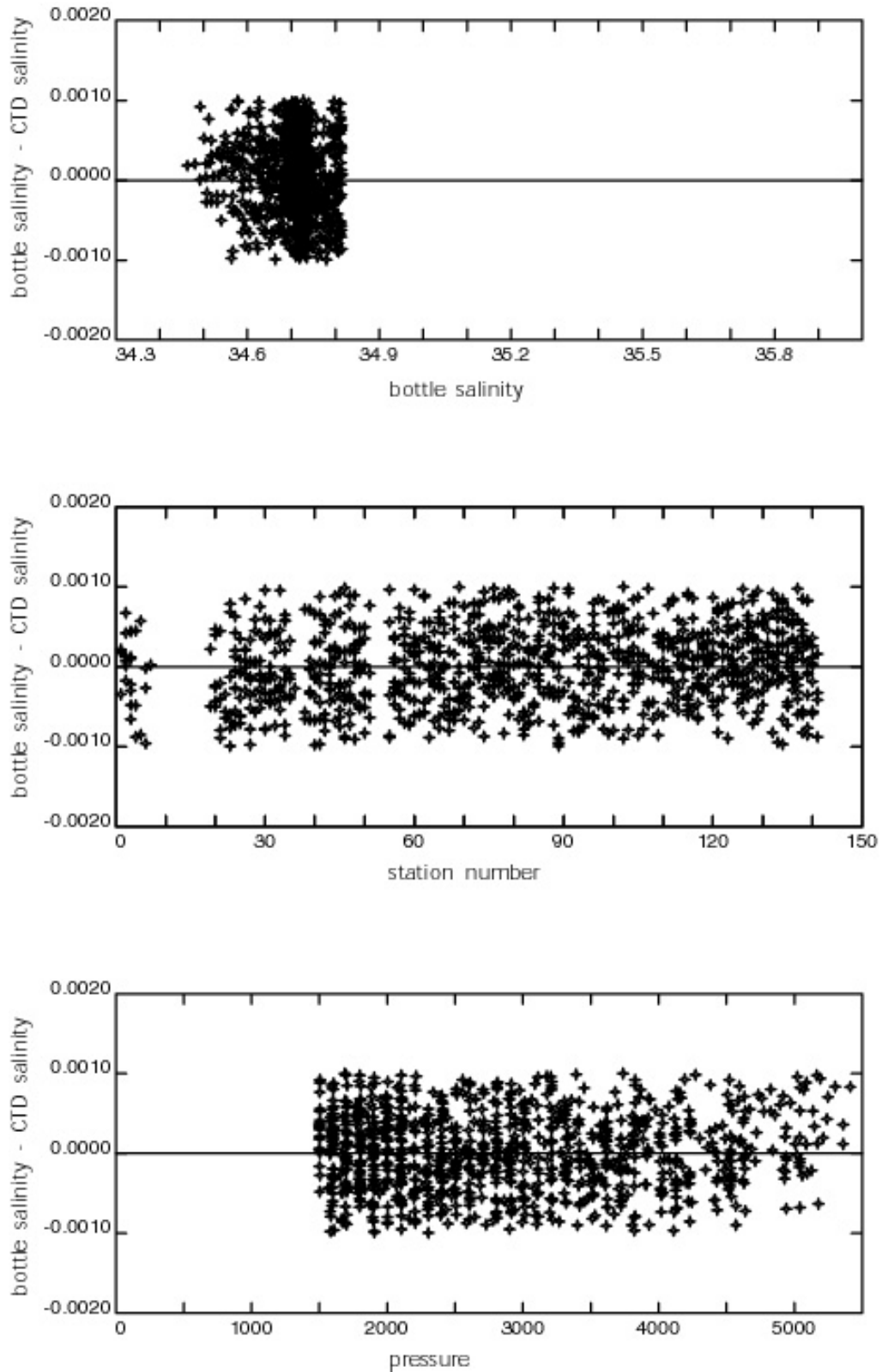


Figure C2b. bottle-CTD salinity (for  $P > 1500$  dbar) versus i. bottle salinity, ii. station number (limits are for  $-0.001 < (bts-s) < 0.001$ ) and iii. Pressure.



indicator of the care with which bottle salinity samples were drawn and analysed. There are no trends in residuals plotted against either bottle salinity or pressure, confirming that the final conductivity corrections were sensible.

Table C11: Bottle-CTD salinity residual means ( $\mu$ ) and standard deviations ( $\sigma$ ).  $n$  number of points in mean and % is percentage of points outside limits, limit is edit criteria applied to (bts-s) for removal of data outliers before mean is calculated.

$\mu$	$\sigma$	<b>n</b>	<b>%</b>	<b>Limits</b>
0.003	0.0013	3018/3100	2.7	$\pm 0.1, \pm 2\sigma, \pm 2\sigma$
0.001	0.0005	1093/1152	5.1	P>1500db, $\pm 0.1, \pm 2\sigma, \pm 2\sigma$
0.0000	0.0005	1016/1152	11.8	P>1500db, $\pm 0.1, \pm 0.001$

### CTD and Sample Processing Paths

#### Sample Path

The object of the sample processing path is to gather the disparate sample data into one PSTAR file.

#### Create ascii text sample files

On the mac "gusto" there is a folder called "samples", and within this folder there are subfolders, one per sample type (e.g. cbn, cfc, nut, oxy, sal, sur). Within each sample folder there is a blank excel file to receive the sample data. Save sample file as text (tab) delimited and with the name format *xxxionnn.txt* where *xxx* is the sample type and *nnn* is the file number e.g. *salio001.txt*.

#### Read ascii text files to UNIX and create PSTAR files

>*xxx.exec*, File in: *xxxionnn.txt* (from mac), File out: *xxxionnn.txt* (ASCII) & *xxxionnn.bot* (PSTAR)

#### Paste sample data into a master sample file

>*pasxxx*, File in: *xxxionnn.bot* is pasted into *samionnn*.

Notes: sur is the file for thermosalinograph salinity samples; each sample file on the mac contains variables sampnum, statnum and botlnum. However, these are only pasted to the master sample file through the sal path; the master sample file (one per station) is created as part of the CTD processing (CTD Path step 12). Use a tick sheet to keep track of which files have been processed and to which stage.

#### CTD Path

To obtain a fully calibrated 2db downcast CTD profile.

- 1 Transfer Sea-Bird CTD files from logging PC to processing PC (zip disk)

2. Sea-Bird processing. Process CTD data using Sea-Bird routines, as described in detail in the cruise report
3. **ftp** processed CTD data from PC to UNIX. PC ftp programme FTP Explorer allows UNIX disk to be mounted on PC, so files can be ftp'd by drag and drop.
4. **>ctd0**: Read in 24hz ascii Sea-Bird file and output to PSTAR. A header time is constructed from times within the Sea-Bird .cnv file. File in: CD139*nnn*.cnv, File out: *ctdionnn*.24hz
5. **>ctd1**: i. process 24hz data to 1hz (median despiked, average on time to 1hz, interpolate pressure to remove any absent data). ii. Average 1hz file to 10s for matching to bottle samples. iii. Note the datacycles in the 1hz file of start downcast, maximum pressure and end upcast. File in: *ctdionnn*.24hz, File out: *ctdionnn*.1hz & *ctdionnn*.10s.
6. **>ctd3**: standard plots of CTD 1hz data;  $\theta/s$ , deep  $\theta/s$  and  $O_2$ /pressure
7. **>fir0**: i. read Sea-Bird rosette firing file into PSTAR. ii. Merge firing file with 10s CTD file to produce file with the 10s averaged upcast CTD variables at the time of bottle firing. iii. Read in winch data using datapup. File in: CD139*nnn*.ros & *ctdionnn*.10s, File out: *firionnn* & *winionnn*.
8. **>sam0**: i. Create a blank sample file for station *nnn* from the master sample file. At the beginning of the cruise create a master sample file with all required variables set to absent. ii. paste firing file into sample file. File in: *sam.master* & *firionnn*, File out: *samionnn*.
9. **>position.exec**: i. creates a file with position at the three times from the *ctdionnn*.1hz file corresponding to the datacycles noted in step 5 at start down, pmax and end up. ii. user is given the choice of adding the position at the bottom of the downcast (nadir position) to the 1hz, 10s, fir, win and sam files. iii. Adds data cycles to *ctd2.exec* so that datacycles do not have to be entered by hand a second time when creating a *ctd2.db* file. File in: *ctdionnn*.1hz and 139gps01 (master gps navigation file), File out: *nnn.position* & *ctd2.exec*.
10. **>ctd2.exec**: runs **ctd2** but has a record of the datacycles at start down, pmax and end up from step 9. File in: *ctdionnn*.1hz, File out: *ctdionnn*.2db & *ctdionnn*.ctu (1 hz file for data cycles between start down and end up).
11. **>adddepth.exec**: add corrected echo sounding depth to the position file. File in: five minute averaged corrected depth, File out: *position.nnn*.
12. **>pbottle.exec**: warning this exec is a complete lash up – wouldn't trust it, but it seemed to work on CD139. In principle: match potemp at upcast bottle stops to downcast potemp and extract downcast oxygen to match to upcast bottles. Writes the downcast CTD oxygen into variable oxygen in the sam file. File in: *ctdionnn*.1hz & *samionnn*, File out: *pbt  
nnn*, *samionnn*.

13. **>sta.sum.exec**: Produces a summary file of ctd station positions, times, depths and bottles.  
File in: position.nnn & ctdionnn.1hz, File out: stn\_sum.ascii

### Calibration

The two execs below calculate calibration variables, and can be run as often as required on any number of stations as set by the user. The principle is that whenever a CTD conductivity or oxygen calibration is done you will want to run these execs to recompute residuals.

1. **>botcond.exec**: Calculate all derived variables required for CTD conductivity and oxygen calibration. The following variables are calculated: botcond=Fn(upcast temp, upcast press, botsal) where temp and press are upcast CTD primary variables, botcond/cond & botcond/cond2, btc-uc=botcond-cond, bts-us=botsal-salin, c2-c=cond2-cond and botoxyM( $\mu\text{mol/kg}$ )=botoxy( $\mu\text{mol/l}$ )/sigoxy(kg/l) where sigoxy is potential density relative to 0 dbar at the fixing temperature of the oxygen samples and finally calculate bto-uo=botoxyM( $\mu\text{mol/kg}$ )-oxygen(ctd downcast found by CTD path step 12,  $\mu\text{mol/kg}$ ). File in: samionnn, File out: samionnn.calib
2. **>sam.calib.append.exec**: i. Appends samionnn.calib files and creates some files where datacycles have been excluded using datpik on press>1500db and  $-0.01 < \text{btc-uc} < 0.01$ . These datpik limits were chosen to isolate deep bottles and to remove obvious outliers. The datpik files were then averaged using **pbins** to provide some statistical estimates of conductivity and oxygen residuals.

### CTD Conductivity

1. **>ctdcondcal.exec**: applies a conductivity correction  $C_{\text{ctdcorr}} = KC_{\text{ctd}}$  to the ctd.1hz file and reworks CTD processing to pass conductivity correction through to the sam file. Dependant variables, salin, potemp and sigma0 in the ctd.1hz file are also recalculated. The values of K must be entered in an array and the exec is set for processing multiple stations. File in: ctdionnn.1hz, File out: ctdionnn.10s, firionnn, samionnn, ctdcondcal.version (record of the version codes changed).
2. **>resid.plot.exec**: plots conductivity residuals with their means and standard deviations: (btc-uc) versus i. botcond, ii. press, iii. statnum and iv. K=botcond/cond versus statnum. Plots with all data cycles or datpiked data cycles are possible.

### CTD Oxygen

1. **>oxy.corr.exec**: applies an oxygen correction curve versus pressure to CTD oxygen in the .1hz file and the sam file. See cruise report for a discussion of oxygen calibration. File in:

ctdionnn.1hz & samionnn, oxy.correction, File out: ctdionnn.1hz & samionnn, oxy.corr.version.

2. >**oxy.corr2.exec**: applies a final station by station offset to oxygen. File in: ctdionnn.1hz & samionnn, oxy.correction File out: ctdionnn.1hz & samionnn, oxy.corr.version.
3. >**resid.oxy.plot.exec**: plots oxygen residuals with their means and standard deviations: (botoxyM-oxygen) versus i. pressure, ii. statnum.

#### Primary and secondary sensors

The UKORS Sea-Bird 911+ CTD's have separate dual conductivity and temperature sensors and these can be examined during the cruise for drift and/or jumps. A third independent measure would tell you which sensor had changed. Generally, only temperature is of relevance, as conductivity performance is monitored against standard seawater.

1. >**pbins.ct.exec**: uses pbins to produce some statistics of variables t2-t and c2-c. File in: sam.append.calib (see botcond.exec & sam.calib.append.exec)
2. > **ct.plot.exec**: plot t2-t and c2-c versus statnum.

#### Others

1. >**osat.exec**: uses a butchered version of oxygn3 to write out oxysat, and then calculates percentage saturations of bottle and CTD oxygens.
2. >**salinom.exec**: divides the measured SSW conductivities by the label conductivity.

#### Units

1 S/m = 10 mmho/cm = 10 mS/cm

#### References

- Lueck, R. G.** 1990 Thermal inertia of conductivity cells: theory. *Journal of Atmospheric and Oceanic Technology*, **7**, 741-755.
- Lueck, R. G. & Pickelo, J.** 1990 Thermal inertial of conductivity cells: observations with a Sea-Bird cell. *Journal of Atmospheric and. Oceanic Technology*, **7**, 756-786.
- Owens, W.B. & Millard, R.C.** 1985 A new algorithm for CTD oxygen calibration. *Journal of Physical Oceanography*, **15**, 621-631.

**Saunders, P.M.** 1990 The International Temperature Scale, *WOCE International Newsletter*, **10**, 10.

**Sea-Bird.** 2001a Computing temperature and conductivity slope and offset correction coefficients from laboratory calibrations and salinity bottle samples. Sea-Bird Electronics, Inc.

**Sea-Bird.** 2001b CTD data acquisition software, SEASOFT, version 4.249. Sea-Bird Electronics, Inc.

**Weiss, R.F.** 1970 The solubility of nitrogen, oxygen and argon in seawater. *Deep-Sea Research*, **17**, 721-735.

Stuart Cunningham and Jeff Benson

## **WATER SAMPLE SALINITY ANALYSIS**

### **Laboratory Set-up**

Two salinometers were set up in the constant temperature (CT) laboratory on *RRS Charles Darwin*. Both the JRD and UKORS salinometers were Guildline 8400B . Although both were set up, the JRD salinometer was the only one used during the cruise. Service and alignment of the JRD Autosal salinometer, s/n 60839, were performed just prior to the cruise. The temperature of the CT laboratory was set to 21 degrees and measurements of room temperature taken before the analysis of each crate indicate the temperature remained in the region 21 - 23°C. The salinometer water-bath was set to 24°C. No serious problems occurred with the salinometer . Only the peristaltic pump switch needed resoldering half way through the cruise. John Wynar performed the resoldering. Jeff Benson also repaired another peristaltic pump that needed a service.

### **Sampling and Analysis**

Water samples for analysis were drawn from each Niskin into 200ml glass sample bottles which were then sealed with clean, dry, disposable plastic stoppers and screw on caps. The neck of the sample bottle is dried prior to insertion of the cap. Samples were then taken into the CT laboratory to equilibrate to room temperature for 24 hours before analysis. During the cruise, samples were also drawn from the non-toxic supply for TSG calibration approximately every four hours. Matt Palmer, John Wynar, and Jeff Benson performed most analyses, with a few carried out by Louise Duncan. On one occasion an untrained scientist performed analysis and the resulting salinity values from stations 52-54 are dubious. Usually a standard seawater sample, batch series P140, was run immediately before and after a crate. Initially the standard reset dial on the autosal was set to 493 but was changed to 490 at station 29. For this reason the CTD salinity calibration had to be considered separately before and after this change. In total 18 replica samples were drawn providing a mean salinity difference of 0.0004 with standard deviation 0.0004.

### **Processing**

Following standard practise, the salinity values were obtained from the conductivity ratio measurements using an Excel spreadsheet, which corrects for offsets from standard readings. These results were transferred to Unix in the form of a tab-delimited ASCII file containing the variables `statnum`, `sampnum`, `botnum`, `botsala`, `botsalb` and `botsal`. No flag was used to indicate good and bad

salinity readings, as in previous cruises. Bottle salinity values were combined with CTD data in samio{num} files.

Correction to the Guildline ratio obtained from the standards throughout the cruise is shown in Figure S1. The corrections range from  $-0.00002$  to  $0.00013$ , or  $0.0004$  to  $0.0026$  Salinity Equivalent. Variability in the standards was very small (s.d.  $0.00001$ ) although a drift in standard readings can be seen over the cruise.

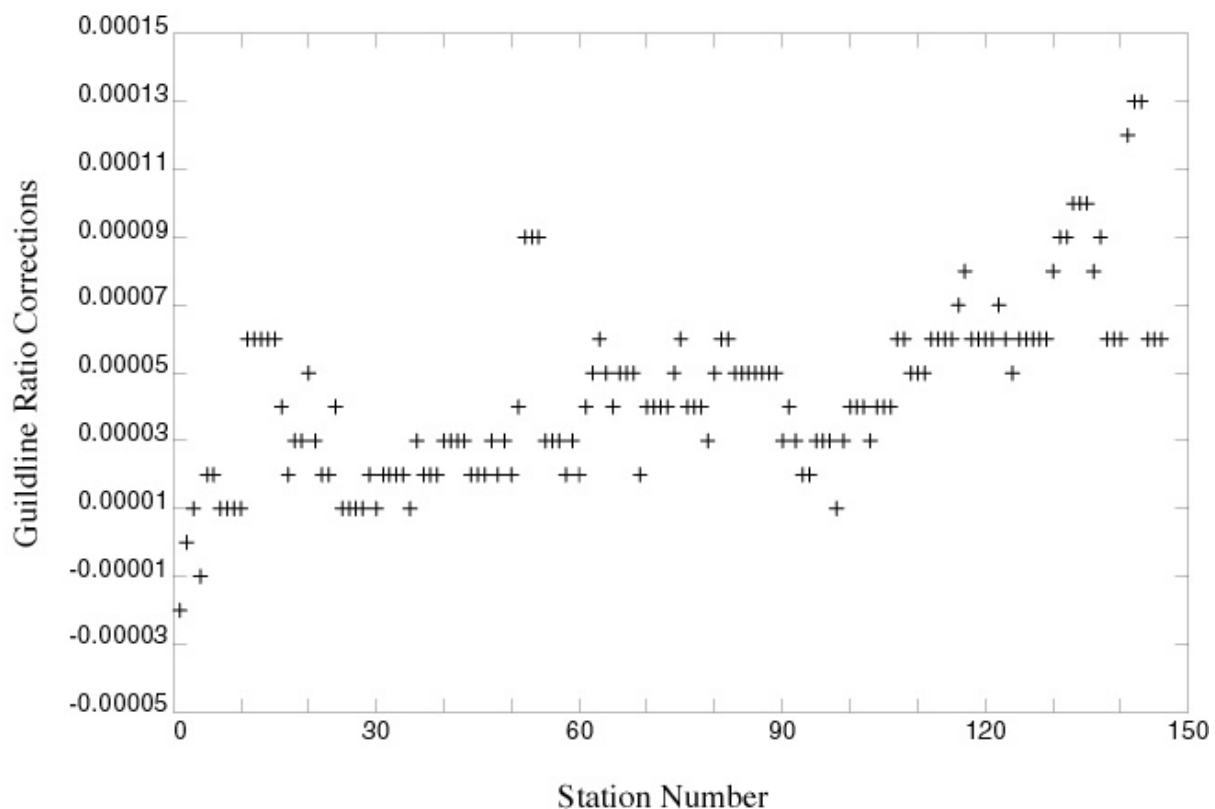


Figure S1. Analysis of Standard Seawater correction to the Guildline ratios for SSW batch P140

Louise Duncan, Matt Palmer, John Wynar and Jeff Benson

## DISSOLVED OXYGEN

### Acquisition

Dissolved oxygen samples were drawn directly from the Niskin bottles into 100 ml volume, calibrated oxygen bottles, their temperature measured and then fixed immediately using alkaline iodide and manganous chloride solutions prepared following Dickson (1994). The dispensers used to fix the samples were thoroughly cleaned in hot water at the start of the cruise and whenever they became sticky. Samples were shaken twice, once on deck and a second time shortly afterwards in the lab and then titrated in the lab within 12 hours.

### Analysis

Dissolved oxygen was measured on all bottles from all CTD casts using a semi-automated whole-bottle Winkler titration unit with spectrophotometric end-point detection manufactured by SIS. Acidification was performed using a 1ml Finn pipette. The user variable parameters in the SIS supplied software are in the parameters screen accessed through the options menu. The following values were determined by trial and error at the start of the cruise and applied throughout: Stepsize 15, Wait time 10, Fast delay 5, Slow delay 5, Fast factor 0.5. This parameter set resulted in titration times of less than three minutes.

One litre batches of sodium thiosulphate (25g/l) were prepared as required during the cruise. This strength solution results in titration volumes of about 1.00 ml. The thiosulphate solution was standardised at the start and end of the batch using a commercially available 0.01N Potassium iodate standard (Ocean Scientific International, Petersfield, Hants). Between these points the thiosulphate breakdown was regularly (every few days) monitored using an in-house solution of Potassium iodate prepared on board by dissolving 0.3567 g reagent grade KIO<sub>3</sub> in 1 litre Milli-Q water. The average volume of thiosulphate required to titrate 5 ml aliquots of the OSI standard to an agreement better than 0.002 ml was used in the calculation of oxygen concentration which was performed on an excel spreadsheet following the equations supplied by Dickson (1994). The reagent blank was evaluated at the start of the cruise and found to be 0.0011 ml and this value was applied to all calculations undertaken. The thiosulphate solution was found to be extremely stable. A minimum of one bottle on each cast was sampled twice to gain an estimate of the analytical precision. The mean difference in calculated oxygen concentration between all the duplicate pairs sampled was 0.38%.



**Reference**

**Dickson, A.G.** 1994 Determination of dissolved oxygen in seawater by Winkler titration. WOCE operations manual, WOCE Report 68/91 Revision 1 November 1994.

Val Latham

## NUTRIENTS

### Background

Water samples for inorganic nutrient analysis were drawn from each Niskin bottle on every station into 40ml polystyrene coulter counter vials after pH, alkalinity, oxygen, CFCs and He/Tr but before salinity. Inorganic nutrient concentrations were measured using a Skalar San Plus autoanalyser purchased by SOC in November 2000. This instrument was last used on *RRS Discovery* cruise D258 (Marine Productivity I). On D258 it was configured according to the manufacturers specifications (Kirkwood, 1995) with the exception that the flow rates through the phosphate line were changed from 0.8 ml/min sample, 0.1 ml/min ascorbic acid, 0.1 ml/min ammonium molybdate solution to 2 ml/min sample, 0.23 ml/min ascorbic acid, 0.23 ml/min ammonium molybdate solution to improve peak reproducibility and definition relative to the results obtained on *RRS Discovery* cruise D253 (FISHES). However, whilst addressing the phosphate peak shape and reproducibility, this change during D253 had the effect of causing frequent (occurring on around 50% of runs) catastrophic deterioration in the phosphate baseline which rendered data from that run unusable.

In an effort to counter this problem for use on *RRS Charles Darwin* cruise D139 the instrument was configured in Durban with a compromise configuration for phosphate consisting of 0.16 ml/min for each reagent and 1.4 ml/min for the sample. In addition large sections of the line, which had previously been made of polypropylene tube were replaced with glass and acidflex pump tubing. These precautions produced an acceptable peak shape and eliminated baseline failures; however, the reproducibility of the measurements was not as good as desired and the matrix effect observed at the interface of samples and the Artificial Seawater (ASW) wash solution was larger than desirable. After a mid-cruise review of the phosphate data, it was decided to revert to the pump tube sizes used on D258 and these were employed for the remainder of this cruise after station 78. This improved the sample resolution, reduced the matrix effect and resulted in only two of the remaining runs suffering catastrophic baseline failure. Thus the modifications to the reaction line undertaken at the start of the cruise must have been effective. The effects of the changes in sample and reagent flow rates on the quality of the P data are discussed later.

### Acquisition

Initially we were equipped with two lap-top PCs, one to run the autoanalyser and one to run the dissolved oxygen analyser. In the past the autoanalyser has been known to abruptly and without warning cease communications with the computer operating it. Often this failure has been associated

with processing data from previous runs. We therefore took the precaution of loading the software for both instruments onto both computers. The autoanalyser stopped communications on three separate occasions, only once in the middle of a run. Fortunately on each occasion we were able to switch immediately to the other machine and reconfigure the offending machine, a process which takes at least two hours. Attempts to write a cd-rom with ready-configured software failed for unknown reasons (but maybe because the software modifies one of the files in the windows directory as well as installing itself into the c:/flowaccess directory). Raw datafiles were processed on laptop PC's and backed up onto zip disks, following compression using winzip and transfer to the PC interfaced to the zipdrive. This procedure was not 100% successful as some of the raw datafiles were too large to be transferred in this manner, and therefore were not backed up. Unfortunately the PC on which they were acquired stopped functioning after station 33 and the raw datafiles for stations 22-32 will have to be recovered from the hard drive of this machine at SOC. Fortunately the raw data had been processed from these stations and results files created; however, the quality control parameters from two of these runs were not recorded. A reserve computer supplied by UKORS was used to acquire the oxygen data following this problem and we thank them for the loan of this instrument.

### **Quality Control**

Under the nutrients system currently in use at SOC the samples are run interspersed with an intersample wash solution consisting of 40 g/l analar sodium chloride in MilliQ (MQ) water, this solution (called artificial seawater, ASW) is also used as the standard matrix. Generally we find that this solution is free of nitrate, phosphate and silicate, although this is checked on each run using a nutrient-free seawater. On this cruise however a large and batch-dependent phosphate contamination was observed in the various batches of ASW made up, ranging from zero to 0.3 M/l. This started about station 54 and had serious effects on the phosphate data from station 54 to the end of the cruise. Every run from that point onwards (with the exception of the final run) had to be manually processed (or reprocessed) in Excel to account for this. This manual recalculation involved combining the computer generated corrected peak heights (which take account of instrument sensitivity and baseline drift) with an additional component corresponding to the contamination in the baseline relative to phosphate-free seawater and then calculating the phosphate concentration equivalent to the combined peak height using the phosphate standards as a standard additions curve. Phosphate concentrations calculated on a station with no phosphate contamination via this method appear to be within 2% of those calculated via the software working alone. It is possible that this phosphate contamination resulted from a fault with the MQ water system on the ship. This appears unlikely given that the conductivity of the MQ water remained constant and that no nitrate or silicate contamination was

observed. A further consequence of this problem was that checking the runfiles became a time-consuming business that had to be undertaken at the same time as acquiring data from the analyser. Fortunately no loss of data resulted from this procedure.

Overall approximately 3250 samples were analysed in 67 separate runs. The performance of the analyser is monitored via two parameters: the baseline value (in Digital Units, DU) and the gradient of the calibration curve (in DU/ M). Figure N1 shows time series of the baseline value. The baseline for all three nutrients moved over the course of the cruise in the manner shown in Figure N1.

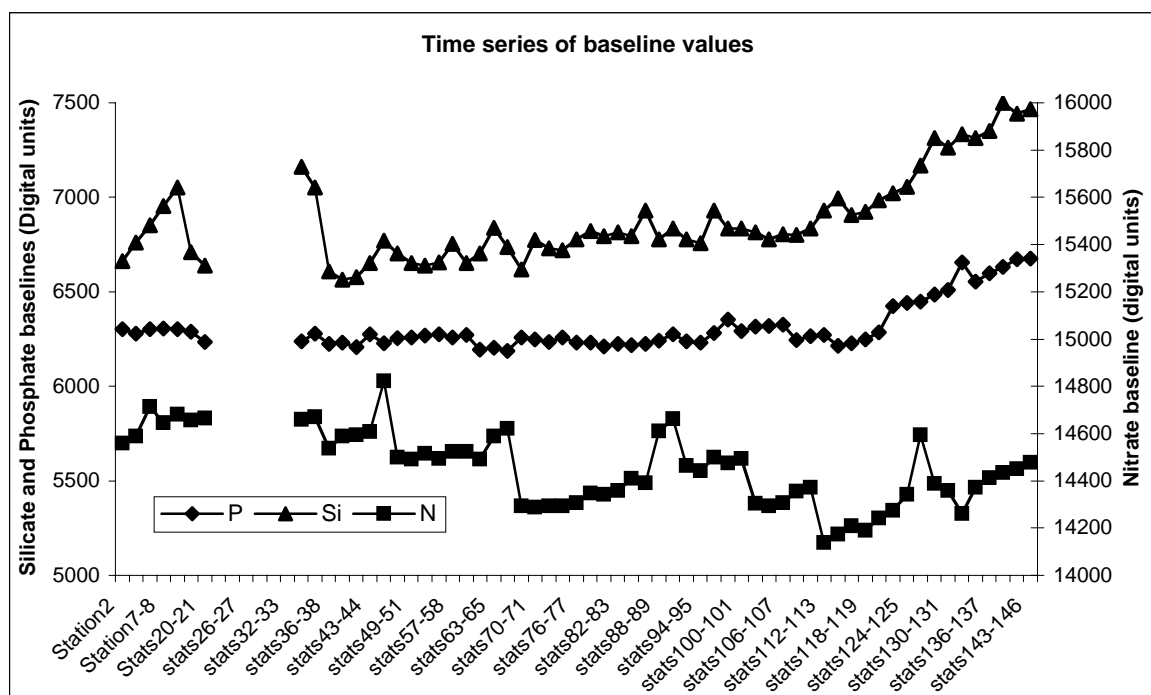


Figure N1. Baseline values for phosphate, silicate and nitrate versus station.

The baseline for all three nutrients varied. Silicate and phosphate both drifted up over the course of the cruise, this may be related to changes in the intensity of the light source which the two methods share. The nitrate baseline decreased over the course of the cruise with a sawtooth pattern imposed on this general decline. This decrease is associated with reagent deterioration.

The gradient of the calibration curve is shown in Figure N2. Of the three nutrients the silicate gain is by far the most stable with only two stations showing deviations from a value of about 60 DU/ M. This resulted from the emergency making up and usage of a new batch of Si reagents in Durban. Note that the silicate time series is only plotted from station 9. The high silicate concentrations encountered on this cruise necessitated the construction of a dilution loop in which the sample was diluted with an equivalent volume of silicate free ASW. This was built in port but could not be tested until sailing. It proved to be inadequate and was modified such that it diluted the sample

with twice its own volume of ASW. Thus silicate data from stations 1-8 were processed using a second order calibration curve. Further examination of this data in SOC may be required. The nitrate gain value drifted up steadily over the course of the cruise. Again, data from the early part of the cruise are not presented. Some of the early nitrate runs required calibration with a second order

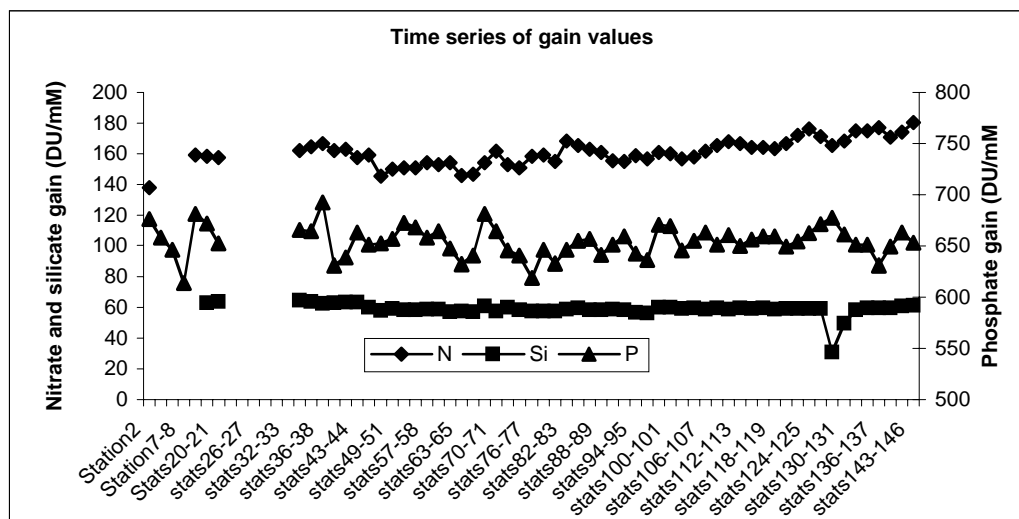


Figure N2. Gain values for nitrate, phosphate and silicate versus station.

polynomial. This problem appeared to resolve itself as the cadmium column bedded in (a single column was used over the course of the cruise, the efficiency of which was 100+/- 3%) and was not directly addressed. Further examination of this data in SOC may be required.

## Duplicates

Two samples per station were run in duplicate. The mean differences between the pairs of samples expressed as a percentage of the top standard were nitrate, 1.1%, phosphate, 0.9%, silicate, 0.43%. When the phosphate data is split into two groups comprising those samples analysed before and after the change in methodology which took place after station 78 the mean differences are 0.4% after the change and 1.3 % before.

The time variability of the differences between duplicate phosphate samples is shown in Figure N3. Clearly the modifications to the phosphate methodology undertaken in mid cruise were beneficial in terms of reducing the difference between pairs of duplicate measurements.

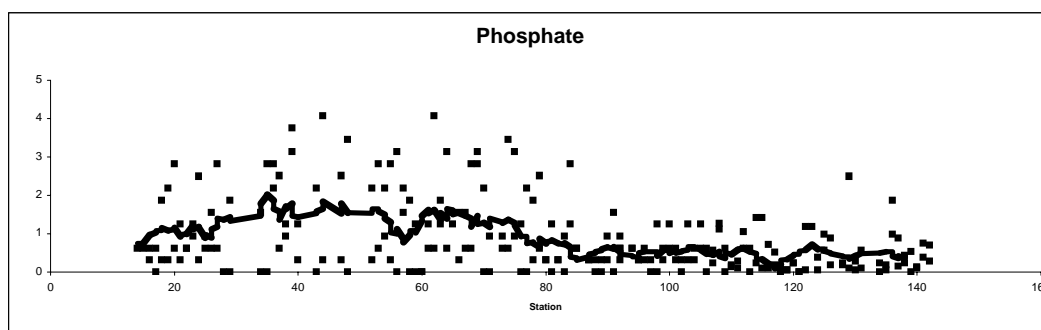


Figure N3. Absolute difference between duplicate phosphate samples versus station.

We investigated the reasons for these differences in duplicate concentrations by evaluating whether or not the second measurement of nutrient concentration was systematically larger or smaller than the first determination. If the error is random then we expect the average difference between the two determinations to be zero. If the error is systematic then we expect the average difference between determinations to be non zero. The average differences for the entire datasets were N, 0.03%, P, 0.43%, Si 0.46%. When this parameter was evaluated for the phosphate data before and after station 78 its value was 0.8% in the early part of the cruise and 0.1% in the latter part of the cruise. A comparison of these values with the mean differences set out earlier suggests that the error in the determination of nitrate concentration is almost entirely random, whereas the error in silicate and phosphate concentrations are substantially systematic (that is replicate 1 is consistently higher than replicate 2 or vice versa), accounting for approximately 70% of the difference between replicate silicate determinations and 50% of the difference between replicate phosphate determinations. This is almost certainly a consequence of carryover of water from one sample to the next and is the first direct evidence we have that this is an issue that should be addressed. Interestingly the modifications to the phosphate line reduced the proportion of the error attributable to systematic causes from approximately 60% to about 20%. In light of this consideration should be given to increasing the flow rate through the silicate line.

The concentration of a bulk nutrient sample collected on WOCE cruise A23 was determined on each run to provide some measure of the internal consistency of the dataset. The results of these determinations are shown in Figure N4 together with the deep N/P ratio. The results of these determinations were Nitrate 34.98 +/- 0.6 mM, Phosphate 2.46 +/- 0.07 mM, Silicate 129.9 +/- 1.9 mM. These are equivalent to errors of 1.63, 1.47 and 2.81% respectively. When the phosphate data is broken into to groups before and after station 78, the errors are 3.8 and 1.8% for the early and late part of the cruise respectively.

Some difficulty was encountered in sampling the bulk seawater standard in a clean manner, particularly for phosphate. Obviously erroneous determinations have been excluded from the errors

calculated above, however these errors represent upper limits. As a further internal consistency measurement we evaluated the deep N/P ratio throughout the cruise, plotted in Figure N4. This showed a high degree of uniformity. The standard deviations of the points used to evaluate this ratio were Nitrate 2.4% and Phosphate 2.56%. This suggests that the internal consistency of the phosphate data is broadly comparable to that of the nitrate data.

## Accuracy

In the absence of a certified reference material an evaluation of accuracy is dependent on a comparison with historical data. This will be undertaken at SOC.

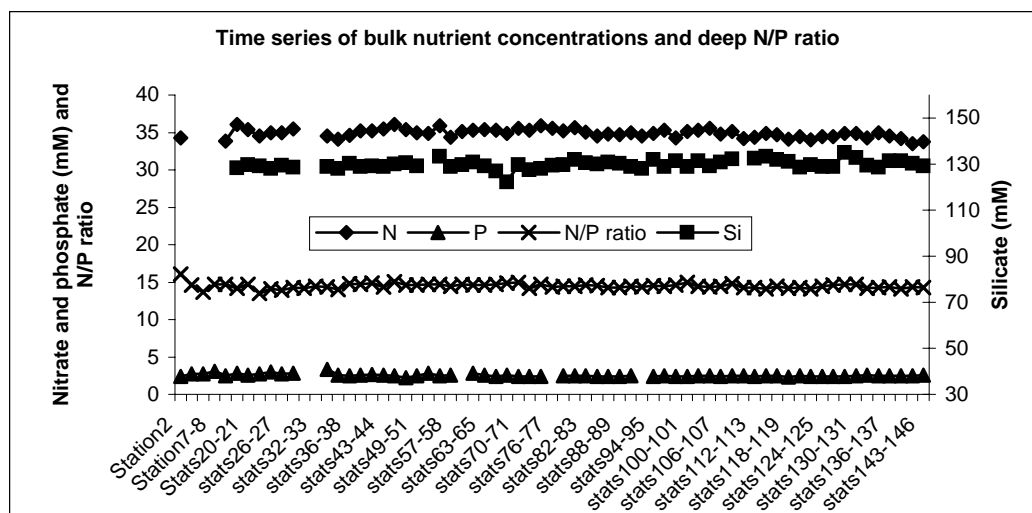


Figure N4. Bulk nutrient concentrations and deep nitrate/phosphate ratio versus station.

## Organic Nutrients

Dissolved organic nutrient samples were drawn from 10 bottles per station into pyrex glass bottles with teflon-lined lids and frozen immediately. A separate set of approximately 400 samples were collected in 40ml sterilin sample pots and also frozen. Chlorophyll samples were taken on one station per day. For these samples 5l of water were filtered through a glass-fibre filter (GFF) and the filter frozen for subsequent analysis back at SOC using HPLC (High Pressure Liquid Chromatography).

## Reference

**Kirkwood, D.S.** 1995 Nutrients: Practical notes on their determination in seawater. ICES Techniques in Marine Environmental Sciences report 17, International Council for the Exploration of the Seas, Copenhagen. 25p. ISSN 0903-2606.

Richard Sanders



## CO<sub>2</sub> COMPONENTS

During the *Charles Darwin* 139 cruise along 32°S in the Indian Ocean, carbon system components pH and alkalinity were sampled and analysed. As well, samples for total inorganic carbon were taken and stored to be analysed on land. Table O1 shows the stations where samples were taken for the different CO<sub>2</sub> parameters.

### pH analysis

pH was measured spectrophotometrically following techniques described by Clayton and Byrne (1993). Roughly, this method consists of adding a dye solution to the seawater sample, so that the ratio between two absorbances at two different wavelengths is proportional to the sample pH.

#### i. Sampling and analytical methods.

Seawater samples for pH were collected after oxygen samples using cylindrical optical glass 10-cm pathlength cells which were filled to overflowing and immediately stoppered. Seawater pH was measured using a double-wavelength spectrophotometric procedure (Byrne, 1987). The indicator was a 1 mM solution of Kodak m-cresol purple sodium salt (C<sub>21</sub>H<sub>17</sub>O<sub>5</sub>Na) prepared in seawater. After sampling all the samples were stabilised at 25 °C. The absorbance measurements were obtained in a thermostatted (25±0.1) cell compartment of a CECIL 3041 spectrophotometer.

After blanking with the sampled seawater without dye, 100 µl of the dye solution were added to each sample using an adjustable repeater pipette. The absorbance was measured at three different fixed wavelengths (434, 578 and 730 nm). pH, on the total hydrogen ion concentration scale, is calculated using the following formula (Clayton and Byrne, 1993):

$$\text{pH}(T) = 1245.69/T + 3.8275 + (2.11 \cdot 10^{-3})(35-S) + \log((R-0.0069)/(2.222-R \cdot 0.133)) \quad (1)$$

where R is the ratio of the absorbances of the acidic and basic forms of the indicator corrected for baseline absorbance at 730 nm ( $R = A_{578}/A_{434}$ ), T is temperature in °Kelvin and S is salinity. Therefore pH values are given on the total scale and referred to 25°C (pH<sub>25</sub>T).

#### ii. Quality control.

In order to check the precision of the pH measurements, samples of CO<sub>2</sub> Certified Reference Material (CRM, batch 55, distributed by Dr. A.G. Dickson from the Scripps Institution of Oceanography) were analysed during the cruise (Figure O1). The mean value for the set of CRM measurements was 7.909± 0.003. The overall precision of the pH measurements during the cruise was obtained from the analysis of duplicate samples (usually 9 cells) drawn from the same bottle. The mean standard deviation of the series of replicates was ± 0.0007.

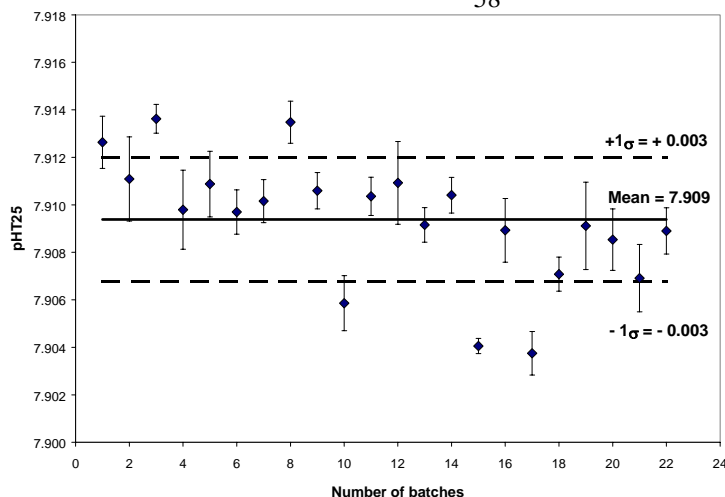


Figure O1. Spectrophotometric pH<sub>25</sub>T measurements on the CRM batch 55 during the cruise. Each batch consists of 8 measurements from the same CRM bottle.

## Alkalinity Analysis

### i. Sampling and analytical methods.

Seawater samples for alkalinity were collected after pH samples in 600 ml glass bottles. Samples were filled to overflowing and immediately stoppered. Total alkalinity was measured using an automatic potentiometric titrator "Titrino Metrohm", with a Metrohm 6.0233.100 combination glass electrode and a Pt-100 probe to check the temperature. Potentiometric titrations were carried out with hydrochloric acid ( $[HCl] = 0.1 \text{ M}$ ) to a final pH of 4.44 and 4.40 (Pérez and Fraga, 1987). The electrode was standardised using a 4.4 buffer made in  $CO_2$ -free seawater (Pérez et al., 2000). Concentrations are given in  $\mu\text{mol/kg-sw}$ .

### ii. Quality control.

Determinations of alkalinity on  $CO_2$  **Certified** Reference Material (CRM, batch 55) were made during the cruise to monitor the Titrino performance (Figure O2).

As well, in order to obtain a more precise determination of alkalinity for each sample, each was analysed twice, a mean and standard deviation were then calculated. 75% of the double determinations had a standard deviation lower than  $1 \mu\text{mol/kg}$  and a further 20% between 1 and  $2 \mu\text{mol/kg}$ . In the test station N° 1, the whole set of bottles were fired at the same depth. The standard deviation of a total of 24 analyses over 12 bottle samples collected for alkalinity was  $1.04 \mu\text{mol/kg}$ .

## Total Inorganic Carbon Sampling

Samples for Total Inorganic Carbon to be analysed at the land laboratory were collected at crossover stations where previous cruises in the Indian Ocean had sampled. Emptied Certified Reference Material bottles were rinsed twice and filled from the bottom, overflowing half a volume while taking care not to entrain any bubbles. Then 0.2 ml of saturated mercuric chloride solution was added to the sample as a preservative and the bottle was sealed with glass stoppers covered with

Apiezon-L grease and stored in the dark at room temperature. Samples for Inorganic Carbon were taken at stations 48, 100, 117 and 134.

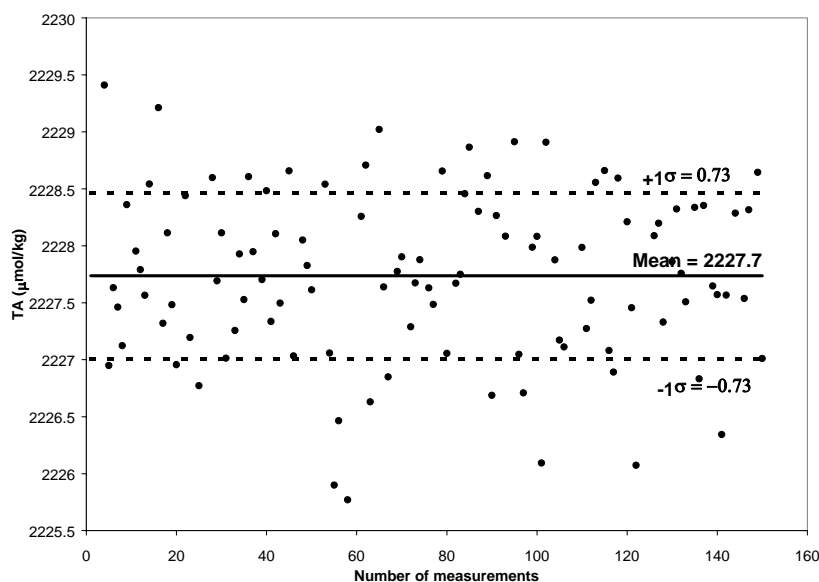


Figure O2. Alkalinity measurements on the CRM batch 55 during the cruise.

## REFERENCES

- Byrne, R.H.** 1987 Standardization of standard buffers by visible spectrometry. *Analytical Chemistry*, **59**, 1479-1481.
- Clayton, T.D. & Byrne, R.H.** (1993). Spectrophotometric seawater pH measurements: total hydrogen ion concentration scale concentration scale calibration of m-cresol purple and at-sea results. *Deep-Sea Research I*, **40**, 10, 2115-2129.
- Pérez, F.F. & Fraga, F.** 1987 A precise and rapid analytical procedure for alkalinity determination. *Marine Chemistry*, **21**, 169-182.
- Pérez, F.F., Ríos, A.F., Rellán, T. & Álvarez, M.** 2000 Improvements in a fast potentiometric seawater alkalinity determination. *Ciencias Marinas*, **26**, 463-478.

**Table O1.** List of sampled stations for pH, alkalinity (TA) and total inorganic carbon (TIC).

St.	pH	TA	TIC
1	+	+	
2	+	+	
3	+		
4	+	+	
5	+	+	
6	+		
7	+	+	
8	+		
9	+	+	
10	+		
11	+	+	
12	+	+	
13	+	+	
14	+	+	
15	+		
16	+		
17	+	+	
18	+		
19	+	+	
20	+		
21	+	+	
22	+		
23	+	+	
24	+		
25	+	+	
26	+		
27	+	+	
28	+		
29	+	+	
30	+		
31	+	+	
32	+	+	
33	+		
34	+	+	
35	+		
36	+	+	
37	+		
38	+	+	
39	+		
40	+		
41	+	+	
42	+		
43	+	+	
44	+	+	
45	+		
46	+	+	
47	+		
48	+	+	+
49	+		
50	+	+	
51	+		
52	+	+	
53	+		
54	+	+	
55	+		
56	+	+	
57	+		
58	+	+	
59	+		
60	+	+	
61	+		
62	+	+	
63	+		
64	+	+	
65	+		
66	+	+	
67	+		
68	+	+	
69	+		
70	+	+	
71	+		
72	+	+	
73	+		
74	+	+	
75	+		
76	+	+	
77	+		
78	+	+	
79	+		
80	+	+	
81	+		
82	+	+	
83	+		
84	+	+	
85	+		
86	+	+	
87	+		
88	+	+	
89	+		
90	+	+	
91	+		
92	+	+	
93	+		
94	+	+	
95	+		
96	+	+	
97	+	+	
98	+	+	
99	+		
100	+	+	+
101	+		
102	+	+	
103	+		
104	+	+	
105	+		
106	+	+	
107	+		
108	+	+	
109	+		
110	+	+	
111	+		
112	+	+	
113	+		
114	+	+	
115	+		
116	+	+	
117	+	+	+
118	+		
119	+		
120	+	+	
121	+		
122	+	+	
123	+		
124	+	+	
125	+		
126	+	+	
127	+		
128	+	+	
129	+		
130	+	+	
131	+		
132	+	+	
133	+		
134	+	+	+
135	+		
136	+	+	
137	+		
138	+	+	
139	+		
140	+	+	
141	+		
142	+	+	
143	+		
144	+	+	
145	+	+	
146	+	+	

## CHLOROFLUOROCARBON (CFC) MEASUREMENTS

Samples for the analysis of dissolved CFC-11 and CFC-12 were drawn from ~2100 of the 3500 water samples collected during the expedition. Samples for carbon tetrachloride ( $\text{CCl}_4$ ) analysis were drawn from ~540 samples. Specially designed 10 liter water sample bottles were used on the cruise to reduce CFC contamination. These bottles have the same outer dimensions as standard 10 liter Niskin bottles, but use a modified end-cap design to minimize the contact of the water sample with the end-cap O-rings after closing. The O-rings used in these water sample bottles were vacuum-baked prior to the first station. Stainless steel springs covered with a nylon powder coat were substituted for the internal elastic tubing provided with standard Niskin bottles.

When taken, water samples for CFC and carbon tetrachloride analysis were usually the first samples drawn from the 10 liter bottles. Care was taken to co-ordinate the sampling of CFCs with other samples to minimize the time between the initial opening of each bottle and the completion of sample drawing. In most cases, dissolved oxygen, alkalinity and pH samples were collected within several minutes of the initial opening of each bottle. To minimize contact with air, the CFC samples were drawn directly through the stopcocks of the 10 liter bottles into 100 ml precision glass syringes equipped with 2 way metal stopcocks. The syringes were immersed in a holding tank of clean surface seawater until analysed. To reduce the possibility of contamination from high levels of CFCs frequently present in the air inside research vessels, the CFC extraction/analysis system and syringe holding tank were housed in a modified 20' laboratory van on the aft deck of the ship.

For air sampling, a 100 meter length of 3/8" OD Dekaron tubing was run from the CFC lab van to the bow of the ship. A flow of air was drawn through this line into the CFC van using an Air Cadet pump. The air was compressed in the pump, with the downstream pressure held at ~1.5 atm. using a back-pressure regulator. A tee allowed a flow ( $100 \text{ ml min}^{-1}$ ) of the compressed air to be directed to the gas sample valves, while the bulk flow of the air ( $>7 \text{ l min}^{-1}$ ) was vented through the back pressure regulator. Air samples were only analysed when the relative wind direction was within 60 degrees of the bow of the ship to reduce the possibility of shipboard contamination. The Air Cadet pump was run for at least 60 minutes prior to analysing each batch of air samples to insure that the air inlet lines and pump were thoroughly flushed.

Concentrations of CFC-11 and CFC-12 in air samples, seawater and gas standards were measured by shipboard electron capture gas chromatography (EC-GC) using techniques similar to those described by Bullister and Weiss (1988). For seawater analyses, a 30 ml aliquot of seawater from the glass syringe was transferred into the glass sparging chamber. The dissolved CFCs in the seawater sample were extracted by passing a supply of CFC-free purge gas through the sparging chamber for a period of 4 minutes at  $70 \text{ ml min}^{-1}$ . Water vapour was removed from the purge gas

during passage through an 18 cm long, 3/8" diameter glass tube packed with the desiccant magnesium perchlorate. The sample gases were concentrated on a cold-trap consisting of a 1/8" OD stainless steel tube with a ~7 cm section packed tightly with Porapak N (60-80 mesh). To cool the trap, isopropanol cooled by a Neslab Cryocool refrigeration system was forced from a reservoir beneath the trap to a level above the packing with a stream of compressed nitrogen. After quickly bringing the isopropanol to the top of the trap, a low flow of nitrogen was bubbled through the bath to reduce gradients and maintain a temperature of -20°C. After 4 minutes of purging the seawater sample, the sparging chamber was closed and the trap was held open for an additional 1 minute to allow nitrous oxide (N<sub>2</sub>O) to pass through the trap and thereby minimize its interference with CFC-12. The trap was isolated, the cold isopropanol in the bath was drained, and the trap was heated electrically to 125°C. The sample gases held in the trap were then injected onto a precolumn (~50 cm of 1/8" O.D. stainless steel tubing packed with 80-100 mesh Porasil C, held at 90°C) for the initial separation of the CFCs and other rapidly eluting gases from the more slowly eluting compounds. The CFCs then passed into the main analytical column (~183 cm of 1/8" OD stainless steel tubing packed with Carbograph 1AC, 80-100 mesh, held at 90°C) for final separation, and into the EC detector for quantification.

The analysis of carbon tetrachloride was made on a separate, but similar apparatus to the EC-GC system used in the analysis of CFC-11 and CFC-12. Samples were drawn in the same type of syringes used for the CFC analysis. In the CCl<sub>4</sub> system, the sample injection port was flushed with 30-40 ml of sample before injecting sample into a calibrated loop (~30 ml). After filling, an additional 30 ml of water was pushed through the loop and allowed to overflow. For analysis, a valve was switched and the water sample held in the loop was pushed into the stripper with the same CCl<sub>4</sub> free nitrogen that was used to strip the sample. The gases removed from the sample were dried while passing through an ~18 cm x 3/8" OD tube of magnesium perchlorate and concentrated on a trap packed with 10 cm of Porapak N and held at -30°C during trapping. At the conclusion of stripping, the trap was heated electrically and the contents swept onto the precolumn (0.53mm I. D. x 30 meters, DB624 capillary column held at 45°C) with clean nitrogen. The desired gases passed on to the main analytical column (0.53mm I. D. x 30 meters, DB624 capillary column, 45°C) before the precolumn vented the later peaks. All other aspects of the analysis were the same as for the CFC analysis.

Both of the analytical systems were calibrated frequently using a standard gas of known CFC composition. Gas sample loops of known volume were thoroughly flushed with standard gas and injected into the system. The temperature and pressure was recorded so that the amount of gas injected could be calculated. The procedures used to transfer the standard gas to the trap, precolumn, main chromatographic column and EC detector were similar to those used for analysing water samples. Two sizes of gas sample loops were present in the CFC analytical system, while four calibrated sample loops were used in the CCl<sub>4</sub> system. Multiple injections of these loop volumes

could be made to allow the system to be calibrated over a relatively wide range of concentrations. Air samples and system blanks (injections of loops of CFC-free gas) were injected and analysed in a similar manner. The typical analysis time for seawater, air, standard or blank samples was 12 minutes on the CFC system and 20 minutes on the  $\text{CCl}_4$  system.

Concentrations of the CFCs and  $\text{CCl}_4$  in air, seawater samples and gas standards are reported relative to the SIO98 calibration scale (Cunnold, et. al., 2000). Concentrations in air and standard gas are reported in units of mole fraction CFC in dry gas, and are typically in the parts-per-trillion (ppt) range. Dissolved CFC and  $\text{CCl}_4$  concentrations are given in units of picomoles per kilogram seawater ( $\text{pmol kg}^{-1}$ ). CFC and  $\text{CCl}_4$  concentrations in air and seawater samples were determined by fitting their chromatographic peak areas to multi-point calibration curves, generated by injecting multiple sample loops of gas from a working standard (PMEL cylinder 33780 for CFC-11, CFC-12, CFC-113 and  $\text{CCl}_4$ ) into the analytical instrument. Full range calibration curves were run at intervals of ~3 days during the cruise. Single injections of a fixed volume of standard gas at one atmosphere were run much more frequently (at intervals of 1 to 2 hours) to monitor short term changes in detector sensitivity.

Extremely low CFC-11 and CFC-12 concentrations ( $<0.01 \text{ pmol kg}^{-1}$ ) and carbon tetrachloride concentrations ( $0.01\text{-}0.02 \text{ pmol kg}^{-1}$ ) were measured in waters between 2800-3200 meters depth along the section east of  $\sim 89^\circ\text{E}$ . Based on the median of concentration measurements in these regions, which is believed to be nearly CFC-free, blank corrections of  $0.007 \text{ pmol kg}^{-1}$  for CFC-11,  $0.004 \text{ pmol kg}^{-1}$  for CFC-12 and  $0.007 \text{ pmol kg}^{-1}$  for carbon tetrachloride have been applied to the data set. If the measured CFC concentration for a sample is very low, these blank corrections can result in a very small negative concentration being reported. On this expedition, based on the analysis of duplicate samples, we estimate precisions (1 standard deviation) of 1% or  $0.005 \text{ pmol kg}^{-1}$  (whichever is greater) for dissolved CFC-11 and CFC-12 measurements and 1.4% or  $0.006 \text{ pmol kg}^{-1}$  for  $\text{CCl}_4$  measurements.

A very small number of water samples had anomalously high CFC or  $\text{CCl}_4$  concentrations relative to adjacent samples. These samples occurred sporadically during the cruise and were not clearly associated with other features in the water column (e.g. anomalous dissolved oxygen, salinity or temperature features). This suggests that these samples were probably contaminated with CFCs or  $\text{CCl}_4$  during the sampling or analysis processes. Measured concentrations for these anomalous samples are included in this report, but are given a quality flag value of either 3 (questionable measurement) or 4 (bad measurement). A total of 11 analyses of CFC-11, 36 analyses of CFC-12 and 7 analyses of  $\text{CCl}_4$  were assigned a quality flag of 3. A total of 13 analyses of CFC-11, 17 analyses of CFC-12 and 6 analyses of  $\text{CCl}_4$  were assigned a quality flag of 4.

## References

**Bullister, J.L. & Weiss, R.F.** 1988. Determination of  $\text{CCl}_3\text{F}$  and  $\text{CCl}_2\text{F}_2$  seawater and air. *Deep-Sea Research*, **25**, 839-853.

**Prinn, R. G., Weiss, R.F., Fraser, P.J., Simmonds, P.G., Cunnold, D.M., Alyea, F.N., O'Doherty, S., Salameh, P., Miller, B.R., Huang, J., Wang, R.H.J., Hartley, D.E., Harth, C., Steele, L.P., Sturrock, G., Midgley, P.M. & McCulloch, A.**, 2000. A history of chemically and radiatively important gases in air deduced from ALE/GAGE/AGAGE. *Journal of Geophysical Research*, **105**, 17751-17792.

David P. Wisegarver and Kevin McHugh



## **SAMPLING FOR HELIUM AND TRITIUM**

### **Background**

In December 2001, following a discussion with Bill Jenkins and Clare Postlethwaite, we decided to attempt sampling for Helium and Tritium during the transindian hydrographic section across 32°S beginning in March 2002. The section (WOCE I5) had been sparsely sampled at the eastern and western boundaries during WOCE and the central region had not previously been sampled at all for Helium and Tritium. Because there was no space for an additional scientist to participate on the cruise to do tracer sampling, the physical oceanographers on the cruise took on the commitment to acquire the samples. The idea was to draw samples in copper tubes for Helium and in one-litre bottles for Tritium for later shore-based analysis at the Noble Gas Laboratory at Southampton Oceanography Centre. It was envisioned that it would be possible to sample about one station each day outside the densely sampled eastern and western boundary regions.

Clare Postlethwaite prepared the materials for surface shipment in early January 2002 and provided about 2 hours training to Louise Duncan and Brian King on how to take and preserve the samples and to maintain the equipment.

### **Sampling**

For Helium sampling, 68 cm pieces of copper tube are cut from 20m reels of copper tube and are labelled as to station, bottle, and with a unique identification number. Each tube is dented in 2 places, + and - 14 cm from the centre of the tube. During sampling (which occurs directly after CFC's) water is syphoned through tygon tubing into the bottom of a copper tube and out of the top draining through more tygon tubing. All bubbles in the water are beaten out of the tubing and copper with a wooden bat; when all bubbles are gone, the tubing is clamped below, then above, the copper tube. Holding the tygon tubing firmly onto both ends of the copper tube, the tube is then sealed with a hydraulic cutter powered by compressed air at one end, then in the middle of the tube, and finally at the other end. In effect the tube ends are sealed by a cold weld. The result is a pair of duplicate samples from each bottle. Re-rounding each tube creates a vacuum inside; if the seal is tight, a sharp flick of the tube creates a click which verifies the integrity of the sample. The copper tubes are later wrapped in bubble wrap and labeled with the unique identification number on the outside of the bubble wrap.

For Tritium sampling, which is the last water sample to be drawn from each bottle, a small piece of tygon tubing is attached to the Niskin bottle, rinsed and used to dribble water down the sides of a one-litre bottle which had been baked under an argon atmosphere and sealed at Southampton Oceanography Centre in January. Each bottle has a unique bar code which is recorded versus station

and Niskin bottle number on the log sheet; at the same time the station and Niskin bottle numbers are written on the label of the sample bottle. The bottles once filled are then sealed with electrical tape to prevent movement of the cap during storage and shipment back to Southampton. A tritium sample was drawn from each Niskin bottle for which helium samples were drawn.

Sampling for Helium and Tritium was principally done during the 0800-1600 watch period. Principal samplers were Louise Duncan, Melanie Witt, Brian King and Harry Bryden. During the cruise, 24 stations were sampled for Helium and Tritium, slightly less than anticipated due to other commitments. As the cruise developed, the goal evolved to sample approximately every 3 degrees of longitude across the width of the Indian Ocean. A total of 375 duplicate copper tube samples for Helium and 375 one-litre bottle samples for Tritium were acquired and shipped back to Southampton Oceanography Centre at the end of the cruise. Details of the sampling are presented in Table H1.

Harry L. Bryden and Louise M. Duncan

Table H1: Sampling for Helium and Tritium

*RRS Charles Darwin 139, March-April 2002.*

<b>Station</b>	<b>Latitude</b>	<b>Longitude</b>	<b>Depth</b>	<b>Samples</b>
21	-31 13.10	030 35.10	2705	18
29	-31 48.20	031 25.50	3315	15
36	-32 53.70	035 00.50	1602	15
41	-33 01.00	036 31.40	4839	18
45	-32 59.60	038 59.70	5091	18
51	-33 00.00	043 02.20	2321	14
58	-33 29.30	047 27.20	3570	14
64	-34 00.30	052 44.70	4478	16
72	-33 58.00	057 02.10	4997	17
76	-33 59.10	059 19.60	5551	17
79	-34 00.20	060 59.60	4946	16
82	-33 59.00	063 59.90	4666	14
85	-34 00.00	067 00.00	4681	16
88	-33 59.70	070 00.90	4219	16
93	-32 45.20	074 29.40	3850	16
98	-30 45.00	078 30.00	3454	15
104	-31 13.40	084 30.40	4068	15
108	-31 44.80	088 09.50	1932	12
115	-32 10.20	090 52.20	4444	15
118	-33 50.00	095 32.00	4558	15
123	-34 30.00	100 27.00	4337	15
128	-33 30.00	105 00.00	5332	16
133	-31 30.00	108 55.00	5327	16
138	-31 30.00	113 09.00	5199	16

## LOWERED ACOUSTIC DOPPLER CURRENT PROFILER

### Summary

During the trans-Indian Ocean section across 32°S (RRS *Charles Darwin* cruise 139) three Lowered Acoustic Doppler Current Profilers (LADCPs) were deployed simultaneously on a specially adapted frame. The intention was to combine the new RDI 300kHz Dual Workhorse configuration of one upward-looking and one downward-looking LADCP, with the more established downward-looking 150kHz Broadband LADCP, to produce an outstanding, comprehensive (and comparable) dataset of direct velocities.

The Dual system was deployed throughout the cruise, except on station 3, with a ping cycle of 1.54 s. Two 150kHz instruments were brought on the cruise: the SOC instrument, and a backup loaned by Teri Chereskin at the Scripps Institution of Oceanography (SIO). Both instruments were deployed with a staggered ping cycle (0.8 s/1.2 s) to eliminate the bottom interference layer. The SIO LADCP has 30 degree beam angles, compared to SOC's 20 degrees, and thus produces horizontal velocities of consistently 20% lower standard deviation.

Interference between the instruments was a concern. The dual system was designed for simultaneous deployment and therefore able to asynchronise pings and avoid interference with one another, but the 150kHz LADCP has no such capability. The 150kHz instrument was deployed alone during one cast and its beam amplitudes from this and another cast examined to assess the effect of interference. Interference from the 300kHz pings was found to affect about 4% of its returns. This reduced the number of good samples collected, but did not appear to have a detrimental effect on the measured velocity profile, which compared favourably to both shipboard ADCP profiles and bottom-tracked velocities. Thus, it was concluded that the instrument was flagging the interference correctly as bad data and thus not introducing errors, except via the slight reduction of good samples.

Comparisons between the instrument measurements revealed that the 150kHz LADCP outperformed the 300kHz LADCPs in most respects. In waters deeper than about 1500 m, where scatterers are few, the higher frequency instruments often did not obtain enough return samples to produce a realistic ocean velocity profile. In contrast the 150kHz LADCP always maintained a return sample number of over 50 (more often over 100) per depth bin. In addition the shear standard deviation of the returns in deep water was generally 34% larger for the 300kHz instruments. Processing the upward and downward-looking 300kHz data simultaneously, and thereby doubling the number of return samples per depth bin, did little to improve the erroneous deep velocities. We conclude that the Dual Workhorse system did not perform well during this cruise, perhaps because of the clear, unproductive Southern Indian Ocean water. This was disappointing, because the same instruments produced good data in the Drake Passage in November 2001.

Comparisons were also made between the established Firing processing technique, with which we had many cruises of experience, and the Visbeck technique which was relatively new to us. In Firing's method a differentiation of velocities into noisier shears is required, whereas in Visbeck's method this is no longer necessary. Therefore, in theory the new technique has an advantage and should produce cleaner velocity profiles. However, on comparing a station of 150kHz data processed using each technique it was found that the Visbeck method underestimated top-to-bottom (first baroclinic mode) shear and created more disparate up-down profiles (causing the classic X-profile). In addition, the reader should be advised that using the Visbeck method with the added constraint of bottom-tracked data, as Visbeck intended, should be conducted cautiously. On deep stations, where it was clear that the 300 kHz data was erroneous due to unrealistically strong deep shears and large bottom velocities, a plausible profile is created using the bottom-tracked velocity constraint, since it prevents the profile from blowing up. However, the resulting velocity profile is quite wrong. During the cruise Visbeck released a modified version of his software which was set up, tested and used on board. Results were much more encouraging, with the obvious underestimate of the shear no longer apparent. The technique holds promise for the future.

In summary, the 150kHz LADCP data is good quality, comparing well with surface velocities from shipboard ADCP and with bottom-tracked velocities from the downward-looking 300kHz instrument. In fact the data is an improvement over measurements collected during ACE, because of the staggered ping deployment. Further improvement of the data is possible through subjective use of the bottom-tracked and on-station shipboard ADCP velocities to adjust the top-to-bottom (first baroclinic mode) shear.

### **Configuration, Deployment, and Recovery**

Two *RD Instruments* 300 kHz Workhorse (WH) Lowered Acoustic Doppler Current Profilers (LADCPs) and one *RD Instruments* 150kHz Broadband (BB) LADCP were secured to a modified CTD frame for simultaneous deployment throughout the cruise. An additional 150kHz Broadband instrument, loaned by Teri Chereskin at the Scripps Institution of Oceanography (SIO), was available as backup. The two 150kHz instruments were identical except for their beam angles. The SOC instrument has a beam angle of  $20^\circ$ , while the SIO instrument has a beam angle of  $30^\circ$ . The 150kHz LADCP was mounted at the centre of the frame, below the rosette mechanism, with a separate battery pack mounted horizontally at the level of the CTD. One of the 300kHz instruments was mounted off-centre at the bottom of the frame, as the down-looker or master Workhorse (MWH). The other was mounted to the side of the rosette at the top of the frame, as the up-looker or slave Workhorse (SWH). The uplooker was protected by an arc segment of frame built on the side of the main frame. The battery pack for both Workhorses was also mounted horizontally at the level of the CTD. To avoid confusion over the different LADCPs, hereafter the Dual Workhorse (DWH)

system, consisting of both 300kHz instruments, will be referred to as DWH, while singularly the up-looker will be referenced as SWH and the down-looker as MWH. Finally the 150kHz LADCP will be referred to as BB (for Broadband).

The workhorse instruments were deployed in master/slave mode, with the master telling the slave when to ping, therefore avoiding interference between the instruments. Otherwise, each instrument was set up identically having ping intervals of 1 s with a 0.5 s snych delay after the slave ping, sixteen bins each of length 10 m, a 5 m blank after transmit, and an ambiguity velocity of  $2.5 \text{ m s}^{-1}$ . Copies of the deployment command files, WHM.CMD and WHS.CMD can be found in the appendix. The workhorses have RDI firmware that obtains bottom-tracked velocities from water-tracking pings (in beam coordinates), thus giving good 'truth' data at the bottom of each cast.

The BB setup during CD 139 was one not previously used by SOC scientists. In previous experiments (such as ACE) the interference layer, which results from the previous ping reflecting off the bottom, has caused a data gap in the BB LADCP profile, causing an uncertain velocity offset of several  $\text{cm s}^{-1}$  between the parts of the profile on either side of the gap. It is possible to set a long ping interval to reduce this problem. For example, a 2 s interval will place the interference layer about 1500 m off the bottom, therefore reducing the strength of the interference signal to insignificance. However, with this approach one loses at least 50% of possible measurements, thus increasing the variance of the resultant velocity profile. Instead, during CD 139 the BB was deployed with a staggered ping. By setting an ensemble time of 0.8 s, with two ensembles per burst of 2 s duration, one achieves a PING PING WAIT pattern, resulting in intervals of 0.8 s and 1.2 s between pings. Thus, one set of pings causes an interference layer about 600 m off, the other about 900 m off, but in neither case is the entire data set contaminated and there is no data gap. Other significant settings for the BB were: sixteen times 16 m bins, a 16 m blank after transmit, and an ambiguity velocity of  $3.5 \text{ m s}^{-1}$ . A copy of the deployment command file for the BB, BB13901.CMD can also be found in the appendix.

Examples of the log sheets, deployment and recovery instructions for LADCP watchkeepers can be found in the appendix. The logsheet was modified to accommodate 'start-pinging' times etc of both instruments (the master and slave) for a DWH cast. The slave entries were left blank in the case of a BB cast. Separate logsheets (of the same format) were used for the DWH cast and the BB cast on each station.

## **Interference**

In deploying the DWH and BB LADCP systems simultaneously there was concern that interference from the pings of one in the returns of the other would cause data degradation. It was clear after the test cast (station 1) however, that the BB produced good velocity profiles during a DWH deployment. As a result both systems were used on each station throughout the cruise, except station

3 when the DWH were not deployed, and stations 97/98 when the SWH was not deployed. These latter stations offered the chance for a more careful examination of interference by comparing BB data from casts with and without simultaneous workhorse deployments.

The beam amplitudes from stations 3 (BB) and 2 (BB + DWH) are shown in Figures L1, L2, plotted as a function of ping number (equivalent to seconds) and bin number. All beams are shown for each bin, so that there are 16 bins each with four beams, making a total of 64 on the y-axis. The large regions of high returns at the beginning and end of each cast represent the subsurface scatter maximum in the water column. Below the scatter maximum the trend from higher to lower amplitudes with distance from the instrument becomes more apparent. In addition to this background gradient there are intermittent high return signals throughout the record, evident in white and pale grey. Figures L3, L4 show a deep region of each cast (approximately 2500-2800 m) in more detail. There are short high-amplitude signals, over only one bin of one ensemble present in station 2 and not in station 3. These are interference from the DWH pings. When the first and second BB pings are separated out (lower plots in Figure L4) we can distinguish a diagonal pattern of these interference signals, as they march through the BB bins at a constant but different rate for each ping interval.

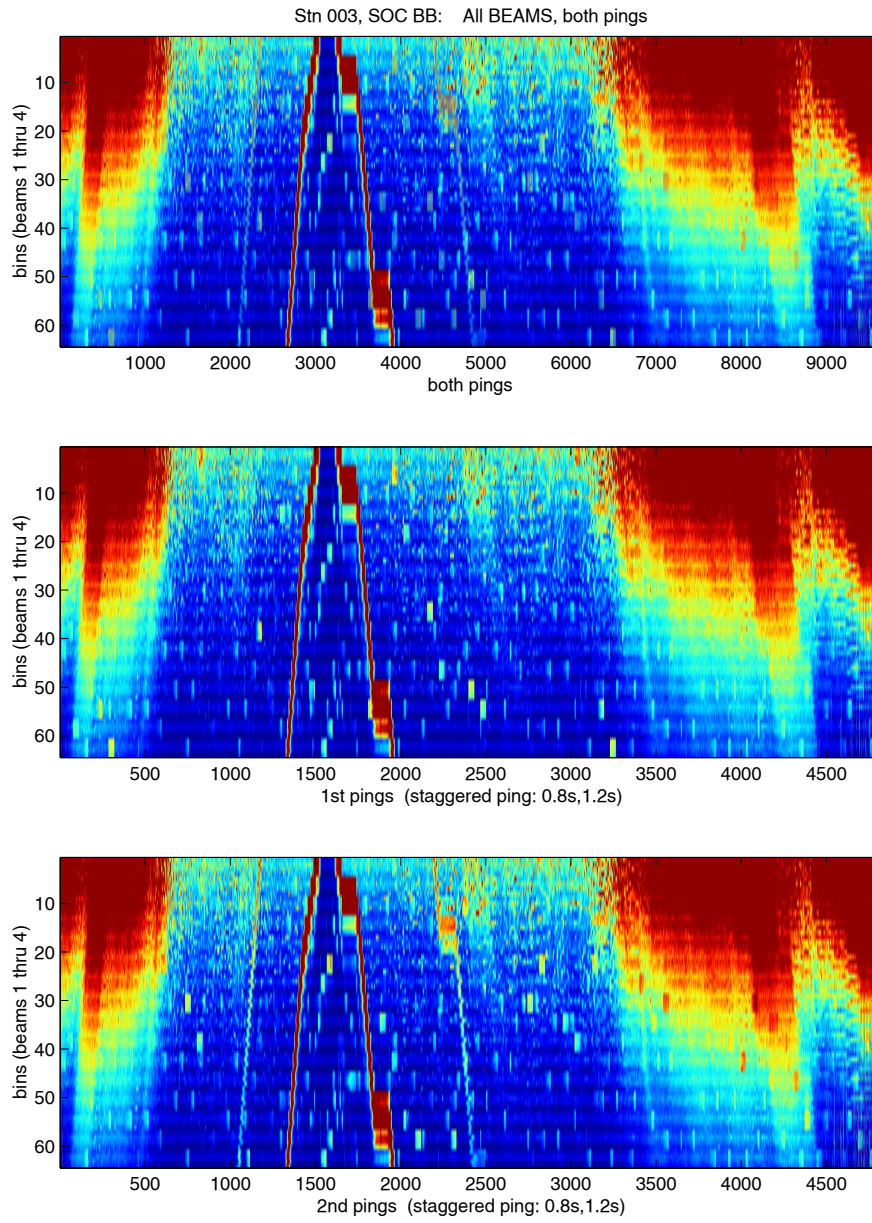
We can estimate the number of BB bins that are contaminated in two ways. First, by adding them up over the 300 pings shown in Figure L3, assuming it is a representative time segment. This indicates that 3.3% of the BB bins contain interference from the DWH pings. Second, by considering the relative ping rates and listening times of the instruments. The BB pings on average once per second and is set to sample 16 bins of 16 m each with a 16 m blank after transmit. Therefore it 'looks out' over 272 m which, taking the speed of sound as  $1500 \text{ m s}^{-1}$ , will require a travel (or listening)-time of 0.36 s. Meanwhile, the DWH has a ping rate of 0.77 s, since each workhorse pings every 1.54 s. Thus, over a period of 300 s the BB will collect  $300 \times 16$  bins of data and listen for 109 s, during which time the DWH will ping 142 times, leading to an estimate of 3.0% contamination. This is smaller than the estimate above taken from the data, because some pings contaminate more than one bin.

Station 97 has no SWH (up-looker) data. A detail of the beam amplitudes over 300 pings is shown in Figure L5. The data shows that contamination from MWH pings alone is about 2.1%, or two thirds the contamination from both workhorses.

## **Processing**

### *Firing Method*

The LADCP provides a full-depth profile of ocean current. However, to obtain the ocean current the unknown package motion must be removed during processing. In the Firing method, overlapping profiles of the vertical shear of horizontal velocity are averaged and gridded, to form a full-



2002- 3-29 19:46

Figure L1: Solo BB deployment: Beam Amplitudes



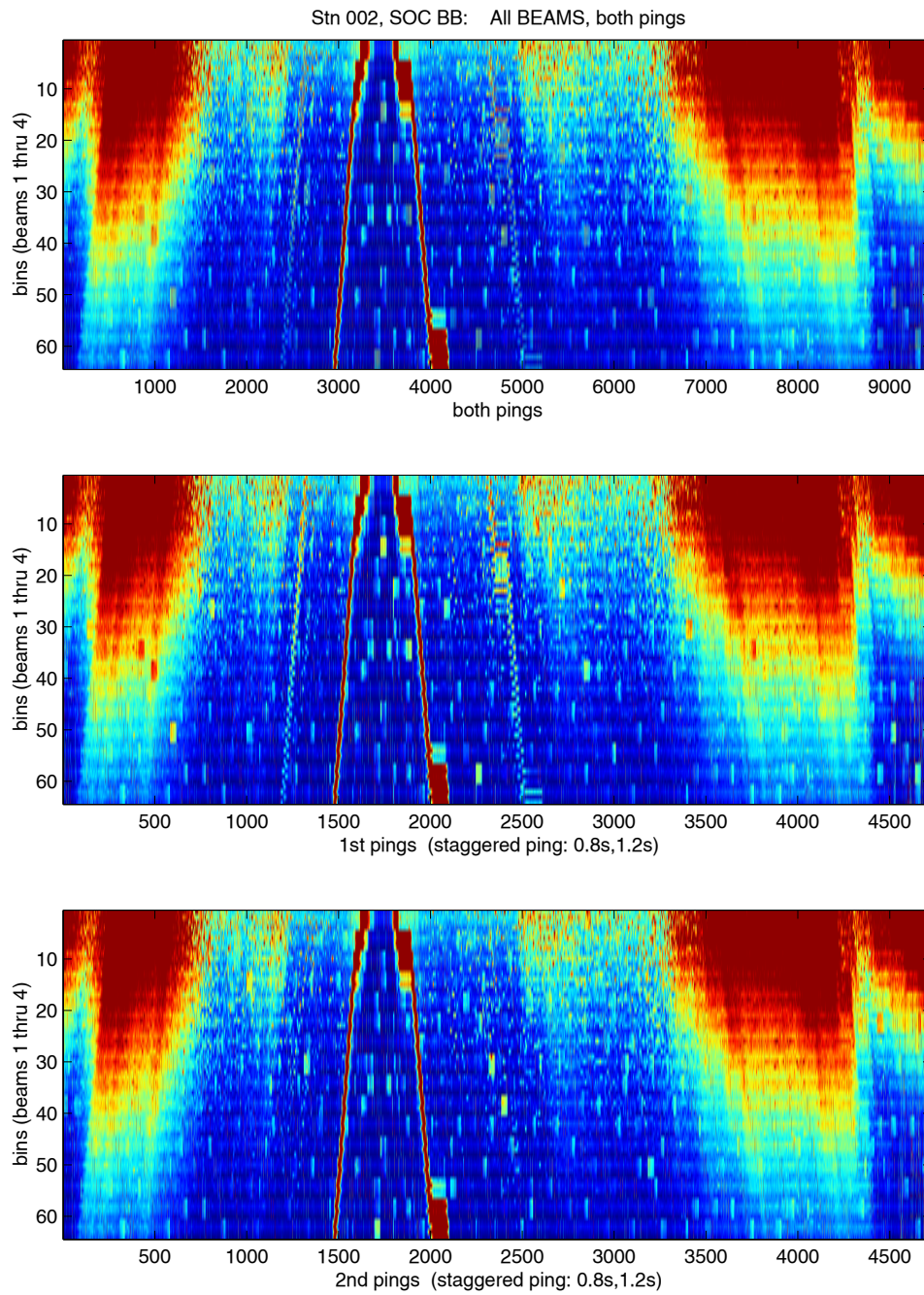


Figure L2: Combined BB and DWH deployment: Beam Amplitudes

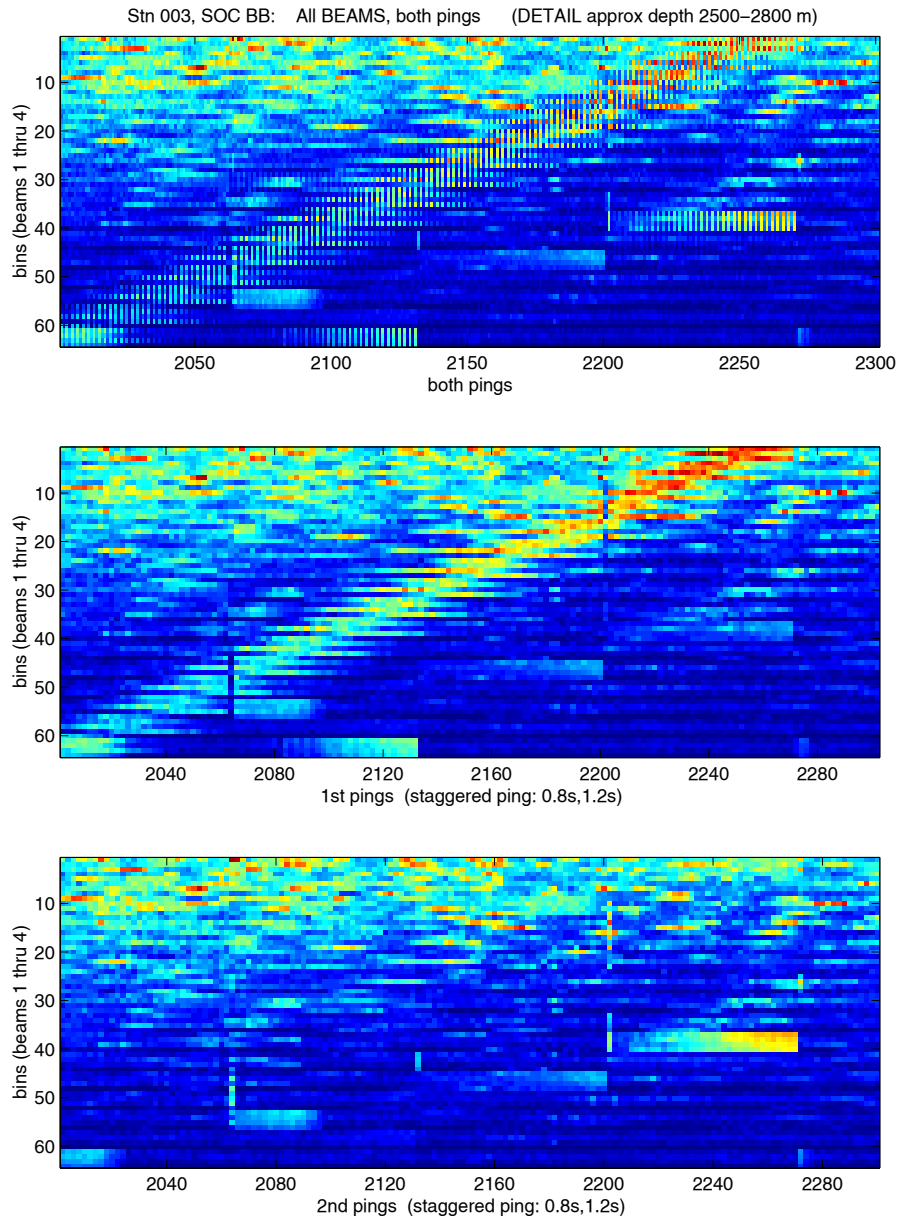


Figure L3: Solo BB deployment: Detail of Beam Amplitudes

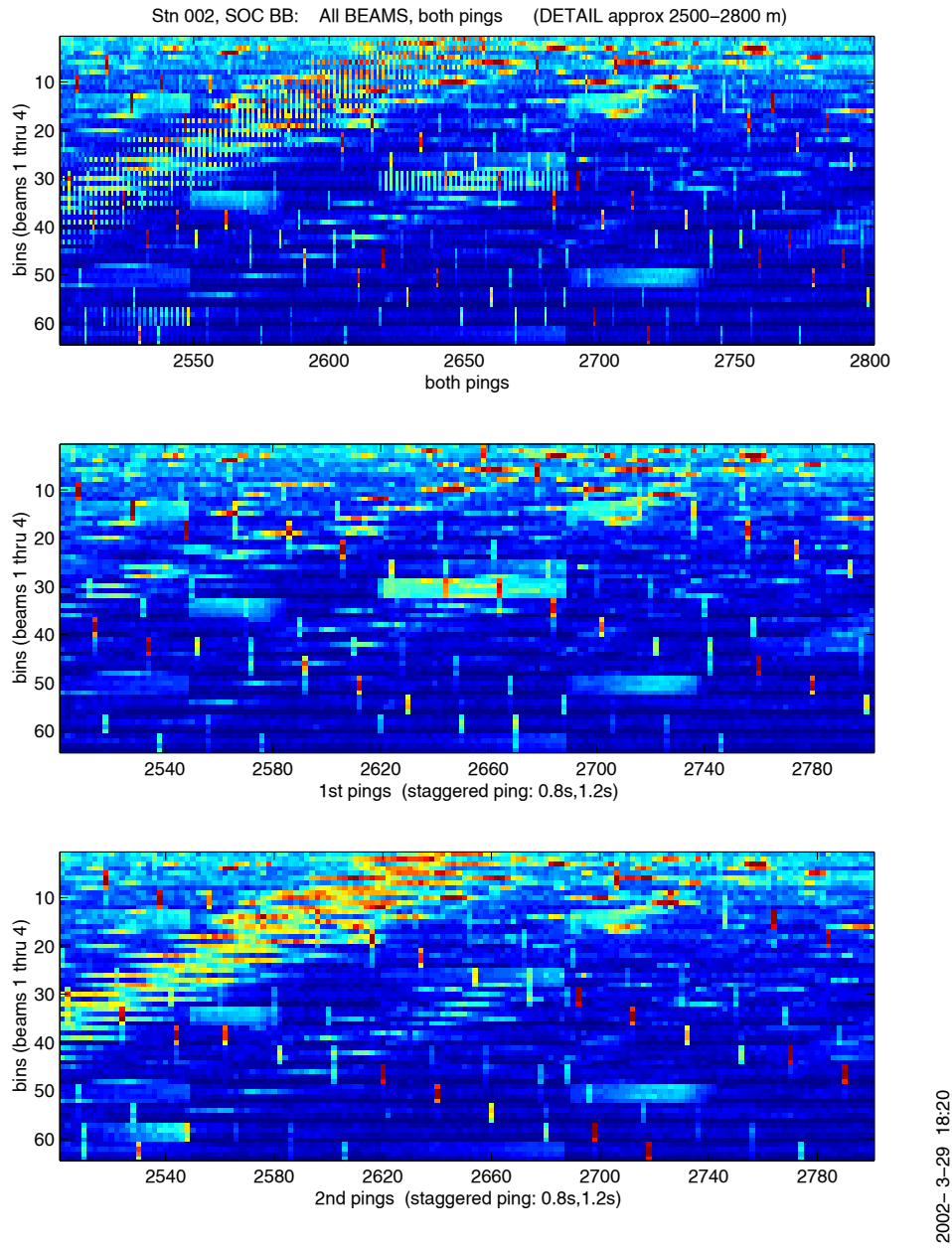


Figure L4: Combined BB and DWH deployment: Detail of Beam Amplitudes

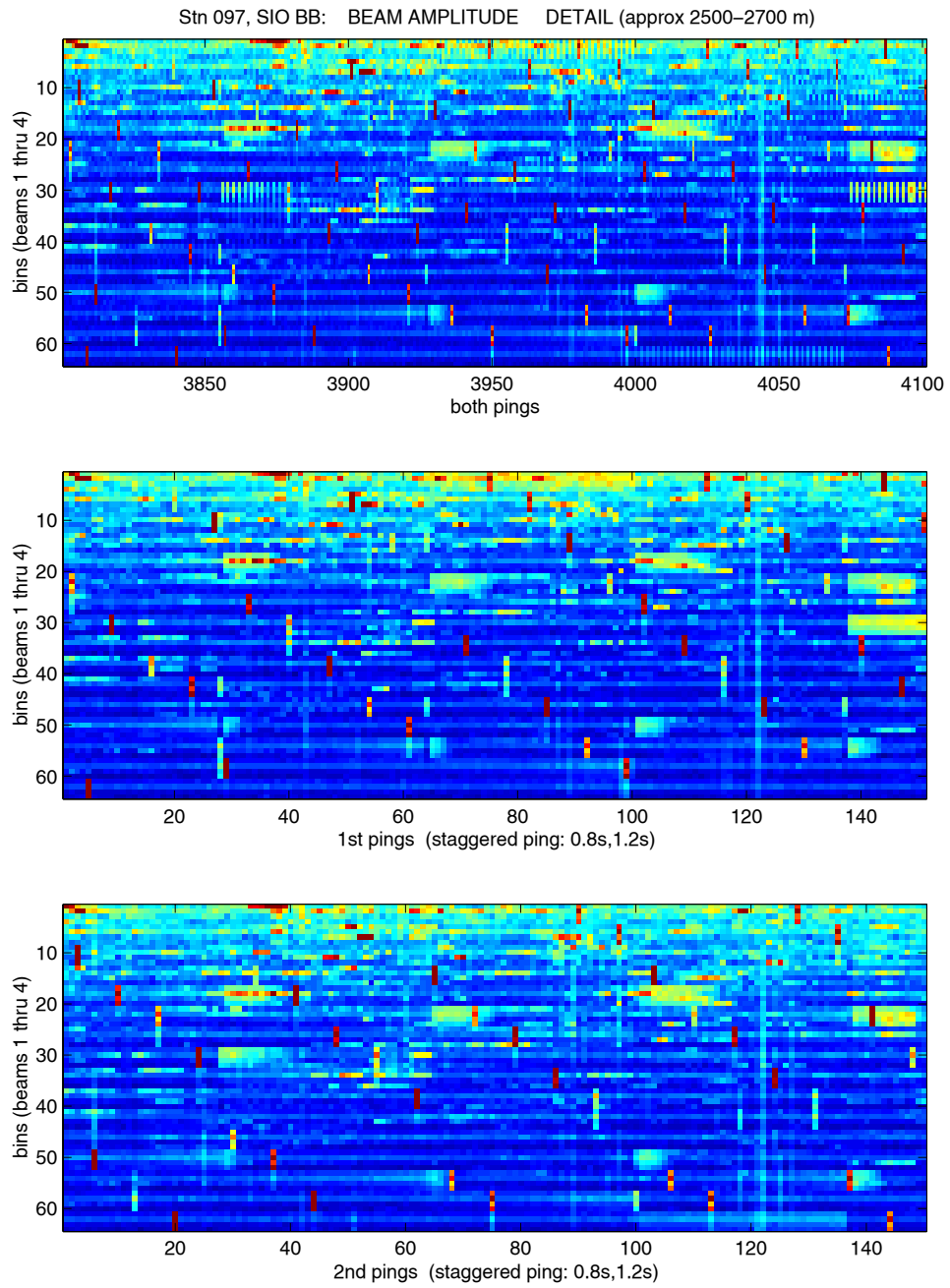


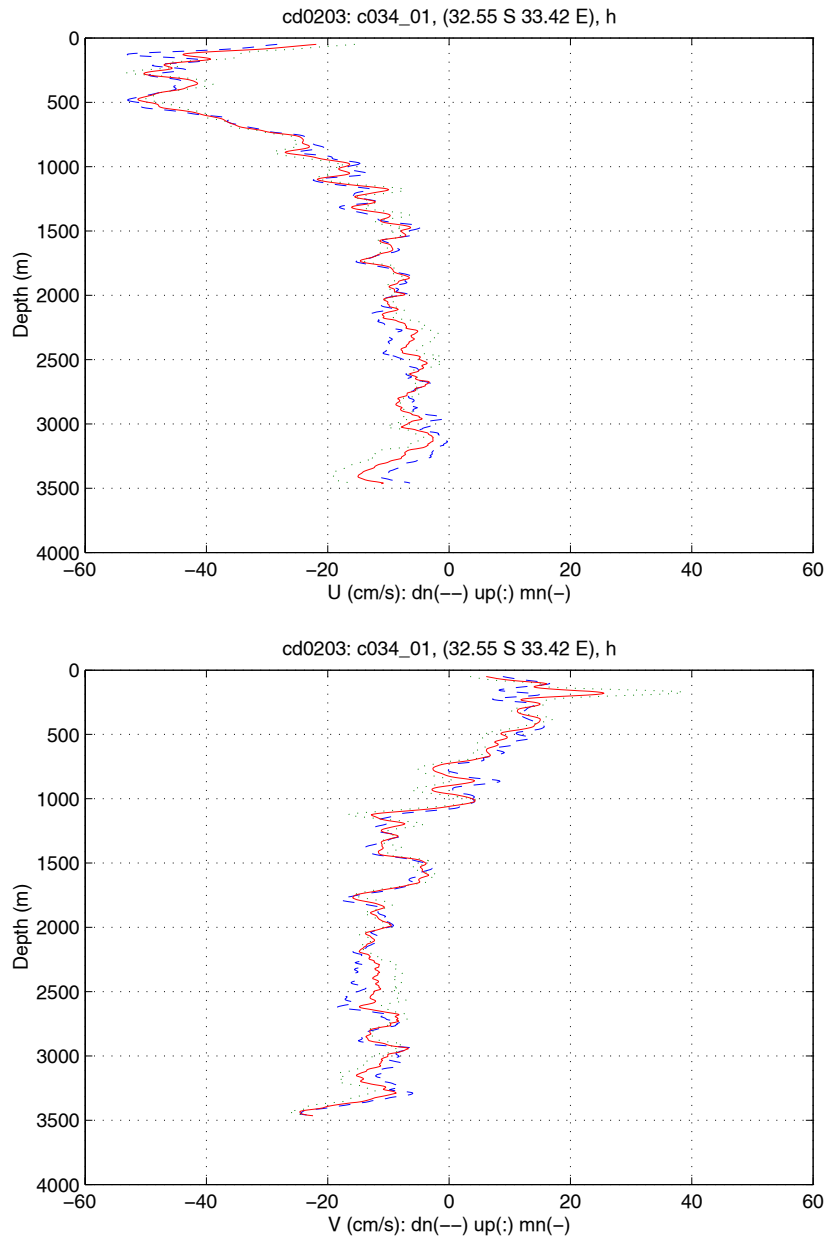
Figure L5: Combination BB and MWH deployment: Detail of Beam Amplitudes

depth shear profile. By differentiating individual profiles the constant velocity of the package has dropped out. The full-depth shear profile is then integrated vertically to obtain the baroclinic ocean velocity, and the resulting unknown integration constant is the barotropic (depth-averaged) velocity. This barotropic component is computed as the sum of the time-averaged, measured velocity and the ship drift (minus a small correction, less than  $1 \text{ cm s}^{-1}$ , to account for a nonconstant fall rate) (Fischer and Visbeck, 1993; Firing, 1998).

Errors in the baroclinic profile accumulate as  $\sum std/\sqrt{N}$  where  $N$  is the number of ensembles (Firing and Gordon, 1990). This error translates to the lowest baroclinic mode and, for a cast of 2500 m depth, it is about  $2.4 \text{ cm s}^{-1}$  (Beal and Bryden, 1999). The barotropic component is inherently more accurate, because the errors result from navigational inaccuracies alone. These are quite small with DGPS, about  $1 \text{ cm s}^{-1}$  (2 to  $4 \text{ cm s}^{-1}$  without). Thus, the errors in LADCP velocities are of the order of the expected oceanic variability, 3-5  $\text{cm s}^{-1}$  (Send, 1994), which is due primarily to high frequency internal waves.

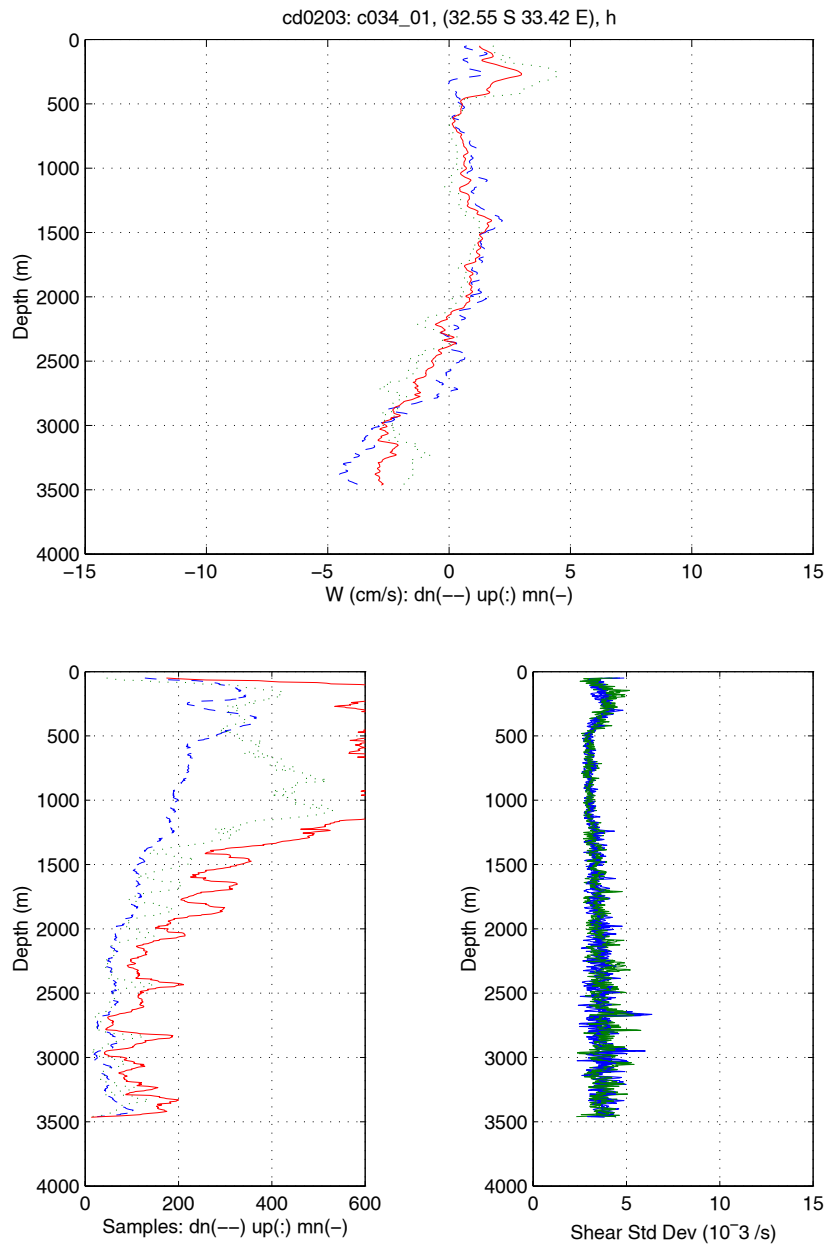
The Firing software was routinely used during CD 139 as the primary technique for obtaining final velocities. This is both because it is well established and because results from the new Visbeck technique were disappointing (see the next section). GPS and CTD data are required to produce final LADCP velocities and therefore Firing's software was slightly adapted by Brian King (BAK) to accommodate pstar data streams. The Firing software directory tree was set up under /data/ladbbuh. A copy of the step-by-step, first-pass processing sheet, as followed by LADCP watchkeepers during the cruise, can be found in the appendix. Typical BB profiles as output from Firing's method are shown in Figures L6, L7. The first figure shows down, up and mean velocity profiles in the east (U) and north (V) directions. The second shows the same for vertical velocity (W), plus plots of the number of shear samples and the ping standard deviation (of U and V shears) as a function of depth. Looking at vertical velocity is a useful proxy for the quality of the full-depth profile: if W is small (as we would expect for the ocean) then data quality is good. The standard deviation indicates the quality of the individual ping returns, which in the case of the BB are almost constant with depth.

A few of the processing steps used during CD139 were a little out of the ordinary and are described here. Bottom interference appeared at approximately 600 and 900 m off the bottom, affecting half the data in each case (at two depths because of the staggered ping). Therefore, a clip\_margin of 15 was set in mergeb\_1.cnt to cut out the affected data. Water (bottom) depth is used during Firing processing to predict the cut off depth of the full-depth velocity profile. It is initially estimated from the integral of vertical velocity, when scan.prl is run on the raw BB cast data, and output to file proc.dat. For final data during CD139, however, the absolute water depth was obtained from MWH height off plus CTD depth. Height off is one of the parameters of RDI bottom-tracked data, part of the data download from the MWH. The absolute water depth is output by Visbeck processing and, together with bottom-tracked velocities, saved in file C(stn)(run name).bot under the Visbeck directory tree. This depth is used to update proc.dat for a final processing run



2002-4-11 14:59

Figure L6: BB eastward and northward velocity profiles processed using Firing method



2002-4-11 14:59

Figure L7: BB vertical velocity, number of samples and standard deviation output from Firing method

(rerun domerge.prl and do\_abs.m). Final velocity data can be found under Firing's proc directory in /matprof/h/\*.mat. MWH bottom velocities are also saved here in matlab format.

We are very grateful to Firing who, immediately prior to the cruise worked on a modification to his software to enable merging of SWH and MWH data. The script, merge\_ud.m, together with required modified versions of two other mfiles, can be found under Firing's proc directory in /dual. To combine up- and down-looker data, 'dual\_system' and 'dual\_method' were set to 1 in matlab, and do\_abs was rerun calling the new scripts (by setting addpath('dual')). Unfortunately, due to the disappointing quality of the DWH data, little use was made of this.

### *Visbeck Method*

The Visbeck processing method has a theoretical advantage over Firing's method, because it does not calculate shear in order to remove the package motion. Thus, there is not the introduction of noise that the shear calculation inevitably causes. Nor is there a random-walk error associated with building up a full-depth shear profile. Instead, Visbeck poses an inverse problem to solve for the package motion using a least squares technique (Visbeck, 2002). The resulting problem is over-determined and as a result should produce robust velocities, provided the weights (or covariances) are considered carefully. Another advantage of the inverse method is that it is possible to add constraints, such as bottom-tracked data and shipboard ADCP data. Visbeck routinely uses RDI bottom-tracked velocities in addition to navigation data to constrain full-depth velocity profiles. Finally, the method allows processing of the Workhorse up- and down-looker data simultaneously.

The Visbeck software directory tree was set up under /data/ladbbvis and all processing steps were carried out from the vis\_ship/pro directory. Originally, Visbeck intended demo.m to be hand modified with position, time, data paths, control settings etc for each station and then run to carry out all the processing steps. In this case some front-end programs were written by BAK to pull in various data streams automatically. Time and position information is fetched from Firing's \*.scn files and from the RVS GPS datastream respectively, using shell script scanexec. Pstar CTD data is modified so that the timestamp has origin at the beginning of the year and then written out in ascii format using ctd\_timadj.exec. Then, the Visbeck processing is run in matlab by calling run\_laproc(stn), where stn is station number. This script was written by Lisa Beal and processes BB and DWH data, both with and without a bottom-tracked-velocities constraint. It calls some more front end (BAK) scripts which load the peripheral data, set paths and control parameters and then runs the Visbeck processing proper. An example of the full-depth velocity profiles output from the Visbeck method is shown in Figures L8, L9. The first figure (from a run with bottom-tracked velocity constraint) is output directly after processing and shows up/down/mean U and V profiles, plus number of samples, velocity error, target strength (like beam amplitude) and the ship drift on station. The latter figure (from a run without bottom-tracked velocity constraint) shows U and V in the same format as the



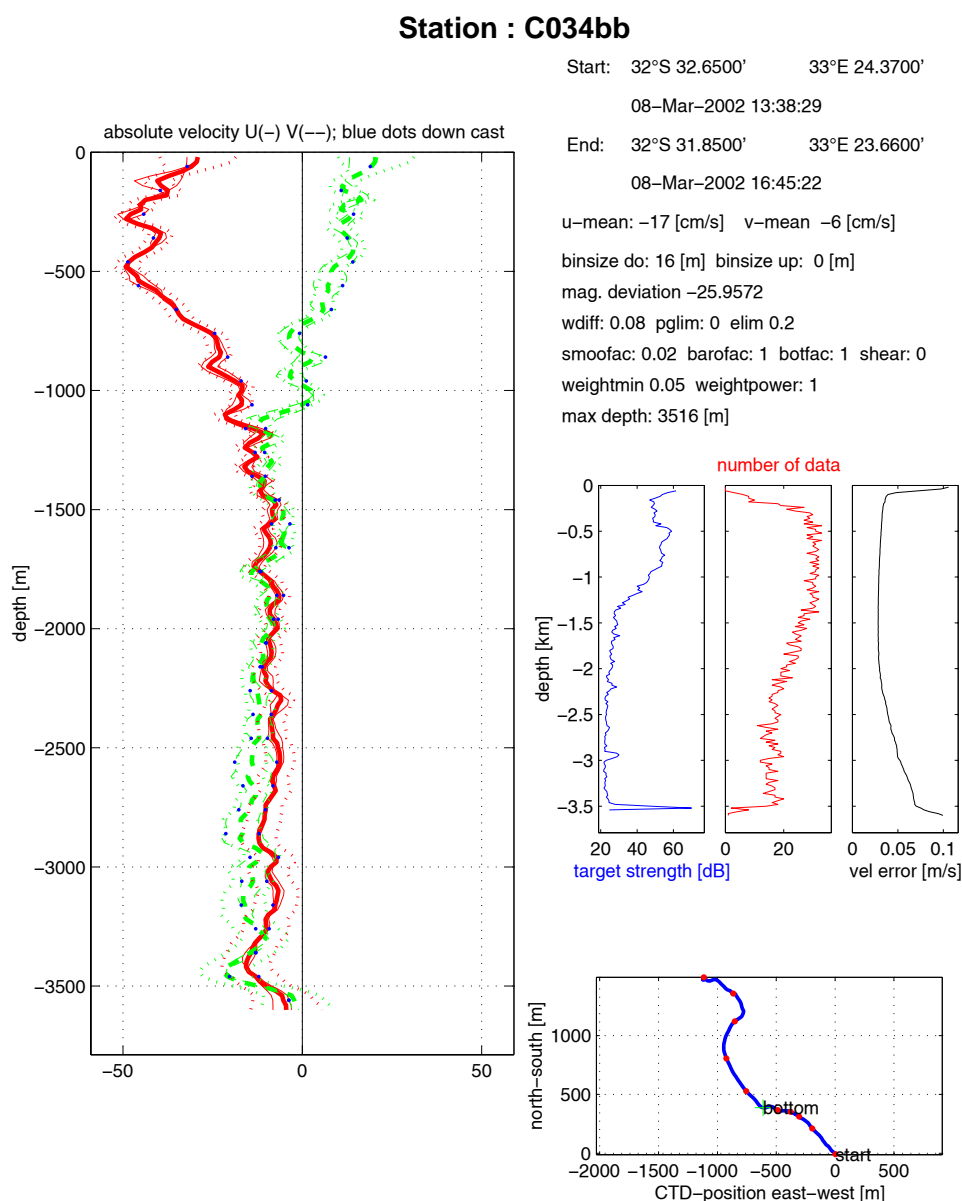


Figure L8: BB velocity profiles, data quality, and ship drift processed using Visbeck method

Firing output to allow a direct comparison.

The MWH collects RDI bottom-tracked velocities (processed internally from water-tracked pings) which are extracted and cleaned during Visbeck processing. If no RDI bottom-tracked velocities are available, as is the case for BB data, then they are estimated during processing, by examining the beam amplitudes to find the bottom returns. It was perceived (although not rigorously tested) that the RDI bottom-tracked velocities were more accurate than those processed from BB.

In practice the Visbeck method was not found to be an improvement over Firing's processing. BB data was processed using both methods, with each set up in a similar manner for a comparison

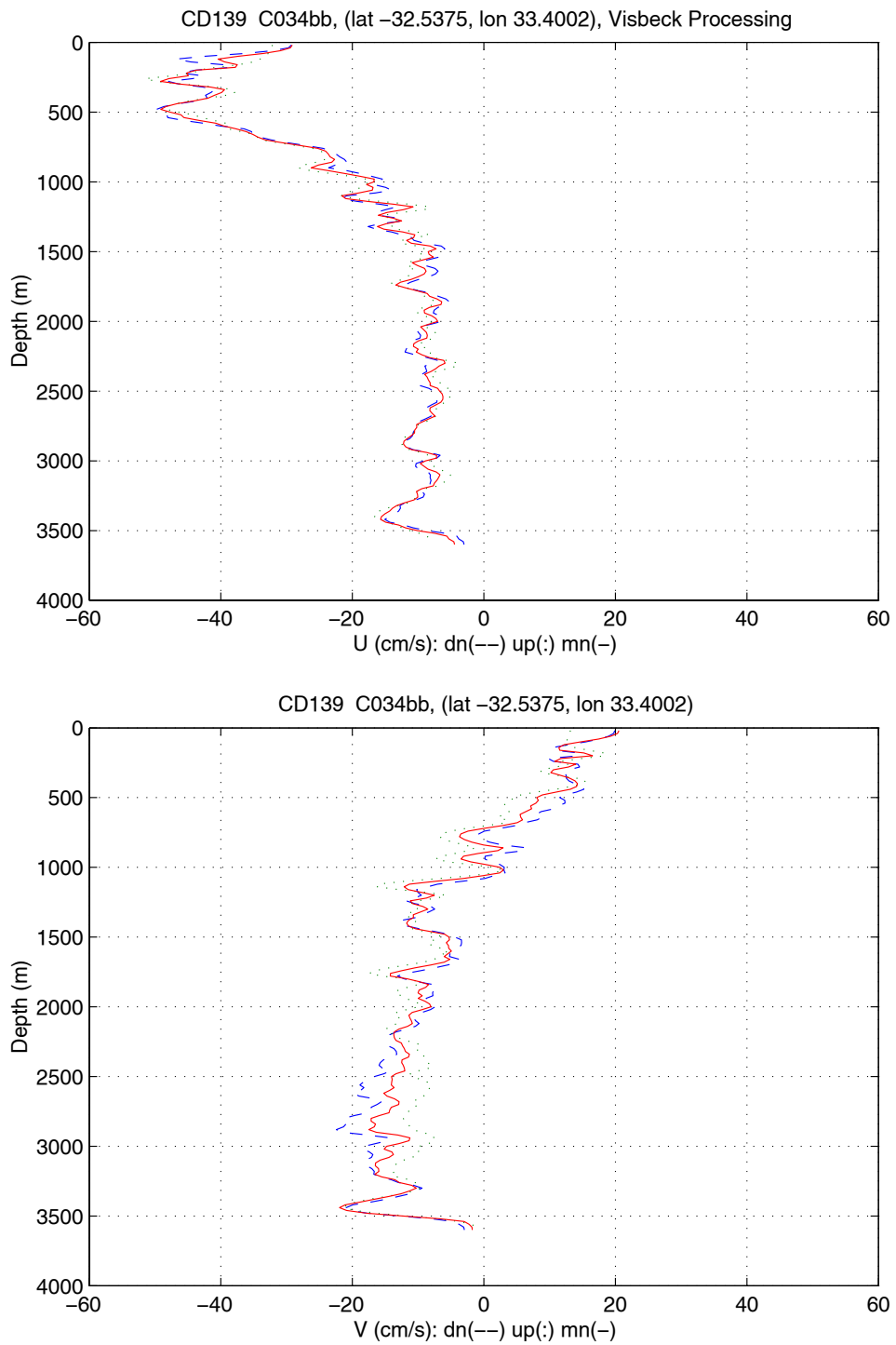


Figure L9: BB eastward and northward velocity profiles processed using Visbeck method

(GPS and CTD data were used, but not the additional bottom-tracked velocities in the Visbeck case). The Visbeck method routinely under-estimated the top-to-bottom shear of the ocean velocity profile, often by more than  $10 \text{ cm s}^{-1}$ . Moreover, it produced dissimilar up and down profiles which, when constrained to a single barotropic current from the navigation, results in the classic 'X-profile'. When produced from the Firing method such profiles are taken as an indication of uncertain velocities.

A new release of Visbeck's software was received via email about half way through the cruise. It has a number of modifications and bug-fixes which result in top-to-bottom BB shears which are much better matched to those from the Firing method. There are also some internal changes to the software which make it incompatible with old data files. As a result we implemented the new version in a new directory tree (`/vis_ship`) and began processing all the station data from scratch. There was not time to properly assess the performance of the upgraded software, but it is apparent that it is much improved and now provides a viable alternative to Firing's software.

The DWH data was processed together using Visbeck's method, but the results were disappointing due to poor data quality below 1500 m or so (see next section), where profiles tended to blow up to unrealistic bottom velocities. However, the DWH profiles were better handled by Visbeck's (modified) method than by Firing's. On a cautionary note, the Visbeck method can produce plausible looking velocity profiles (with totally manufactured shears) from bad data when the bottom-tracked velocity constraint is employed. We strongly recommend that processing is always run with this constraint off (`botfac=0`) as a first pass, so that bad data will not slip by unnoticed.

In conclusion, we are indebted to Eric Firing and Martin Visbeck who worked on additions and improvements to their software in time for this cruise, in response to feedback from BAK after taking the new DWH system to Drake Passage in November 2001. This report summarises achievements during CD139, but the software issue is by no means closed and discussions will continue subsequently.

## **Data Quality**

During the cruise there were a number of deployments made with unusual configurations in order to test (or try to improve) data quality. Some of these have been described above in the section on interference. Station 003 was deployed with BB alone (no DWH) to compare BB data with and without DWH interference. Stations 097 and 098 have no SWH (up-looker) deployment, allowing an assessment of its interference with the BB. For station 117 the DWH were configured with a 0.95 s ping rate, so that they were pinging at twice the rate of the BB. On station 134 DWH was deployed in a broader band mode, giving better quality pings but reduced range. Tests were also conducted on DWH compass error, because the poor DWH profiles appear to be dominated by biased errors, rather than random noise. Each workhorse was rotated in turn through  $360^\circ$  in steps of  $90^\circ$  per cast in order

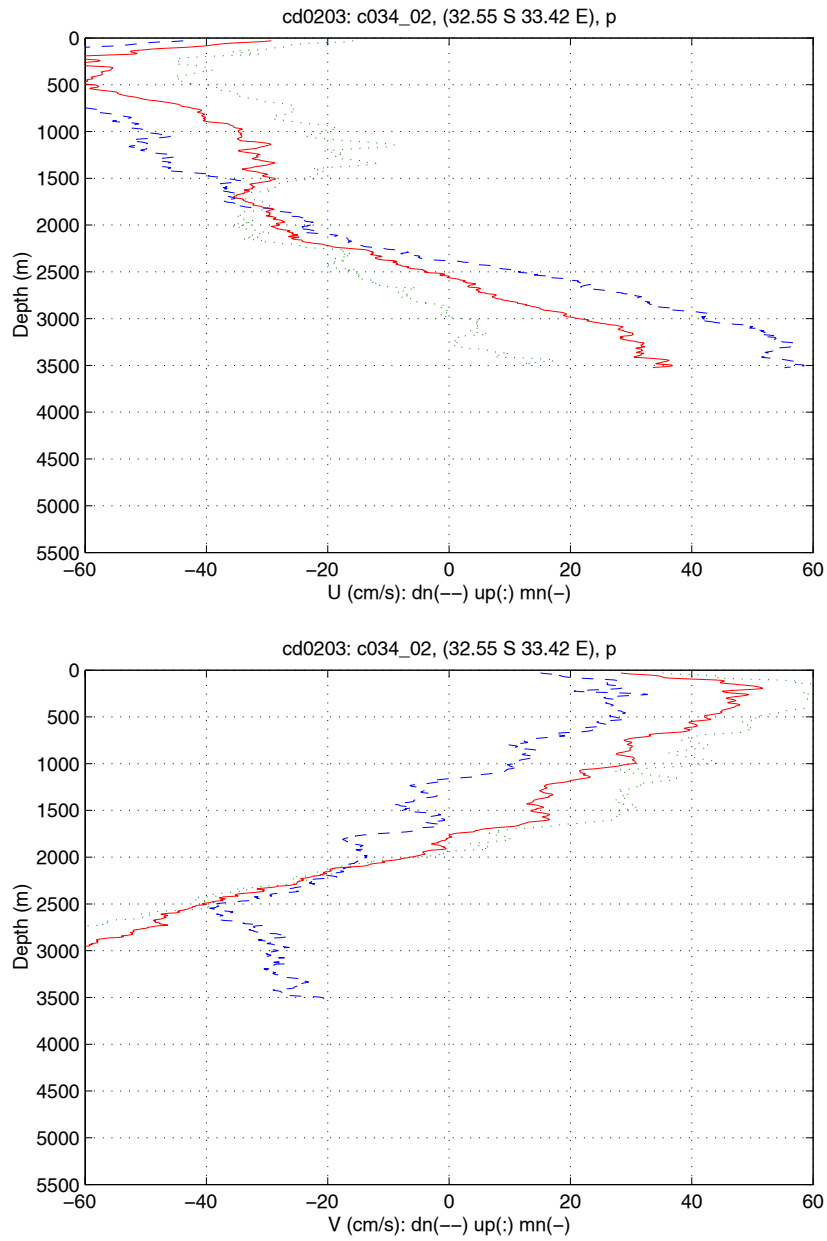
to untangle heading related errors. The BB configuration was not altered during the cruise (except for swapping from SOC to SIO instruments at station 062), since it was considered optimum.

Results from the compass tests and from stations 117 and 134 are described in the DWH section below, beginning with a summary of the instruments' general performance. Following this the BB is assessed by comparing its velocity profiles to on-station shipboard ADCP and to bottom-tracked velocities. Finally the two systems, BB and DWH, are compared quantitatively for range and ping quality.

### *Dual Workhorse*

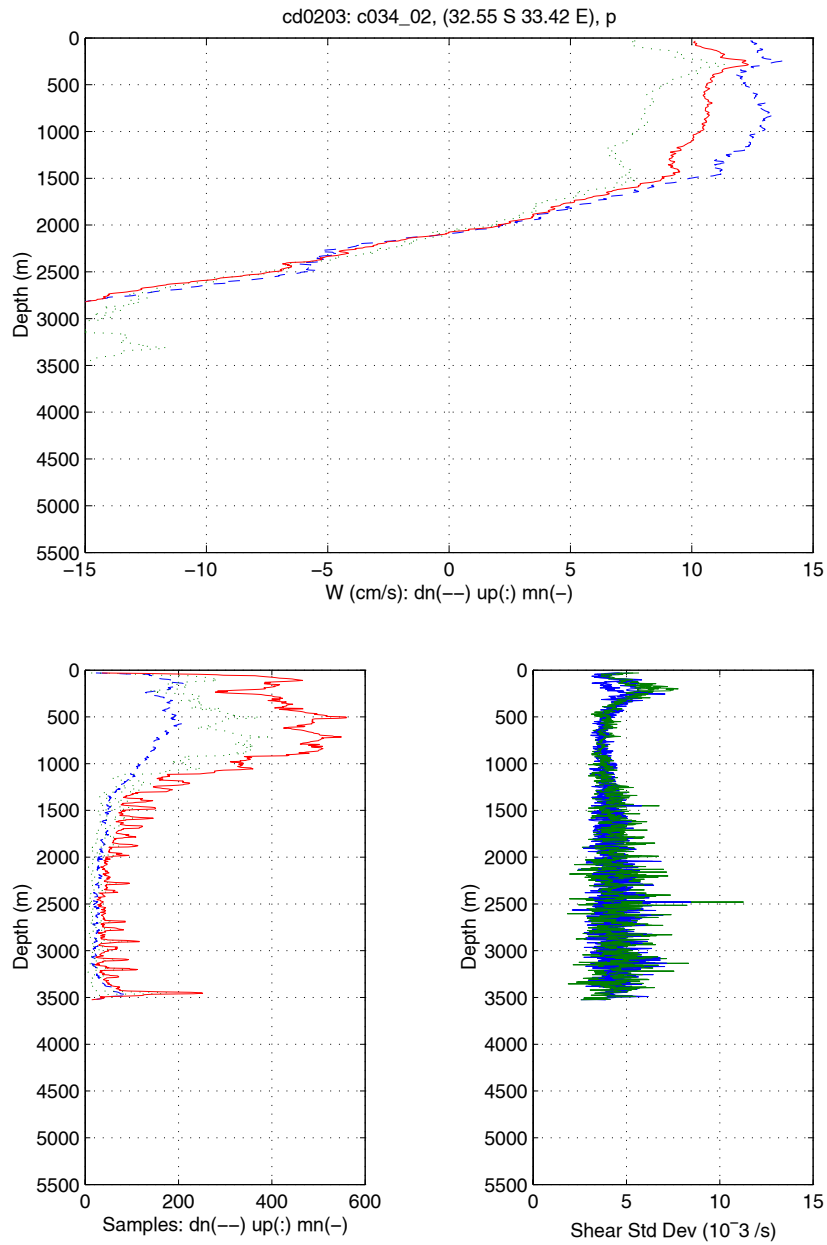
In general the workhorses performed very poorly. DWH data from the Agulhas Current was the best quality, with most profiles resembling their BB counterparts. This is because the stations were relatively shallow. There was no evidence that the DWH provided better data than the BB, however. Elsewhere, DWH velocity profiles blew up in deep water, exhibiting unrealistically strong, unidirectional shears and large bottom velocities. For example, Figures L10, L11 show a typical DWH profile as processed by the Firing dual method. The workhorses were not getting enough returns (samples) below about 1500 m to maintain a good full-depth velocity profile from the Firing shear technique. There is some improvement using Visbeck's inverse technique (Figure L12), probably because strong shears are penalised, but still the profiles compare unfavourably with the BB profile. Note that the Visbeck solution should be treated with caution when implementing the bottom-tracked velocity constraint. By pulling in the blown up deep velocities the constraint can make a bad profile look plausible. This is dangerous because, as Figure L13 shows, the deep shears are manufactured.

There seems to be two issues. The first is that the WHs suffer from a much greater loss of ping returns in the deep water than does the BB. Often the number of DWH (both 300 kHz instruments) returns per 5 m depth bin (of the full-depth profile) drops to less than 50 below 1500 m (the up-looker always performs worse), whilst the BB collects 100 or more. Evidently, the higher frequency WH signal does not scatter as well from deep marine particles as the lower frequency BB. The second is that the individual WH pings are of lower quality in the deep water (about 34% higher standard deviation) than the BB pings. As a result we would require more returns (twice as many) to obtain a full-depth profile of the same quality as the BB, whereas we are actually obtaining far fewer. This second issue could perhaps be alleviated by choosing a higher ping rate and/or smaller bins. However, the fact that the quality and number of the DWH returns is compromised in deep water to a much greater extent than those of the BB must be based on the physics of deep marine scatterers and is therefore insuperable.



2002-4-1 18:26

Figure L10: DWH eastward and northward velocity profiles processed using the Firing method



2002-4-1 18:26

Figure L11: DWH vertical velocity, number of samples, and variance processed using Firing method

## Station : C034dwh

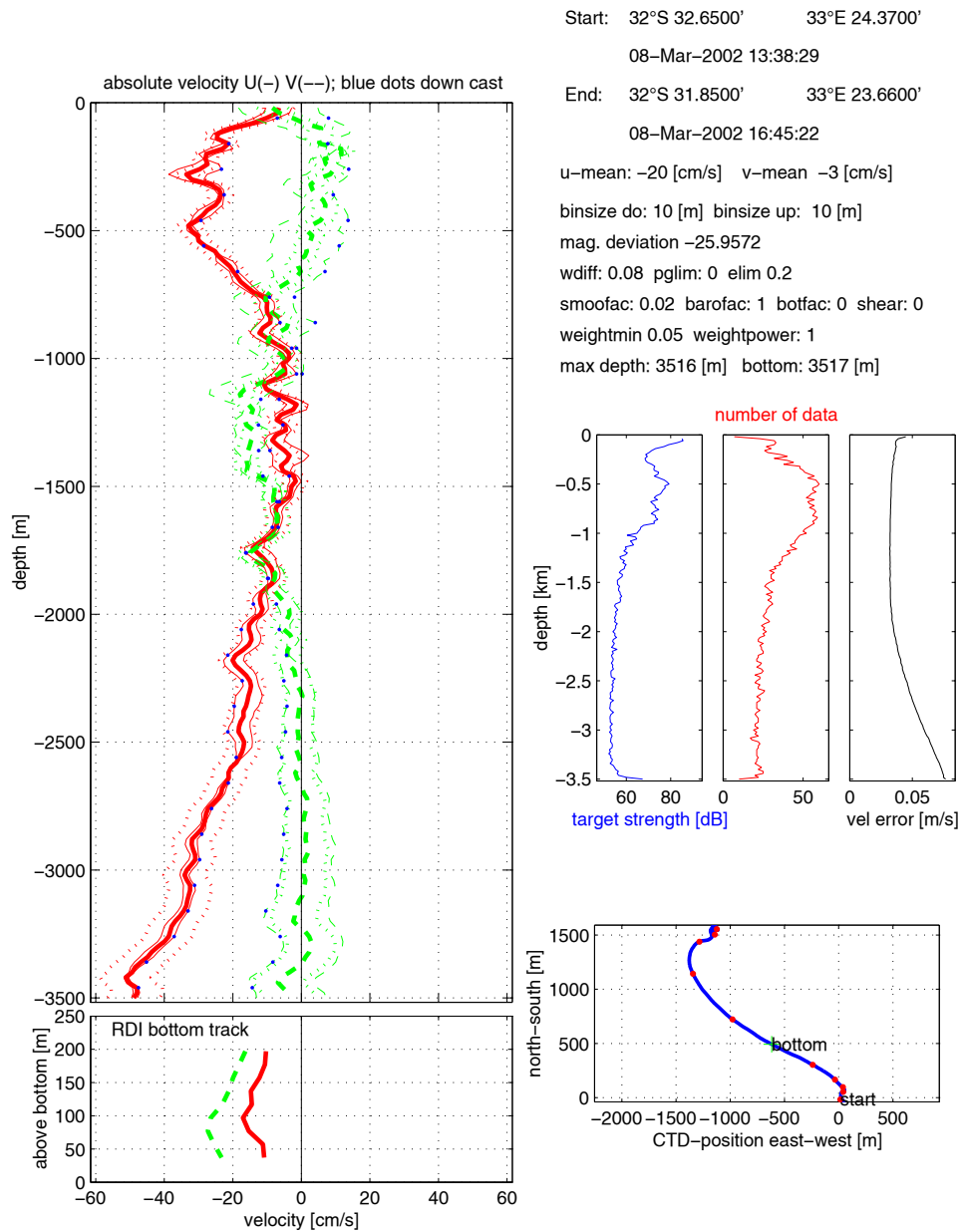


Figure L12: DWH velocity, data quality and ship drift processed using Visbeck method without bottom-tracked velocity constraint

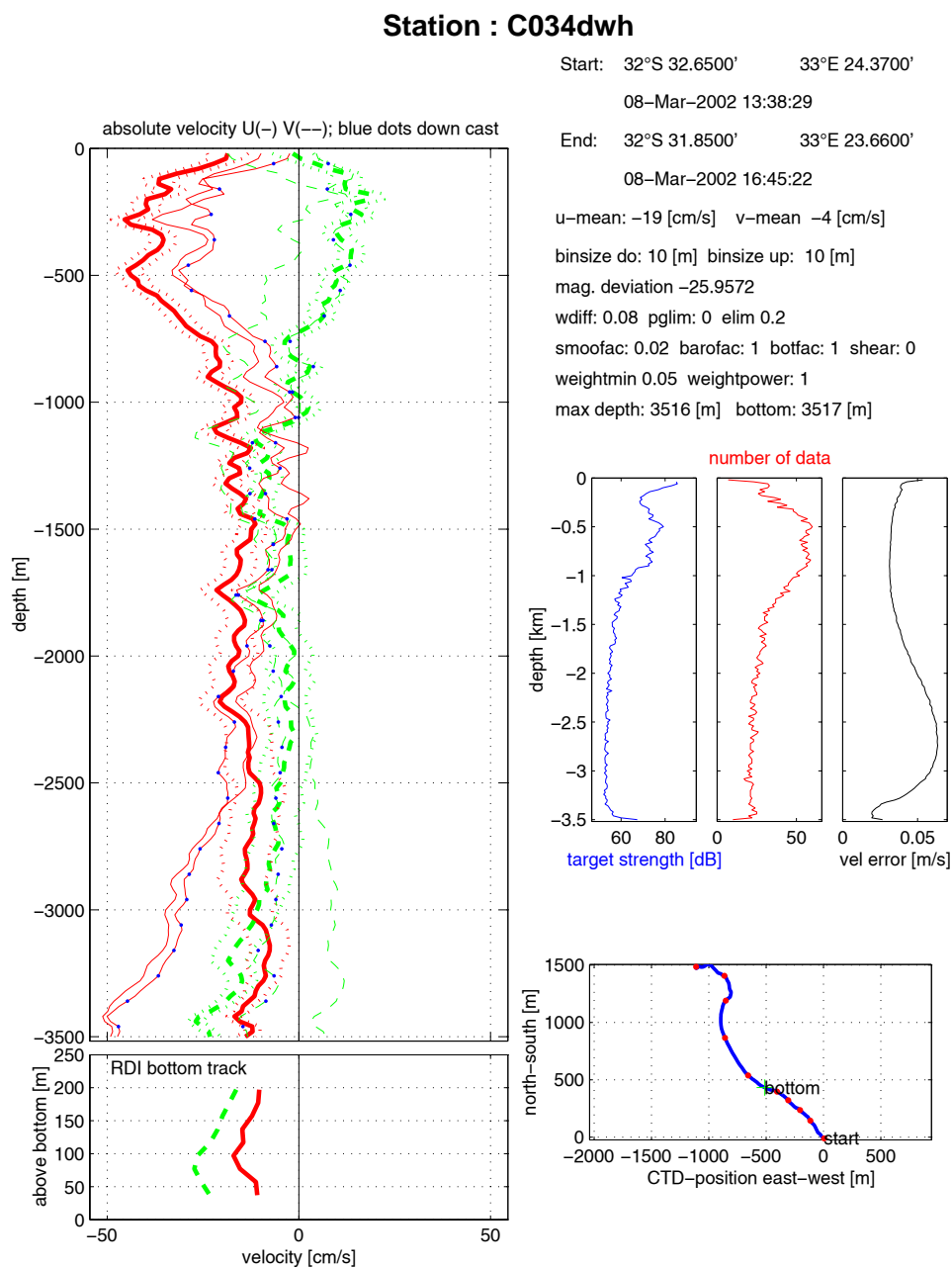


Figure L13: DWH velocity, data quality and ship drift processed using Visbeck method WITH bottom tracked velocity constraint



### Fast ping deployment

The motivation for a fast ping deployment of the DWH was to even out the mean standard deviation statistics of the 5 m shears with those from the BB. It was noted that the deep shear standard deviation (per ping) of the DWH was about  $4.7 \times 10^{-3} \text{ s}^{-1}$ , while that for the BB was  $3.5 \times 10^{-3} \text{ s}^{-1}$ . By dividing the square of these terms, this implies that the number of DWH samples required to obtain data of equal quality to the BB is 1.8 times the number of BB samples collected. Therefore the DWH were set to ping every 0.95 S, providing more than twice the number of BB pings. This was accomplished by re-setting the ping interval (TP) in the command file to zero and reducing the wait time (SW) of the asynchronous ping to 0.3 s.

The results from station 117 were disappointingly similar to previous casts. Qualitatively there did appear to be some improvement, with more realistic fine scale shears, but there is still a bias, in this case in the V component, which dominates the data and blows up the deep velocities. The bias could be related to a mean package tilt.

### Broader bandwidth deployment

There are two modes of deployment for the workhorses: mode 0 (LW0) is the default broad bandwidth configuration and mode 1 (LW1) is a narrower bandwidth pulse with a greater range, but increased standard deviation. When using the DWH as a lowered system mode 1 is recommended (Visbeck, 2001), and this is how the instruments were deployed in the main. On station 134 the DWH was switched to mode 0. The motivation was that since the DWH were losing so much range at depth, is it not better to have better quality pings at the expense of more range? The answer is emphatically, no. Below 2000 m depth the DWH in this mode collected no good samples and there was complete data drop out. This was surprising, since it implies that even those data in bins right next to the instruments were flagged bad.

### Dual Workhorse heading related compass errors

An investigation was carried out into the magnetic compasses of the WHs. The motivation is that heading related and relative compass errors of the two instruments play a large part in resulting velocity profile errors.

From the analysis that follows, we expected to be able to determine the instruments compass errors. Unfortunately, the results are puzzling, as will be described. The experiment consisted of comparing differences of reported heading between the two instruments, with the instruments being rotated in their clamps between casts.

The instrument headings returned by the compasses are subject to errors from two sources. First, distortion of the local magnetic field by the CTD frame and possibly by the instrument itself,

and second, instrumental error whereby it fails to measure the local field perfectly. Let the local field error, presumed to be caused chiefly by the influence of the frame, be denoted by  $F$ . Let the instrument error be  $I$  and the measured heading be  $H$ . Then at some instant, the true heading  $T$  of the underwater package (e.g. the direction in which the fin was pointing) is given by

$$T = H + O + F + I \quad (1)$$

where  $O$  is the offset between beam 3 of the instrument and the nominal true package heading. The sense of  $F$  and  $I$  is that they are corrections that must be applied. All elements of (1) are dependent on time  $t$ , except for  $O$ . We assume that  $F$  is a function of  $T$ . That is to say, whenever the package points in the same direction,  $F$  has the same value. We also assume that  $I$  is a function of  $H$ : whenever the instrument measures a heading of, say  $90^\circ$ , it will be subject to a reproducible error. Thus, in full,

$$T(t) = H(t) + O + F(H(t)) + I(H(t)) \quad (2)$$

Now (2) applies for both uplooker (subscript 1) and downlooker (subscript 2) instruments,

$$T = H_1 + O_1 + F_1(T) + I_1(H_1) = H_2 + O_2 + F_2(T) + I_2(H_2)$$

Taking the difference of the two equations, and noting that the true package heading is the same for both instruments, gives

$$H_1 H_2 = O_2 O_1 + F_2 F_1 + I_2 I_1. \quad (3)$$

Suppose that  $H_1 - H_2$  has been measured for a complete range of headings, with instrument positions we will denote by subscript A. (Note on many casts, the package completes one or more complete rotations, but on some casts this was not the case.) Thus,  $H_1 - H_2$  is considered to be known as a function of  $T$ . Now suppose that one of the instruments is rotated on the frame, and the new geometry is denoted by B. To preserve generality, we will suppose that each instrument is rotated by an amount  $\delta$  counterclockwise viewed from above. Of course, for any adjustment we chose to keep either  $\delta_1$  or  $\delta_2$  as zero, rotating just one instrument. Thus, on cast A

$$T = H_1 + O_{1A} + F_1(T) + I_1(H_1),$$

and on cast B

$$T = H_1 + O_{1B} + F_1(T) + I_1(H_1),$$

where  $O_{1B} = O_{1A} + \delta_1$  and similarly,  $O_{2B} = O_{2A} + \delta_2$ .

Consider (3) for two casts before and after a rotation. At some true package heading (estimated from the uplooker, for instance, by assuming that  $F$  and  $I$  are small),

$$H_{1A} - H_{2A} = O_{2A} O_{1A} + F_{2A}(T) F_{1A}(T) + I_{2A}(H_{2A}) I_{1A}(H_{1A})$$

$$H_{1B} - H_{2B} = O_{2B} O_{1B} + F_{2B}(T) F_{1B}(T) + I_{2B}(H_{2B}) I_{1B}(H_{1B})$$

Subtract these two equations to discover the change in  $H_1 - H_2$ . Assuming that the error terms are small, we can write, for example,  $H \sim TO$ , so  $I(H) \sim I(T - O)$ ,

$$\begin{aligned} (H_{1B} - H_{2B})(H_{1A} - H_{2A}) = & \\ & + \{(O_{2B} - O_{2A})(O_{1B} - O_{1A})\} \\ & + \{(F_{2B}(T) - F_{2A}(T)) - (F_{1B}(T) - F_{1A}(T))\} \\ & + \{I_{2B}(T - O_{2B})I_{2A}(T - O_{2A})\} \\ & - \{I_{1B}(T - O_{1B})I_{1A}(T - O_{1A})\}. \end{aligned}$$

Now assume  $F_{1B}(T) = F_{1A}(T)$  and  $F_{2B}(T) = F_{2A}(T)$ , *i.e.* the frame induced error is assumed to be unchanged by rotation of the instrument in the frame, then

$$\begin{aligned} (H_{1B} - H_{2B})(H_{1A} - H_{2A}) = & \\ & + \{\delta_2 \delta_1\} + zero \\ & + \{I_{2B}(T - O_{2A} - \delta_2)I_{2A}(T - O_{2A})\} \\ & - \{I_{1B}(T - O_{1A} - \delta_1)I_{1A}(T - O_{1A})\}. \end{aligned}$$

Now, we also assume that the functional form of  $I(H)$  has not changed, so  $I_1$  and  $I_2$  do not need subscript A or B. Finally if, for example  $\delta_1$  is zero, then the last line of the above equation is zero, so

$$(H_{1B} - H_{2B})(H_{1A} - H_{2A}) = \delta_2 + \{I_2(T - O_{2A} - \delta_2)I_2(T - O_{2A})\} \quad (4)$$

Thus the double difference (change in heading differences) resulting from the rotation of an instrument in the frame has a mean offset equal to the rotation of the instrument, and a functional form (as a function of  $T$ ) that arises from a phase shift of  $I_2$ .

Next, we observe that the left hand side (LHS) of (4), is found to be roughly sinusoidal in shape, with amplitudes up to 5 degrees either side of the mean. If  $I = \sin(H)$ , then LHS should be described by a sine curve, however this did not fit the results satisfactorily. Therefore assume,

$$I(H) = A_1 \sin(H + \phi_1) + A_2 \sin(2H + \phi_2).$$

In principle, the four coefficients  $A_1, A_2, \phi_1, \phi_2$  can be determined from a single rotation of amount  $\delta_2$ . Indeed, it was found that this functional form fitted the measurements very well. The residuals of LHS after fitting were invariably less than  $1^\circ$ . Now,

$$\sin(H - \delta) \sin(H) = 2 \cos(H - \delta/2) \sin(-\delta/2)$$

and (4) becomes,

$$\begin{aligned} LHS - \delta_2 = & \\ & 2A_1 \cos(T - O_{2A} + \phi_1 - \delta_2/2) \sin(-\delta_2/2) + 2A_2 \cos(2(T - O_{2A}) + \phi_2 - \delta_2) \sin(-\delta_2). \end{aligned}$$

Table L1: Rotations and switches of Workhorse LADCPs during CD 139

Orient- ation	Station range	H1-H2 (degs)	O1 (degs)	O2 (degs)	$\delta_1$ (degs)	$\delta_2$ (degs)	Comments
A	001-028	183	39	222	39	0	M 1855, S 1881
B	029-076	222	0	222	0	0	S CW*
C	077-079	320	0	320	0	98	M 90° CCW
D	080-084	34	0	34	0	172	M 90° CCW
E	085-106	125	0	125	0	263	M 90° CCW
F	107-112	34	91	125	89	263	S 90° CCW
G	113-126	128	91	219	91	357	M 90° CCW <sup>†</sup>
H	127-131	37	182	219	182	357	S 90° CCW
I	132-135	305	274	219	274	357	S 90° CCW
J	136-141	307	272	219	272	357	M 1881, S 1855 <sup>‡</sup>
K	142-146	37	272	182	272	357	S 90° CW

Table notes: *M* is master workhorse, *S* is slave. Instruments are identified by serial numbers 1881 and 1855. All rotations  $\delta$ , are given relative to configuration B. \*SWH turned to put CTD wire between beams. <sup>†</sup>MWH back to its original position. <sup>‡</sup>Instruments switched top-to-bottom. (Values of  $\delta_1$  and  $\delta_2$  in orientation J were determined by comparing offsets between MWH and BB on stations 135-141.)

The unknown coefficients and phases were determined from the lowest two modes of an FFT of  $(LHS - \delta_2)$  in Matlab. Note that if  $\delta_2$  is exactly  $180^\circ$ , the  $\cos(2H)$  term cannot be determined.

A series of adjustments to the WH positions was made, as summarised in the table, to attempt to solve for the unknown amplitudes and phases of the instrument error.

If all our assumptions were correct, any move of the MWH should enable us to determine the SAME  $A$  and  $\phi$  coefficients for  $I_2$ . However, we don't find this is to be the case. Instead different coefficients are found for different orientations (A to J) of the two instruments. One or more of the assumptions must be wrong. At present, we consider the most likely difficulty to be the assumption that when the master is rotated,  $F_2(T)$  is unchanged. We also need to consider that the problem may arise from comparing  $H_1(T + O_1)$  with  $H_2(T + O_2)$ , when in fact it should be  $H(T + O + F + E)$ , although we expect this effect to be small.

The goals of this piece of work have not been achieved as of the end of the cruise. However, the experimentation with instrument orientation, and the mathematical description of the problem described here has laid the groundwork to be able to solve for instrument compass errors back at SOC.

### *Broadband*

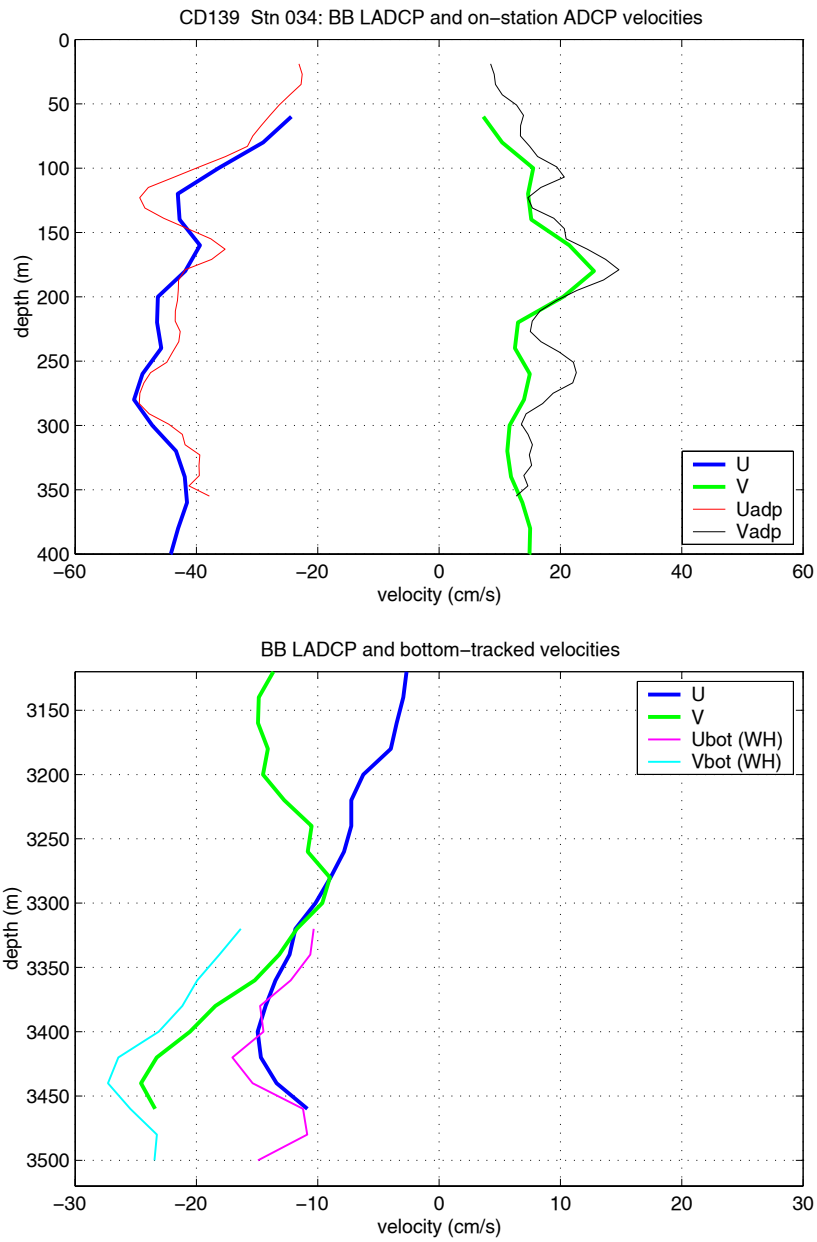
The broadband data, in comparison to the DWH, is very good. However, there may be large errors, especially on deep casts, and these are highlighted by comparing the BB full-depth profile with independent observations at the surface and at the bottom. These comparisons have been done qualitatively (see Figure L14), but a more thorough post-cruise statistical analysis is required. On-station ADCP velocities were, almost without exception, well matched (within  $4 \text{ cm s}^{-1}$ ) to the BB profiles. At the bottom, both RDI bottom-tracked velocities from the MWH and processed bottom-tracked velocities from the BB were used to compare to the BB full-depth profile. About 45% of the profiles matched to bottom-tracked velocities within  $5 \text{ cm s}^{-1}$ . The deeper the cast, the larger the W velocities at the bottom, and the worse the match appears (although this is not always the case). Deep stations suffer from increases in velocity error not only because of the random walk of the single ping standard deviation when ensembles are strung together for the full-depth profile (see processing section), but also because the standard deviation itself increases with depth and the range decreases.

As outlined in the processing section above, the dominant errors in the Firing-processed BB data propagate into the first baroclinic mode. The barotropic velocity is known really quite well, since it is dominated by ship drift which is determined by GPS positioning and not by the BB. Therefore, we strongly advise that BB profiles be adjusted to better match ADCP and bottom-tracked data using constant shear and not constant velocity.

It is worth mentioning here again that the Visbeck processing method will not suffer from errors introduced by the calculation of shear, or by the random walk described above. The LADCP community is in agreement that the inverse method is an advance from the Firing shear method. A few bugs were apparent in the original version of Visbeck's software however, which caused a large underestimate of the shears, as described above. A modified version of the software was received half way through the cruise, so that by the time the new version was set up, tested, and station processing got up to date (Visbeck's processing is significantly slower than Firing's) there was not sufficient time to investigate the quality of the profiles. It is clear that the profiles are much improved and may provide a better estimate of the ocean velocity, particularly on deep stations. A comparison of Visbeck profiles to SADC and bottom-tracked velocities is needed, as done for the Firing profiles during the cruise.

### *Performance statistics (range and variance) of BB and DWH pings*

The W shear variance and number of samples are good proxies for the data quality of a lowered velocity profile. The latter is closely correlated with the range of the instrument. In order to assess the performance of the BB and MWH at depth these two parameters were studied in the downcast (to avoid bottle stops) at 200 m and at 2000 m, well below the 'scatter-cline'. The results are shown



2002-4-8 20:50

Figure L14: BB velocity profile (Firing processed) compared to on-station ADCP and MWH bottom-tracked velocities

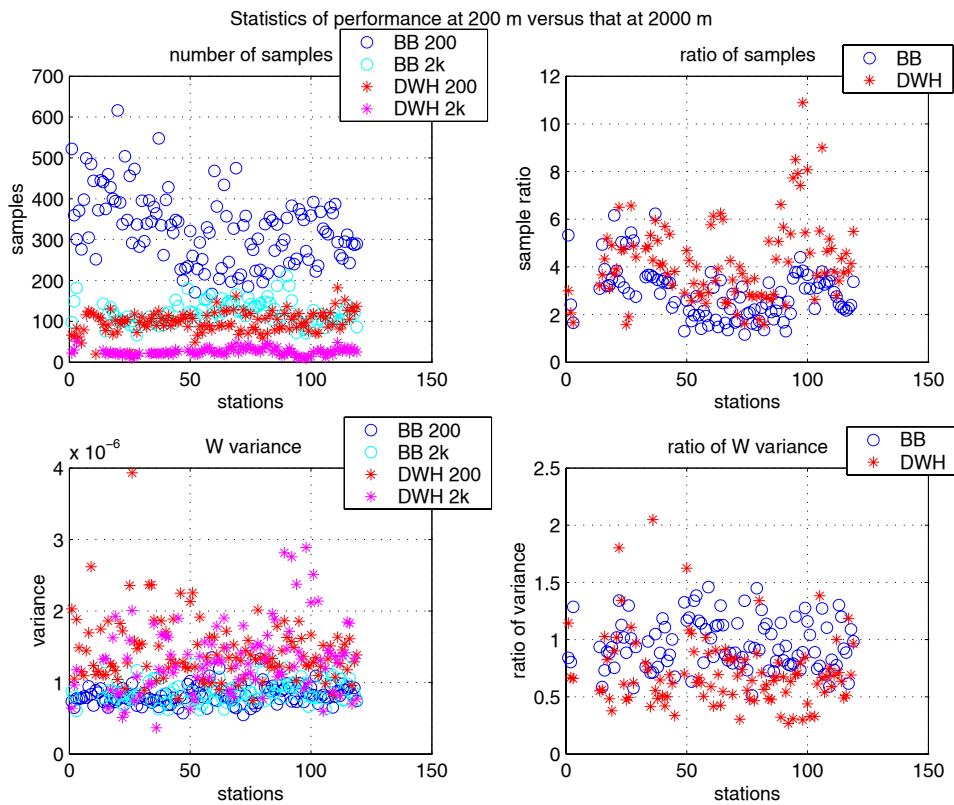


Figure L15: Performance statistics of BB and MWH

in Figure L15, where the left hand plots give the ratio of the instruments' performance at 200 m to that at 2000 m. On average (for all stations up to 115) the W shear variance ratio is 0.96 for the BB, and 0.71 for the MWH. In other words, the quality of BB pings is hardly effected, while the MWH pings decrease in quality by over 40%.

As for the range, the cruise sample ratio (samples at 200 m / samples at 2000 m) is 2.88 for the BB and 4.24 for the MWH. So the range loss is quite dramatically worse for the MWH. There is a possibility that the BB could see farther at 200 m than the 256 m that the instrument is configured for. This would bias the BB sample ratio low. To test this the samples at 1000 m were compared to those at 3000 m and the resulting ratios were found to be not significantly different. The blue water of the Southern Indian Ocean is attenuating the 150kHz signal to less than 250 m penetration even at 200 m. The relatively poor performance of the higher frequency MWH appears to be real. The only factor that can explain the poor performance of the MWH compared to the BB is the physics of deep marine scatterers, which must backscatter the 150kHz signal in preference to the 300kHz signal.

**References**

- [1] Beal, L. M., and H. L. Bryden, 1999, The velocity and vorticity structure of the Agulhas Current at 32°S, *J. of Geophys. Res.*, 104, 5151-5176
- [2] Firing, E. F. and R. Gordon, 1990, Deep ocean acoustic Doppler current profiling, *Proceedings of the IEEE Fourth International Working Conference on Current Measurements, Clinton, MD*, Current Measurement Technology Committee of the Ocean Engineering Society, 192-201
- [3] Firing, E., 1998, Lowered ADCP development and use in WOCE, *WOCE NOTES*, 30, 10-14
- [4] Firing, E., Erratum, 1998, *Intl. WOCE Newsletter*, 31, 20
- [5] Fischer, J. and M. Visbeck, 1993, Deep velocity profiling with self-contained ADCPs, *J. Atmos. and Oceanic Tech.*, 10, 764-773
- [6] Visbeck, M., 2002, Deep velocity profiling using lowered acoustic Doppler current profiler: Bottom track and inverse solutions, *J. Atmos. Oceanic Technology*, 19, 794-807
- [7] Send, U., 1994, The accuracy of current profile measurements - effect of tropical and mid-latitude internal waves, *J. Geophys. Res.*, 99, 16229-16236



**Appendix***LADCP Command Files*Down-looker Workhorse Configuration

## WHM.CMD

PS0 CR1 CF11101 EA00000 EB00000 ED00000 ES35 EX11111 EZ0111111 TE00:00:01.00  
 TP00:01.00 LD111100000 LF0500 LN016 LP00001 LS1000 LV250 LJ1 LW1 LZ30,220 SM1  
 SA001 SW05000 CK CS

Up-looker Workhorse Configuration

## WHS.CMD

PS0 CR1 CF11101 EA00000 EB00000 ED00000 ES35 EX11111 EZ0111111 TE00:00:01.00  
 TP00:01.00 LD111100000 LF0500 LN016 LP00001 LS1000 LV250 LJ1 LW1 LZ30,220 SM2  
 SA001 ST0 CK CS

Broadband Configuration

## BB13901.CMD

CR1 PS0 CY CT 0 EZ 0011101 EC 1500 EX 11101 WD 111100000 WL 0,4 WP 00001 WN  
 016 WS 1600 WF 1600 WM 1 WB 1 WV 350 WE 0150 WC 056 CP 255 CL 0 BP 000 TP 000000  
 TB 00000200 TC 2 TE 00000080 CF11101 &?

## Processing instructions

Instructions to Watchkeepers as at Jday 67.

Now that things are settling down, it is worth asking watchkeepers to push the LADCP processing a bit further after each cast. It is important to see that the instruments, particularly the BB, are producing complete and plausible casts after each station.

1) After download, check the log sheets have been completed, and the file names are right. Please complete 'bottom of cast' details on BOTH logsheets. Check the three data file names have been changed correctly.

CnnnB.000

CnnnW.000

CnnnS.000

These now all reside in one directory on unix.

2) On the laptop:

```
start / run / ftp darwin2
```

```
lcd ladcp'bb
```

```
cd /data33/bbraw
```

```
binary
```

```
put CnnnB.000
```

3) on the WH PC:

a) Copy 000 files to ZIP; insert ZIP in 'walknet' PC.

b) Open FTP explorer window

c) select unix directory 'bbraw'; doubleclick. This brings up the contents of bbraw in the right hand half of the window.

d) drag and drop files from ZIP into right hand half of FTP explorer window.

e) return zip disk to zip drive of WH PC.

4) On unix: log on to sohydro6 as pstar

5) start a new terminal window

6) > cd /data33/ladbbuh

7) > source LADall

8) > cd proc

9) > cd Rlad

You should now be in the directory where all the raw ADCP data sit. In order to process all data together, the three instruments are referred to as casts 01, 02, 03 for B, M, S data. Firing's data handles multiple casts more gracefully than multiple instruments.

10) Check the raw data file names.

11) > l.exec nm [this makes links from the file names that Firing requires, such as c027 01, to the raw files.

12) > cd proc

Lisa M. Beal and Brian King

## SHIPBOARD INSTRUMENTATION AND COMPUTING

### Data logged to LevelC

SURFMET	PC
ADCP	PC
WINCH	PC
EA500 D1	MKII LevelA
GPS_4000	MKII LevelA
LOG_CHF	MKII LevelA
GYRONMEA	MKII LevelA
GPS_ASH	MKII LevelA
GPS_G12	MKII LevelA
GPS_NMEA	MKII LevelA

### Ashtec ADU

The Ashtec ADU2 is the most precise GPS-based three-dimensional position and attitude determination system available, providing real-time heading, pitch, and roll measurements. The technology is based on differential carrier phase measurements between 4 antennas connected to the receiver. The ADU2 employs a 4 channel/12 channel configuration with the ability to select the best eight of twelve channels to use in Position and Dilution of Precision (PDOP)- based satellite searching and tracking. This improves solution integrity, allowing close to 100% attitude availability, providing two meter position accuracy and attitude angles can be as accurate as 1 milliradian (0.057°) or better in real-time at a 2 Hz update rate.

Before the start of the cruise it was recognised that the quality of data obtained by the ADU2 installed on the *RRS Charles Darwin* was not up to specifications. After thorough research it was decided that the only way to improve the performance was to replace the antenna cables. The cables installed initially were within the specifications, but were inferior to available alternatives. Four cables were prepared at SOC and brought out to Durban for installation during ship mobilisation. Once work had started it was soon realised that two of the cables were of insufficient length, and no spare connectors or cables were available on board. It was decided to source some locally, which was done, and at the last minute the two short cables were extended to complete the job.

Finally it was possible to perform a calibration of the ADU2. The results from this were fed back into the receiver. Once a fair amount of data had been gathered, it was clear that replacing the cables had improved the signal to noise ratio as well as the quality of data received overall.

## Calibration Details

	<b>X</b>	<b>Y</b>	<b>Z</b>
1-2	-0.504	0.495	0.000
1-3	0.000	0.996	0.000
1-4	0.496	0.498	-0.011

**General Navigation**

GPS receivers: GPS 4000, GPS G12, and GPS Ashtec are logged to the level C as gps\_4000, gps\_g12, and gps\_ash respectively. The GPS 4000 and G12 receive differential corrections from the Fugro SeaStar 3000L DGPS receiver, which is housed in the same case as the G12 receiver. The Churnikeef Log magnetic speed log is recorded as log\_chf. The gyrocompass is recorded as gyronmea. Navigation processing includes automatic correction of navigation error due to receiver error or breakdown. The processed files relmov and bestnav are available as 10 second interval datafiles.

**Underway measurements**

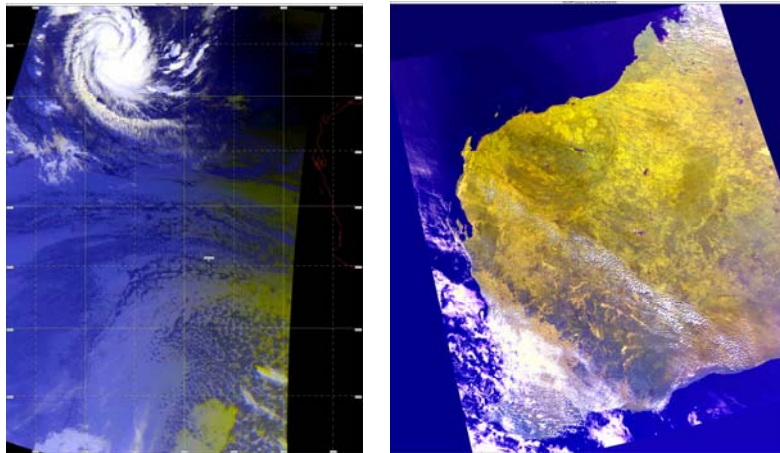
The SIG Surfmet instruments are logged through a PC known as the Surfmet PC. The data is displayed on the PC screen, and logged directly to the levelB computer. A processed wind data stream provides calculated absolute wind speed and direction using bestnav as the navigation input file.

The EA500 echo sounder is logged as ea500d1. Depth corrections were performed daily using the prodep command which produces Carter Area corrected depth measurements using the bestnav navigation data.

The hull mounted ADCP is logged directly to the LevelC. The CLAM winch monitoring system logs directly to the LevelB.

## Dartcom

The Dartcom system consists of a satellite tracking antenna mounted in a large dome above the bridge, and a rack-mounted control system incorporating a processing PC running Windows. Most operations are performed on the PC, using the familiar Windows environment. The system tracks and downloads images from the passing NOAA and Feng Yun weather satellites. The resulting images are an aid to predicting the weather and avoiding storms.



Dartcom images of tropical cyclone Ikeda

## LevelC and Networking

A Network hub was placed in the main lab. Seven computers were added to the network, 1 Sunblade, 3 Windows Pcs, and 3 Macs. An HP1600CM colour printer was also connected, as well as several roaming laptop computers. There was a shortage of network cables, this could have been avoided if computers being brought on board came with their own network cables.

Various drives were cross-mounted between the Sunblade (sohydro6) and levelC system to enable files to be shared for processing by the pstar/pexec processors. The following drives were mounted on sohydro6

darwin3:/data31

darwin3:/data32

darwin3:/data33

darwin1:/rvs/raw\_data

darwin1:/rvs/pro\_data

darwin1:/rvs/def7

darwin2:/nerc/packages/rvs

darwin2:/nerc/packages/gmt

Backups were done on a daily basis to DLT tape from the darwin3 unix machine. Daily backups included: /data31 /data32 /data33 /rvs/raw\_data /rvs/pro\_data /rvs/def7/control and /users, and were performed on a two day rotation basis.

## **Printers**

The following printers were available: HP Laserjet 4, HP 2000C, HP1200C/PS, HP Designjet 750C, and HP1600CM (not RVS/OED). After a few days the HP2000C printer broke down due to a failed printhead. A replacement printhead was not available on board, so this printer was rendered useless. The aged HP1200C was given a quick overhaul, involving repairing the slippery rollers and worked flawlessly throughout the rest of the cruise. The Laserjet started to develop a squeak towards the end of the cruise, perhaps this printer requires service.

## **Email**

The Novell server that was previously in use on *Charles Darwin*, failed on a previous cruise, and although a replacement was sent out prior to this cruise, there was an error with the configuration which meant it could not be used as the main email server. The solution was to setup a POP3 email server on the levelC computer system. The program qpopper was installed on Darwin2 at the start of the cruise, which was hoped would enable conventional email programs such as Eudora, Outlook Express, and Netscape Mail to be used to receive mail. The email transfer machine, Darwin4 was used as the SMTP (outgoing mail) server and Darwin2 as the POP3 (incoming mail via Darwin4) server. Email users were given a unix account on Darwin2, and the option of using Netscape Mail on the unix system or to use their own email client of choice on their own computer. This arrangement worked satisfactorily throughout the cruise, apart from a few hiccups mostly to do with Darwin4.

## **Other PC problems**

The main computer room PC (ibmpc2) running Windows98 experienced strange problems throughout the trip. It would unexpectedly freeze even when not being used, and CD writing was hopeless at best. The virus checker was removed because it seemed to blame for the PC not starting Windows properly. Later information was to leave a zip disk in the zip drive at all time. The USB Cdwriter was dismantled and the drive was installed inside the main computer case, and it worked first time without problems associated with buffer underruns and failure to recognise the drive.

The Master's PC was looked at on several occasions. This aged computer was struggling to run Windows 95/98, with a somewhat split personality. Eventually after a spectacular crash, Outlook Express stopped functioning, even after reinstalling it and the operating system. The Chief Engineer's PC running Windows95 had trouble sending attachments to email, this too was looked at, but a solution could not be found.

Martin Bridger



## NAVIGATION

### Background

Data from three scientific navigational instruments on *RRS Charles Darwin* were processed. Position, heading and attitude were primarily obtained from the Trimble 4000 GPS receiver, Ashtech ADU-2 GPS receiver and the Arma Brown MK10 Gyrocompass. Using a seaSTAR receiver, GPS correction data were passed to the Trimble 4000 to allow it to operate in differential mode (DGPS). On two occasions, no corrections were obtained due to crossing the boundary between different satellite coverage areas. All instruments were logged to the RVS Level A system before being transferred to RVS Level C system. Six Unix scripts were used to process the navigation data in 24 hour periods from 0000 to 2359. Each script, which required the JDAY as input, had to be altered slightly from the original version to deal with JDAY = 100.

### Trimble 4000

The Unix script `gpsexec0` was used to process the GPS data. Initially `datapup` transfers data from the RVS datastream `gps_nmea`, converting it into binary `pstar` format. The raw data flag is reset and new `dataname` and header details are created using `pcopya` and `pheadr` respectively. Data are edited using `pdop` (position dilution of precision based on the number of satellites to fix position). At the start of the cruise, the script was set to remove any data outside  $\text{pdop} < 4$ . However, as we headed eastward away from South Africa the number of data fixes reduced causing `datpik` to eliminate too much reasonable data. A greater amount of interpolation was required later to fill in the gaps, which caused problems when merging GPS with ADCP data. To eliminate problems we narrowed the editing to data outlying  $\text{pdop} < 7$ . This change took place on 17 March (JDAY 76) and the new criterion remained until the end of the cruise. Daily files `139gps[JDAY]` were appended to a master file `139gps01`.

### Ashtech ADU-2

Ashtech GPS data is used to correct heading errors in the ships gyrocompass before the gyrocompass is used in the ADCP processing. This correction is necessary because of the inherent error in the gyrocompass which causes it to oscillate for several minutes after a manoeuvre. Processing the ashtec data was broken down into four execs.

Ashexec0: The initial exec retrieves the raw data from the RVS datastream gps\_ash. The raw data flag is reset and header information set using pcopya and pheadr respectively. The output file created is 139ash[JDAY].raw.

Ashexec1: This exec merges the raw ashtech data with the master gyro file using pmerg2. The difference between the ashtech and gyro headings are calculated and set in the range between -180 and 180. The output file created is 139ash[JDAY].mrg.

Ashexec2: This exec edits the merged file 139ash[JDAY].mrg using a series of pexec programs: datpik removes data outside the limits for the following variables:

heading 0 360

pitch -5 5

roll -7 7

atf -0.5 0.5

mrms 0.00001 0.01

brms 0.00001 0.1

a-ghdg -5 5

pmdian removes shortlived spikes in 'a-ghdg' greater than 1 degree with a five point mean.

pavrg creates a two minute averaged file 139ash[JDAY].ave

phisto is run on the averaged file to determine the mean pitch and its limits.

datpik then removes further spikes from the average file, namely those outside the pitch limits calculated by phisto and where mrms is outside 0 and 0.004.

pavrg puts the file back into two minute average.

pmerge remerges the gyro heading from the master file onto 139ash[JDAY].ave.

pcopya then reorders the variables in the average file.

Output files are 139ash[JDAY].edit and 139ash[JDAY].ave.

Ashedit.exec: The final stage in the ash processing is running ashedit.exec. This allows final interactive editing of 'a-ghdg' with plxyed to remove any outlying data points. The resulting file is then interpolated to fill in missing data values to allow the easy merge of adcp data later on in the processing. The daily output files are 139ash[JDAY].dspk, which were appended to the master file 139ash01.

No ashtech data was recorded on one occasion (JDAY 090 00:40 - 01:10). The reason for this is unknown.

## Gyrocompass

The most continuous information available on ship's heading can be obtained from the gyrocompass. It is used in Acoustic Doppler Current Profiler (ADCP) and meteorological processing. The gyrocompass was processed with the script gyroexec0. Raw data is read in from the RVS data stream gyronmea using the pexec program datapup. The raw data flag and header information is set using pcopya and pheadr. Data is forced to lie between 0 and 360 degrees before being sorted on time. The output file 139gyr[JDAY].raw is created daily and appended to the master file 139gyr01.

The processing stages for gps, gyro and ash (first three execs) were combined into one UNIX script (called dailynav1) for daily processing .

## Investigating the EM-log

On JDAY 073 an investigation was carried out to compare the ships speed as determined from the VMADCP and emlog. It was observed that the emlog was apparently reading ship speeds higher than expected. This was affecting our progress overground, and we wanted to speed things up a little!

Initially, the first row from the master adcp file adpall was copied out from the beginning of jday 060 to the end of jday 070. The first row from the VMADCP provides the closest data to the surface with which we can compare emlog data. Heading data was merged on from the master gyrocompass file, 139gyr01 (ver AQ), and the calibrated ADCP velocities were converted to speed and direction of the ship over water. By subtracting the gyrocompass heading from the VMADCP direction we determined the direction of the ship over the water relative to the ships heading, 'dirn\_rel'. The VMADCP speed and dirn\_rel were reconverted to give the speed of the ship from the adcp in the fore-aft and port-starboard directions. The output file created was emlog\_05.

Data from the emlog was retrieved from the RVS datastream, log\_chf, using datapup. After averaging into two minute intervals (to match the adcp time) the emlog fore-aft and port-starboard speeds were merged on time to the adcp emlog\_05 file. A comparison was made of the VMADCP and emlog fore-aft and port-starboard speeds.

Results from our investigation are summarised in the table below. Plots of ADCP ship speed versus emlog ship speed indicated the emlog was reading higher, by approximately 5% in the slope and 5% in the offset, than expected. For example, at a speed of 10 knots the emlog was reading speeds 10% higher. Therefore, during station 55 (JDAY 73) new coefficients were entered as shown in the table. A repeat investigation made after station 55 on JDAY 76 showed the difference was minimal.

Table v1. Change in calibration of EM Log

<b>EMLOG speed (knots)</b>	<b>Initial calibration (knots) (what speed should be)</b>	<b>After jday 75 calibration (knots) (what speed should be)</b>
2.81	3.77	2.99
3.87	5.03	4.19
7.77	9.69	8.62
9.88	12.06	10.88

Louise Duncan and Brian King

## VESSEL-MOUNTED ACOUSTIC DOPPLER CURRENT PROFILER (VMADCP)

### Instrument Configuration

The Acoustic Doppler Current Profiler (ADCP) on the *RRS Charles Darwin* is an RD Instruments 153.6 kHz unit. Situated within a recess of the hull, the ADCP is orientated such that the transducer head is offset by 45° to the fore-aft direction. This offset is corrected for in daily processing using 139adpexec0a.

Data from the VMADCP was set to record in 64x8m bins, in ensembles of two-minute duration. The 'blank beyond transmit' was set to 4m and the approximate transducer depth was set to 5m. This gives a centre depth for the first bin as 17 metres.

The system uses 17.10 firmware and version 2.48 of RDI Data Acquisition Software, run on an IBM-type 300 MHz PC. With the PC interfaced to GPS, the Userexit program four (UE4) is able to correct the PC time using the GPS time. This eliminates the need for clock correction later in the data processing. Two-minute ensembles of data are passed directly to the Level C.

At the beginning of the cruise, working just off the South African coast, the system was set to record in bottom track mode. However, as we entered deeper water after station 16 (JDAY 63) we switched to water track mode. No bottom track data was collected again until after station 143 (JDAY=104), just off the Australian coast. The instrument was set to make one bottom track ping for every four water track pings using command FH00004.

### Data Processing

Data were processed in 24-hour periods, from 00:00 to 23:59, using six Unix scripts. Each script was altered slightly from the original to deal with JDAY inputs after JDAY = 99.

Reading in Raw Data (139adpexec0): Data were read in from the RVS level C system and separated into non-gridded data, such as heading, temperature, depth and bottom track velocities; and gridded data, such as water velocities and bindepth. Velocities are converted into millimetres per second. The two output files created were 139adp[JDAY] and 139bot[JDAY].

Rotating transducer heading (139adpexec0a): The heading of the VMADCP transducer was rotated by -45° in the bottom track non-gridded file.

Clock correction (139adpexec1): In previous cruises, the VMADCP data stream has been time-stamped with a clock other than the ship's master clock. This often resulted in time drifts in the raw data files. However, no clock correction was required on CD139 as the ship's master clock was used to time-stamp the VMADCP data stream. The exec was run nevertheless to keep file names and procedures the same as in previous cruises. The time difference of zero was applied to the data. The output files from the exec are 139adp[JDAY].corr, 139adp[JDAY] and clock[JDAY].

Ashtech corrections (139adpexec2): The VMADCP determines water velocities relative to the ship. To calculate absolute velocities the ships heading is required. The gyrocompass is used in ADCP processing as it can provide continuous measurements of heading. However, after manoeuvres the gyrocompass can oscillate for several minutes, which can be corrected using the Ashtech GPS. Since the Ashtech system does not provide continuous data, corrections are made on an ensemble-by-ensemble basis (See navigation section). The ashtech-minus-gyro heading correction ('a-ghdg') from the master ashtech file 139ash01 is merged with the VMADCP water track file, 139adp[JDAY].corr, and bottom track file, 139bot[JDAY].corr, on time; and the velocities are then corrected for this heading error. Output files are 139adp[JDAY].true and 139bot[JDAY].true.

Calibration (139adpexec3): Two further corrections required for the VMADCP are

- i) A an inherent scaling factor associated with VMADCP velocities
- ii)  $\phi$  the misalignment angle between the ashtech antenna and the VMADCP transducers heading

Initial values for A and  $\phi$  were set as  $A = 1$  and  $\phi = 6.35$ .

Data from the first four days of the cruise were used to determine the ADCP calibration. In this period two long steams occurred: a) from Durban to the first test station, travelling perpendicular to the coastline; and b) between stations 13 and 14 travelling parallel to the South African coastline.

The two-minute ensembles of bottom-track data were initially merged with the master GPS file, 139gps01, on time to retrieve navigation. Following a 30-minute average, the ship velocities and bottom velocities were converted into speed and direction. On station data were removed from the calibration by discarding bottom track speeds outside the range 100-750 cm/s.

A and  $\phi$  were calculated using

$$A = U_{GPS}/U_{VMADCP}$$

$$\phi = \phi_{GPS} - \phi_{VMADCP}$$

where  $U_{GPS}$ ,  $\phi_{GPS}$ ,  $U_{VMADCP}$  and  $\phi_{VMADCP}$  are the 30-minute average speed and direction from both the GPS and VMADCP respectively. The direction of  $\phi$  was reversed to put it in the correct orientation and then put in the range  $-180^\circ < \phi < 180^\circ$ . Excluding major outliers, we derived

$$A = 1.0035 \text{ and } \phi = 6.00.$$

Data were reprocessed with the new calibration values for A and  $\phi$  to produce correct water velocities relative to the ship. The new output files are 139adp[JDAY].cal and 139bot[JDAY].cal.

At the end of the cruise, we made another bottom-track calibration run, to verify the first calibration. After station 147, we steamed back along the cruise track to station 143 before heading back towards the shore on a heading of 130 degrees (the same track heading off South Africa). The same steps described above were made to find the new calibration. Excluding major outliers, we derived a new calibration

$$A = 1.0038 \text{ and } \phi = 5.80$$

This new calibration was not applied at the end of the cruise.

Calculate absolute velocities (139adpexec4): The master GPS file was merged with bottom track data on time to calculate the ship's velocity over two minute periods. The ship's velocities were then merged onto the water track file 139adp[JDAY].cal and absolute velocities calculated. Absolute velocities were output to the files 139adp[JDAY].abs and 139bot[JDAY].abs. The final daily ADCP files 139adp[JDAY].abs and 139bot[JDAY].abs were appended onto master files adpall and botall respectively.

All the ADCP processing stages were put into two UNIX scripts called dailynav2 and dailynav3.

### Separating Processed VMADCP Data into On-Station and Off-Station Data

For analysis, the master adpall file was separated into on-station, cast and steaming data for each cast. A single bin file, at a depth of 51 m, was used to work out when the ship was in these three different states. Using changes in the ship's speed and heading to determine when the ship was on-station and steaming, and the ctd/ladcp cast times to determine time in water, we listed appropriate datacycle numbers from bin5. These datacycles corrected for the complete gridded data were then used to extract the appropriate part of file adpall. Output files were called 139[NUM]S, 139[NUM]C and 139[NUM]A, where NUM is station number, for on-station, cast and between-station data respectively.

### Results

Various analyses on the ADCP data were performed. During the cruise, daily figures of ten-minute averaged ADCP data were made from 51 metres depth. One of the first analyses followed the completion of the Agulhas section, where transport estimates were made. These results are shown in Table A1.

Table A1: Estimates of the Agulhas Current Transport from Vessel Mounted ADCP

	<b>Transport above 60</b>	<b>Transport above 200</b>	<b>Transport above 280</b>
	<b>m (Sv)</b>	<b>m (Sv)</b>	<b>m (Sv)</b>
Stn 14 – 32	-3.8	-14.5	-19.4
Stn 14 – 31	-4.0	-14.8	-19.8
Stn 14 – 27	-3.7	-13.5	-18.1

Accumulated transport between stations 14 (the start of the final Agulhas section) and station 145 were calculated for the ADCP data. The station data was combined using `papend` and station pair averages calculated using `adcponsta2.m`, creating the output file `trans14-145.1`. The transport across the section, between the depths 60 and 200 metres, was calculated by accumulating the difference in distance between the stations multiplied by the depth multiplied by the velocity average for the stations. The final output file is `trans14-145.10`. Figure A1 shows the alongtrack and cross-track accumulated transports.

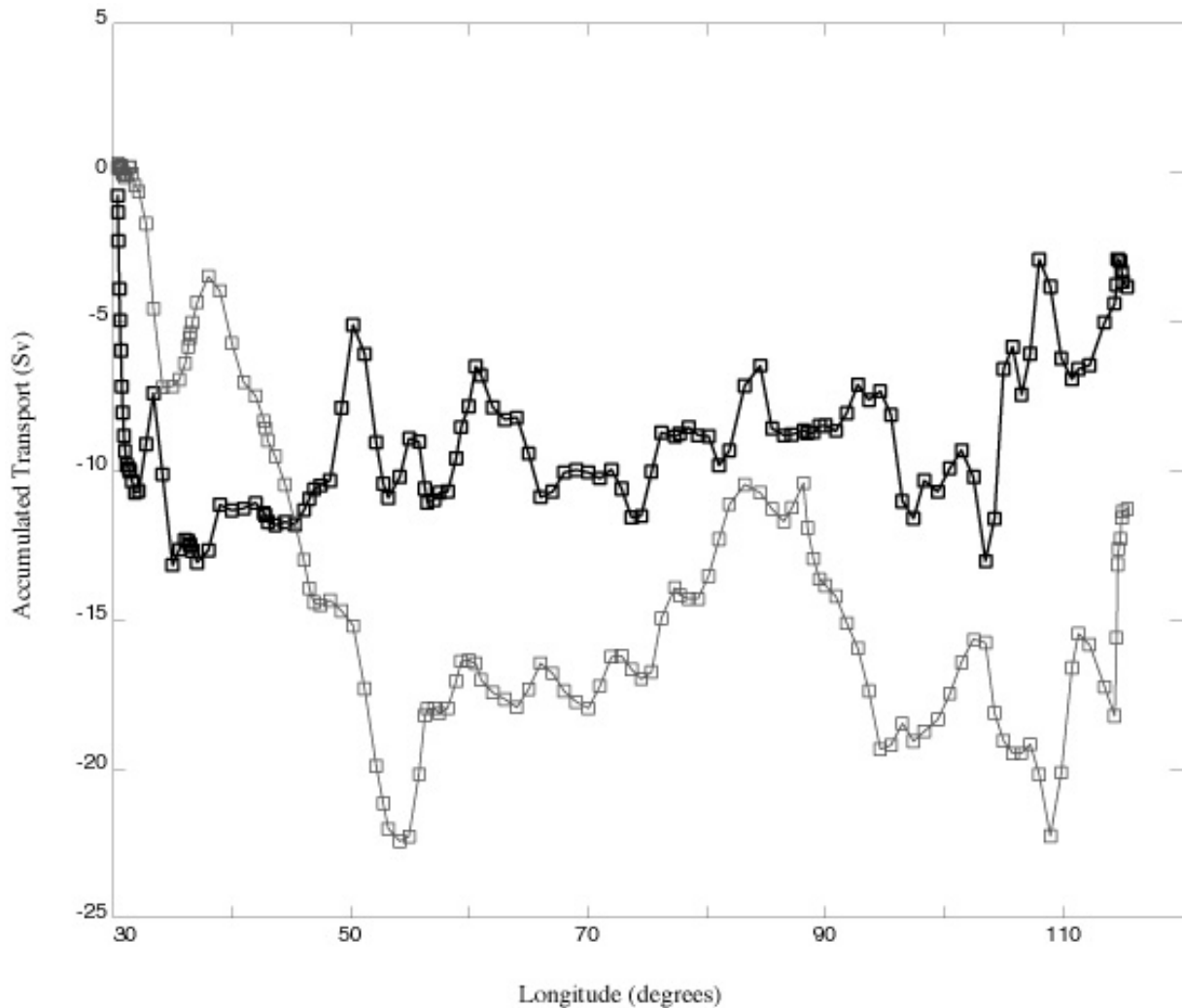


Figure A1. The accumulated transport perpendicular to (darker curve) and along (lighter curve) the cruise track from stations 14 to 145, between the depths of 60 and 200 m.

Louise Duncan and Matt Palmer



## UNDERWAY METEOROLOGICAL MEASUREMENTS

### Instrumentation

The RVS Surfmet system was used throughout the cruise to record near-surface meteorology and sea surface temperature and salinity. The instruments used with their serial numbers and manufacturer are shown in Table U1.

Table U1. Instruments used in Surfmet system on board RVS *Charles Darwin*.

Instrument	Manufacturer	Serial Number
OTM (Temperature) Housing	FSI	1334
OTM (Temperature) Remote	FSI	1401
Barometric Pressure (PTB 100A)	Vaisala	S3440012
OCM (Conductivity)	FSI	1353
Anemometer	Vaisala	S45517
Wind Vane	Vaisala	R05426

Unfortunately, the vane direction 0°/360° was set to be fore-ship, so that on-station when the wind was blowing towards the bow the vane registered values alternately in the ranges 0° to 10° and 350° to 360°. When one-minute averages were made of these one-second vane readings, a meaningless average vane direction was arrived at. Because one-minute averages are archived and subsequently processed, wind-direction values for on-station periods are not generally useful.

### Processing

From JDay 95 (6 March) a number of c shell scripts were used to process the underway data on a daily basis. Data up until JDay 94 were processed as a single batch.

Surexec0: This script transferred the data from the surfmet system to PSTAR format producing files 139sur\*\*\* and a master file 139sur01, where \*\*\* are consecutive numbers.

Surexec1: This merged the ship's position, speed and heading from the navigation system to the surfmet data and calculated thermosalinograph (TSG) salinity using housing temperature, conductivity and a zero pressure value. It also removed absent data values and performed a de-spiking function. The temperature variables were corrected with values taken from the most recent calibration sheet according to the equations below where T is the measured temperature.

$$\text{OTM (Temperature) Housing} = -6.96 \cdot 10^{-2} + 1.00(T) - 4.5 \cdot 10^{-5} (T)^2 + 1.1 \cdot 10^{-6} (T)^3$$

$$\text{OTM (Temperature) Remote} = -1.66 \cdot 10^{-4} + 1.00(T) - 8.66 \cdot 10^{-5} (T)^2 + 1.9 \cdot 10^{-6} (T)^3$$

The data were then further edited using PLXYED to manually remove obvious spikes remaining in the data. This created file 139sur02.

### **Salinity Calibration of Underway Data**

Samples were drawn every four hours from the uncontaminated seawater supply for salinometer analysis. The resulting bottle salinities were then used to calibrate the underway salinity values as follows.

Sur.exec: This script reads data from excel files containing salinity data for the uncontaminated seawater samples into PSTAR format. The files created are called surio\*\*\*.

Surexec2: This script converts the time from days, hours and minutes to total seconds to enable comparisons with the underway data. This master file was called 139tsg.samples.

The underway salinity data were added to the 139tsg.samples file and a new variable was formed of bottle salinity-TSG salinity(s-corr). This was then made into a continuous function and smoothed with a three point moving average. This smoothed function was then subtracted from the continuous salinity values to produce calibrated salinity data, (sal+corr).

Melanie Witt

## **ATMOSPHERIC SAMPLING**

### **Background**

Atmospheric input, primarily via precipitation, is now recognised as a major source of metals to the oceans. There has been much interest in the atmospheric transport of metals such as Cd, Pb, Hg, Cu, and Zn as these have been observed in atmospheric deposition in concentrations high enough to be harmful to aquatic organisms (Galloway et al, 1982). Aerosol samples collected at remote marine regions give important information regarding background concentrations and the extent of transport of continental material to the oceans. Material released as a result of biomass burning and dust transported from desert regions may be delivered to remote marine environments via the atmosphere.

### **Aerosol Collection**

During this cruise aerosol samples were collected using high volume aerosol samplers positioned on the port side of the crane deck (Table M1). Samples were only collected when there was a headwind to avoid contamination from ship's emissions. There were a number of periods during the crossing when sampling was not possible due to tailwinds.

Initially sampling was only undertaken during passage and the samplers were switched off with the filters still in place 15-20 minutes prior to arriving at stations and only switched back on 15-20 minutes after leaving the station. Several rust coloured spots were noticed on the filter papers when they were retrieved after sampling which indicated they had been contaminated by the ship. To avoid this when the samples were not being collected the filter paper was covered with metal plates. When tailwinds were following the ship's course samples were collected while on station as this involved turning the ship to head into the wind.

### **Trace Metal Analysis**

Aerosol samples collected during this passage are to be analysed for a number of trace metals. The concentrations of metals such as lead, copper, zinc, nickel, cobalt and cadmium will be investigated with graphite furnace atomic absorbance spectrometry(GFAAS), a technique with the low detection limits that are required to measure the low concentrations expected.

The aerosols for trace metal analysis were collected on acid cleaned filter papers and the material will be extracted with a number of solutions. A determination of the total metal content involving total digestion of a part of the filter with HF, a weak acid digest and extraction with artificial rain and seawater are planned for other parts of the papers. This will investigate the solubility of the metals to help to establish the availability of metals delivered via the atmosphere.

Table M1. Sampling locations and dates during the Indian Ocean Cruise

Sample No.	Longitude of sample (°E) at ~32°S.	Sample Time (Hours)	Sampling Dates (2003)	Volume of air sampled in trace metal sample (m <sup>3</sup> )
Durban 30.4 °E				
1 (Size segregated)	31.9 - 32.6	5.7	2 -3 March	353
2 (Size segregated)	31.6 – 30.3	3.2	4 March	217
3	32.8 – 36	19.2	8-9 March	797
4	36.8 – 43	31.7	10-13 March	1559
5	43.3 – 46.2	25.7	13-14 March	1719
6	47.4 – 58.1	20.4	15-19 March	1152
7	59.4 – 68	23.7	20-23 March	1337
8	73.8 – 77.7	22.6	25-28 March	1376
9	78.5 – 78.5	3	29 March	190
10	85.5 – 88.5	24	1-2 April	1865
11	88.5 - 93.7	13.5	2-4 April	1042
12	96.5 - 103.5	23	5-8 April	1274
13	105 – 107	9.5	9-10 April	628
14	107 – 114	23.7	10-13 April	1352
Perth 115.4°E				

### Major Ion Analysis

A second aerosol sampler has been used with filter papers not exposed to acid. These filters are to be analysed with ion chromatography for major ions such as sulphate and chloride. This should help to correct for seasalt collected on both samples. Phosphate analysis through the formation of molybdo-phosphoric acid and spectrophotometry will be used to establish the importance of the atmosphere in providing nutrient phosphate to oceans.

### Lead Isotope Signatures

Lead has four naturally occurring long lived isotopes (<sup>204</sup>Pb, <sup>206</sup>Pb, <sup>207</sup>Pb and <sup>208</sup>Pb). The amount of each isotope present in an iron ore is unique and is determined when it is formed. Each ore thus has its own isotopic lead signature. During environmental and industrial processes this isotopic ratio remains unchanged as there is no further fractionation (Doe, 1970). As different regions of the world use lead from different ores, analysis of the isotopic ratio of lead in the atmosphere may be used as a tracer of the source of anthropogenic lead.

Lead isotope measurements are planned on the aerosol samples collected on this cruise with a multi-collector inductively coupled plasma mass spectrometer (MC-ICP-MS). The ratios of the stable lead isotopes present in the aerosols along with back trajectories of air masses and weather maps of the region should help to identify the source of the aerosols sampled and the extent of transport of pollutant lead to the Indian ocean.

## Rain Collection

A number of rain samples have been collected from the monkey island above the bridge. Samples were taken in acid cleaned bottles and funnels for trace metal analysis; for major ion work the bottles and funnels were cleaned without the use of acid. The samples are stored frozen and a similar suite of analysis to the aerosol samples is planned for the rain samples on return to the laboratory at University of East Anglia . This should enable both the wet and dry flux of metals to the Indian Ocean to be investigated. Along with total metal concentration determinations electrochemical measurements of the organic complexation of copper in rainwater is also planned.

There have been several large rain events during passage across the ocean and this has enabled samples to be collected both close to the South African coast and in remote marine regions. A summary of the rain samples gathered during the cruise is shown in Table M2.

Table M2. Rain Samples Collected

<b>Date sampled</b>	<b>Position</b>	<b>Volume sampled</b>	<b>Volume sampled</b>	<b>pH</b>
<b>2002</b>		<b>(Major Ion Sample)</b>	<b>(Trace Metal Sample)</b>	
7 <sup>th</sup> March	31° S, 31° E	100 ml	150 ml	4.5
23 <sup>rd</sup> - 25 <sup>th</sup> March	34° S, 70° E	150 ml	500 ml	4.5
25 <sup>th</sup> -26 <sup>th</sup> March	33° S, 72° E	200 ml	300 ml	4.5
26 <sup>th</sup> March	32° S, 75° E	50 ml	50 ml	
31 March-1 April	31° S, 84° E	500 ml	50 ml	5.0
4 <sup>th</sup> April	32° S, 92° E	400 ml	250 ml	5.0
6 <sup>th</sup> April	34° S, 96° E	500 ml	500 ml	4.0

## Organic Copper Complexation

Copper is an essential nutrient at low concentrations but becomes toxic at elevated levels. Copper also plays an important role in atmospheric chemistry for reactions such as oxidation of SO<sub>2</sub> and production of OH radicals (Losno, 1999). Its bioavailability and catalytic capabilities are strongly influenced by chemical speciation with the free metal ion being the most readily available biologically and chemically (Sunda and Guillard, 1976).

Strong organic complexation of copper has already been observed in rain samples collected at UEA. Measurement of the free copper, and organic ligand concentrations along with total copper analysis in rain samples collected on this cruise will establish how widespread this complexation is.

**References**

**Doe, R.B.** 1970 Lead Isotopes. Springer-Verlag, Berlin.

**Galloway J.N., Thornton J.D., Norton S.A., Volchok H.L. & McLean R.A.N.** 1982 Trace metals in atmospheric deposition, a review and assessment. *Atmospheric Environment*, **16**, 1677-1700.

**Losno R.** 1999 Trace metals acting as catalysts in a marine cloud: a box model study. *Physical Chemistry of the Earth (B)*, **24**(3), 281-286.

**Sunda W. & Guillard R.R.L.** 1976 The relationship between cupric ion activity and the toxicity to phytoplankton. *Journal of Marine Research*, **34**(4), 511-529.

Melanie Witt

## ARGO FLOATS

### Setup

25 APEX floats from Webb Research were deployed, as a contribution to the Argo programme. The floats were purchased through the UK Met Office. Funding was from Met Office Argo funds and JRD. Initial enquiry was made about the possibility of sea freighting the floats directly to Durban, but the Webb agent in Europe believed this to be too great a challenge. The floats were therefore delivered to SOC and travelled to the ship in the JRD container. The floats were packed in 13 crates, 12 with 2 floats plus one single. Before leaving Durban, all float crates were opened, the numbers checked, and the crate lids secured with just two screws. This made the task of accessing the floats later in the cruise much easier. Floats were stored in the JRD container and brought into the main lab one at a time when needed.

A depth table of 55 depths had been defined based on examination of data from the 1987 cruise (Table F1). Compared with the table of 70 depths used for the UK's North Atlantic floats, there are fewer depths near the surface, but some extra entries deeper. Thus 12 different Argos messages make up the complete profile. All floats were set to drift at 2000 m, and profile once per 10 days.

In view of the fact that the depth table was shorter than is sometimes the case, and because the float activation times could be chosen to be optimal relative to the passes of the Argos satellites, it was decided that a time on the surface of 6 hours would be sufficient. Satellite pass predictions were based on satellite orbit data from January 2002. The satellite pass times in January 2002 had been compared with data from 6 months earlier and had not changed significantly. Argos data are relayed using the multi-satellite service. The satellites returning data in March 2002 were NOAA 11(H), 12(D), 14(J), 15(K), 16(L). At optimum times of day, and with a 45 second repetition rate, a 6 hour surface period is expected to return about 150 messages. Even allowing for change of satellites or orbits during the lifetime of the floats, this should be sufficient to ensure all data are recovered.

The floats had a nominal Argos repetition rate of 45 seconds. In practice this meant 44 or 46 seconds. The time of activation of floats was monitored. Where two floats were expected to be on the surface at the same time (i.e., activated 10 or 20 days apart) they were chosen where possible to have different repetition rates. This avoids the possibility that their entire transmissions will be exactly synchronised, which can result in data loss. The satellites cannot receive two transmissions simultaneously. An instance had been noted in the N Atlantic where two floats surfaced and were transmitting simultaneously, with the same repetition rate. Very few data were acquired from one of the floats until the second float ceased transmission and dived.

Floats were tested and reprogrammed using the laptop also used for the BroadBand LADCP. The terminal programme was used with settings 1200/8/N/1 and Xon/Xoff. The test sessions were saved to ASCII files by cutting and pasting into Notepad.

Table F1. Argo profile sample depths.

Sample point	Pressure	Sample point	Pressure	Sample point	Pressure
1	2000	20	750	39	160
2	1900	21	700	40	150
3	1800	22	650	41	140
4	1700	23	600	42	130
5	1600	24	550	43	120
6	1500	25	500	44	110
7	1400	26	450	45	100
8	1350	27	400	46	90
9	1300	28	360	47	80
10	1250	29	330	48	70
11	1200	30	300	49	60
12	1150	31	280	50	50
13	1100	32	260	51	40
14	1050	33	240	52	30
15	1000	34	220	53	20
16	950	35	200	54	10
17	900	36	190	55	4 or surf
18	850	37	180		
19	800	38	170		

## Deployment

Early in the cruise, two floats were deployed in 'dive mode', that is to say the initial period of 6 hours had elapsed, so the floats dived immediately. This was due to a mismatch between the optimum reset time and the CTD station timing. For the early deployments it was considered preferable to deploy the float when steaming away from the station. Later on, with greater familiarity all round, floats were deployed either when approaching or when leaving stations. Float number 1 (Argos 09410) was deployed three hours after dive time. Previous consultation with Webb Research had suggested that while this is not ideal, a delay of a few hours should not be a problem. In Jan 2001, the first batch of Irminger floats (17127 et al.) had been reset several days before deployment. Some floats had taken a few cycles to settle down to the correct park depth. If the float attempts to dive but finds pressure not increasing, it will tend to adjust the dive piston position to an incorrect value. Float number 2 was deployed 90 minutes after the dive time. All other floats were deployed before the dive time.

Floats were deployed by lowering off the starboard quarter, at speeds between 0.5 and 2 knots. Difficulty was experienced with only one float, number 21, Argos 09390. When the loose end



of the rope was paying through the hole in the damper plate, the last metre or so managed to get snagged between the anode and the sensor head assembly, such that it would not run through and release the float. It was decided that the float would need to be hauled back on board and redeployed. As the float was lifted out of the water and more weight came on the rope, it freed itself and the float dropped back into the water from a height of no more than 2 metres. No sign of damage to the sensor head was observed.

Three extra floats were deployed after leaving station 117. This was for the purpose of setting up a dispersion experiment. A float was deployed at 117 as normal, with further floats at a range of 5, 15 and 35 miles along track, so the 6 pairs of initial separations are 5, 10, 15, 20, 30, 35 miles. The floats were reset as near to simultaneously as possible, subject to satisfactory Argos tests.

All floats transmitted to Argos after reset. We have only a short amount of Argos data from Float 1. Due to a misunderstanding, it was carried from the lab to on deck only shortly before the end of transmissions. Floats 1 and 6 have not surfaced. Other floats appear to be functioning normally, and are returning good data. Table F2 contains float deployment details. All floats were set with UP = 12, DOWN = 228, P9 = 8. The expected rise time is about 6 hours, giving 6 hours on the surface. The details for four other floats operating in the area, deployed from Charles Darwin in 2001, are included for reference, although of these, 10309 has not reported since 23 Nov 2001.

Brian King

Table F2: Deployment details for CD139 floats. For reference, some details of four other floats in the region are given. Dive times represent the nominal dive times on a day number near the start of CD 139. Positions of these floats are latest positions relayed to the ship during the cruise. Float 10309 has not reported since 23 Nov 2001.

CD139 no	WRC Apex no	Argos decimal	Argos hex	WMO no	Test time	Reset time	Deploy time	Dive time	Argos rep rate	CTD stn no	Deploy lat	Deploy lon
1	485	09410	930AC		066/1034	066/1201	066/2108	066/1801	44	031	-32°08'	031°52'
2	466	09315	918C6		068/1129	068/1200	068/1930	068/1800	44	039	-33°01'	036°21'
3	465	09309	91763		070/1123	070/2225	070/2319	071/0425	44	046	-33°01'	040°00'
4	427	09108	8E527		071/2215	071/2224	072/0350	072/0424	44	050	-33°00'	042°50'
5	435	09208	8FE11		074/1010	074/1200	074/1421	074/1800	44	059	-33°33'	048°16'
6	451	09213	8FF5D		075/2112	075/2200	076/0049	076/0400	44	063	-34°01'	052°10'
7	458	09214	8FFA8		077/0901	077/1200	077/1735	077/1800	46	070	-34°00'	056°15'
8	469	09348	9210F		079/2025	079/2058	079/2319	080/0258	46	078	-34°00'	060°32'
9	470	09349	9215C		081/0930	081/1000	081/1103	081/1600	46	083	-34°00'	064°59'
10	462	09218	90082		082/2005	082/2100	082/2317	083/0300	46	087	-33°59'	069°00'
11	461	09217	90077		084/0746	084/0907	084/1220	084/1507	46	091	-33°35'	072°49'
12	460	09216	90024		087/0740	087/0800	087/0930	087/1400	44	097	-31°07'	077°44'
13	459	09215	8FFFB		089/0734	089/0800	089/0918	089/1400	44	100	-31°11'	080°10'
14	467	09322	91AAB		090/1002	090/1008	090/1416	090/1608	44	103	-31°13'	083°12'
15	468	09347	920E5		092/0649	092/0803	092/1232	092/1403	44	109	-31°47'	088°29'
16	481	09385	92A70		093/0730	093/0759	093/1314	093/1359	46	113	-32°08'	090°52'
17	464	09255	909C3		094/2040	094/2058	094/2359	095/0258	46	117	-33°31'	094°37'
18	471	09350	921A9		094/2018	094/2059	094/2359	095/0259	44	117	-33°32'	094°42'
19	463	09219	900D1		094/2034	094/2100	095/0056	095/0300	46	117	-33°36'	094°52'
20	478	09351	921FA		094/2026	094/2101	095/0249	095/0301	44	117	-33°44'	095°14'
21	482	09390	92B9A		096/0635	096/0804	096/0853	096/1404	46	121	-34°31'	098°20'
22	484	09397	92D7E		097/1742	097/1754	097/2139	097/2354	44	125	-34°30'	102°29'
23	483	09391	92BC9		099/1752	099/1755	099/2050	099/2355	44	130	-32°30'	106°29'
24	480	09382	929A4		101/0803	101/0808	101/1326	101/1408	44	134	-31°30'	109°52'
25	479	09352	9222E		103/0303	103/0555	103/0621	103/1155	44	138	-31°31'	113°10'
		10313						071/0800	44		-32°26'	046°30'
		10310						072/0400	44		-30°24'	049°39'
		10309						072/2000	44		-28°22'	042°25'
		10308						073/1630	44		-31°13'	033°48'